Technical Report Documentation Page

1. Report No.	2. Government Accession No.	3. Recipient's Catalog No.
TX / 98/1388-2		

4. Title and Subtitle	5. Report Date
Development Length of 0.6-inch (15-mm) Diameter Prestressing Strand at 2-inch (50-mm) Grid Spacing in Standard I-shaped Pretensioned Concrete Beams	June 1999
	6. Performing Organization Code

7. Author(s)	8. Performing Organization Report No.
William R. Burkett and M. Metin Kose	

9. Performing Organization Name and Address	10. Work Unit No. (TRAIS)
Texas Tech University Department of Engineering Technology Box 43107 Lubbock, Texas 79409-3107	11. Contract or Grant No. 0-1388

12. Sponsoring Agency Name and Address	13. Type of Report and Period Cover
Texas Department of Transportation Research and Technology P. O. Box 5080 Austin, TX 78763-5080	TTU/C40 Project Summary Sept 1995 – Aug 1998
	14. Sponsoring Agency Code

15. Supplementary Notes
Study conducted in cooperation with Texas Department of Transportation and the US Department of Transportation, Federal Highway Administration

16. Abstract
The research conducted at Texas Tech University (TTU) is an integral part of a larger, joint research project conducted with the University of Texas at Austin (UT) designed to provide additional test data for consideration toward lifting the FHWA moratorium. This joint project was to provide additional full scale test data on the transfer and development lengths of 0.6-inch (15-mm) diameter prestressing strand for two key variables, concrete strength and strand surface condition, for fully bonded and various combinations of bonded and debonded strand using AASHTO Type I (Texas Type A) I-beams. Three concrete strength ranges and two extreme strand surface conditions were used in the joint TTU/UT project to evaluate their effect on transfer and development lengths. Concrete strengths were 5,000-7,000 psi (34.4-48.2 MPa), 9,500-11,500 psi (65.4-79.2 MPa), and 13,000-15,000 psi (89.6-103.4 MPa) and strand surface conditions were mill bright or rusty. For each combination of concrete strength and strand surface condition, beams were tested for three other variations in the strand: all strands fully bonded, 50% of the strands debonded, and 60% or 75% of the strands debonded. TTU's portion of the project and the data reported herein is limited to concrete strength in the 5,000-7,000 psi (34.4-48.2 MPa) range and strand with a rusty surface condition for the each of the three strand variations listed above with a maximum debonded limit of 60%. Six beams and therefore 12 tests for both transfer and development lengths were conducted by TTU and reported herein. Transfer and development lengths that were experimentally determined during TTU's portion of this project are compared to current code requirements for both transfer and development lengths for ACI-318, AASHTO-Standard, and AASHTO-LRFD. In addition, these results are compared to two predictive equations for both transfer and development lengths: one that was proposed by C. Dale Buckner and one that was proposed by Susan N. Lane.

17. Key Words	18. Distribution Statement
pretensioned concrete, 0.6-inch diameter prestressing strand, transfer length, development length, debonded strand	No restrictions. This document is available to the public through the National Technical Information Service, Springfield, Virginia 22161

19. Security Classif. (of this report)	20. Security Classif. (of this page)	21. No. of Pages	22. Price
Unclassified	Unclassified	105	

Form DOT F 1700.7 (8-72)

DEVELOPMENT LENGTH OF 0.6-INCH (15-mm) DIAMETER PRESTRESSING STRAND AT 2-INCH (50-mm) GRID SPACING IN STANDARD I-SHAPED PRETENSIONED CONCRETE BEAMS

by

William R. Burkett

M. Metin Kose

Research Report Number 0-1388

conducted for

Texas Department of Transportation

by the

DEPARTMENT OF ENGINEERING TECHNOLOGY

TEXAS TECH UNIVERSITY

June 1999

Implementation Statement

The use of 0.6-inch (15-mm) diameter prestressing strand has become necessary with the development and use of high-strength / high-performance concrete in standard I-beam sections to effectively utilize the higher concrete strength. However, the Federal Highway Administration (FHWA) placed a moratorium on the use of 0.6-inch (15-mm) diameter prestressing strand in pretensioned concrete I-beams in October of 1988. This moratorium was imposed because of some apparent unconservatism in the code requirements addressing transfer and development lengths of 7-wire prestressing strand. It should be noted that at the time of the writing of this report that there has been a partial lifting of the FHWA October, 1988, moratorium due to positive results of additional research. The use of 0.6-inch (15-mm) diameter prestressing strand at a 2-inch (50-mm) grid spacing is now allowed in pretensioned applications, but the development length requirement of AASHTO equation 9-32 is to be multiplied by a factor of 1.6.

Transfer and development length values experimentally determined during TTU's portion of the project were for beam concrete strengths in the 5,000-7,000 psi (34.4-48.2 MPa) range and for strand with rusty surface condition. All experimentally determined short-term and long-term transfer length values, except one, met current code requirements. One short-term transfer length value exceeded the ACI-318 and AASHTO-Standard Specification requirement of $50d_b$ by only 1.6%. In addition, all experimentally determined transfer length values were less than the values predicted by both the Buckner equation and the Lane equation, with the Lane equation yielding overly conservative results. All experimentally determined development length values met current code requirements and were also less than the values predicted by both the Buckner equation and the Lane equation. In addition, the extra FHWA factor of 1.6 for fully bonded strand development length was unnecessary.

It should be noted that the data reported herein is a small portion of the overall project data, and any final conclusions should be weighed carefully against the total data from the project as well as other compatible test data in the literature.

Acknowledgements

The authors gratefully acknowledge the support of Ms. Mary Lou Ralls of the Texas Department of Transportation and of Dr. Ned H. Burns and Mr. Robert W. Barnes of the University of Texas at Austin.

Prepared in cooperation with the Texas Department of Transportation and the U.S. Department of Transportation.

Disclaimer

The contents of this report reflect the views of the authors, who are solely responsible for the facts and the accuracy of the data presented herein. The contents do not necessarily reflect the official view or policies of the Texas Department of Transportation. This report does not constitute a standard, specification, or regulation.

Patent Disclaimer

There was no invention or discovery conceived or first actually reduced to practice in the course of or under this contract, including any art, method, process, machine, manufacture, design or composition of matter, or any new useful improvement thereof ,or any variety of plant which is or may be patentable under the laws of the United States of America or any foreign country.

Engineering Disclaimer

This is not intended for construction, bidding, or permit purposes. The engineer in charge of the research study was William R. Burkett, P.E., Texas 81893.

Trade Names and Manufacturers' Names

The United States Government and the State of Texas do not endorse products or manufacturers. Trade or manufacturers' names appear herein solely because they are considered essential to the object of this report.

SI* (MODERN METRIC) CONVERSION FACTORS

APPROXIMATE CONVERSIONS TO SI UNITS

Symbol	When You Know	Multiply By	To Find	Symbol
	LENGTH			
in	inches	25.4	millimeters	mm
ft	feet	0.305	meters	m
yd	yards	0.914	meters	m
mi	miles	1.61	kilometers	km
	AREA			
in^2	square inches	645.2	square millimeters	mm^2
ft^2	square feet	0.093	square meters	m^2
yd^2	square yards	0.836	square meters	m^2
ac	acres	0.405	hectares	ha
mi^2	square miles	2.59	square kilometers	km^2
	VOLUME			
fl oz	fluid ounces	29.57	milliliters	mL
gal	gallons	3.785	liters	L
ft^3	cubic feet	0.028	cubic meters	m^3
yd^3	cubic yards	0.765	cubic meters	m^3
NOTE: Volumes greater than 1000 l shall be shown in m^3.				
	MASS			
oz	ounces	28.35	grams	g
lb	pounds	0.454	kilograms	kg
T	short tons (2000 lb)	0.907	megagrams (or "metric ton")	Mg (or "t")
	TEMPERATURE (exact)			
°F	Fahrenheit temperature	5(F-32)/9 or (F-32)/1.8	Celcius temperature	°C
	ILLUMINATION			
fc	foot-candles	10.76	lux	lx
fl	foot-Lamberts	3.426	candela/m^2	cd/m^2
	FORCE and PRESSURE or STRESS			
lbf	poundforce	4.45	newtons	N
lbf/in^2	poundforce per square inch	6.89	kilopascals	kPa

APPROXIMATE CONVERSIONS FROM SI UNITS

Symbol	When You Know	Multiply By	To Find	Symbol
	LENGTH			
mm	millimeters	0.039	inches	in
m	meters	3.28	feet	ft
m	meters	1.09	yards	yd
km	kilometers	0.621	miles	mi
	AREA			
mm^2	square millimeters	0.0016	square inches	in^2
m^2	square meters	10.764	square feet	ft^2
m^2	square meters	1.195	square yards	yd^2
ha	hectares	2.47	acres	ac
km^2	square kilometers	0.386	square miles	mi^2
	VOLUME			
mL	milliliters	0.034	fluid ounces	fl oz
L	liters	0.264	gallons	gal
m^3	cubic meters	35.71	cubic feet	ft^3
m^3	cubic meters	1.307	cubic yards	yd^3
	MASS			
g	grams	0.035	ounces	oz
kg	kilograms	2.202	pounds	lb
Mg (or "t")	megagrams (or "metric ton")	1.103	short tons (2000 lb)	T
	TEMPERATURE (exact)			
°C	Celcius temperature	1.8C + 32	Fahrenheit temperature	°F
	ILLUMINATION			
lx	lux	0.0929	foot-candles	fc
cd/m^2	candela/m^2	0.2919	foot-Lamberts	fl
	FORCE and PRESSURE or STRESS			
N	newtons	0.225	poundforce	lbf
kPa	kilopascals	0.145	poundforce per square inch	lbf/in^2

* SI is the symbol for the International System of Units. Appropriate rounding should be made to comply with Section 4 of ASTM E380.

(Revised September 1993)

TABLE OF CONTENTS

List of Tables viii

List of Figures ix

CHAPTER I – INTRODUCTION 1

CHAPTER II – BACKGROUND 3

2.1 Terminology 3

2.1.1 Transfer Length 3

2.1.2 Bond 3

2.1.3 Flexural Bond Length 4

2.1.4 Development Length 4

2.1.5 Embedment Length 5

2.1.6 Strand Surface Condition 5

2.1.7 Fully Bonded & Debonded Strand 5

2.2 Current Code and Proposed Equations 6

2.2.1 Transfer Length 6

2.2.1.1 Current Code Requirements 6

2.2.1.2 Buckner Equation 7

2.2.1.3 Lane Equation 8

2.2.2 Development Length 8

2.2.2.1 Current Code Requirements 8

2.2.2.2 Buckner Equation 10

2.2.2.3 Lane Equation 10

2.3 Project Overview 11

CHAPTER III – FABRICATION AND TESTING 13

3.1 Introduction 13

3.2 Beam Fabrication and Transfer Length Measurements 14

3.3 Deck Slab Fabrication and Composite Beam Set-up 19

3.4 Instrumentation and Test Measurements 22

3.5 Development Length Tests 24

CHAPTER IV – TEST RESULTS 28
4.1 Transfer Length 28
4.2 Development Length 38
4.3 Effect of H-Bars 45
CHAPTER V – SUMMARY AND OBSERVATIONS 46
5.1 Summary 46
5.2 Observations 48
APPENDIX A BEAM REINFORCEMENT DETAILS 52
APPENDIX B CONCRETE COMPRESSION STRAINS AND PROFILES 56
APPENDIX C LOAD – DEFLECTION CURVES 81
APPENDIX D LOAD – END SLIP CURVES 94
APPENDIX E NOTATION 103
APPENDIX F UNIT CONVERSIONS 104
REFERENCES 105

LIST OF TABLES

2.1 Test Matrix and Material Target Values 12
3.1 Length of Mounted Demec Points 19
3.2 Concrete Material Properties 20
3.3 Test Geometry 26
4.1 Short-Term Transfer Length 32
4.2 Long-Term Transfer Length 33
4.3 Calculation of Transfer Length Using Buckner and Lane Equations 34
4.4 Summary of Development Length Results 39
4.5 Maximum End Slip Values 43
4.6 Calculated Values of Development Lengths 44
4.7 Comparison of Development Lengths 44

LIST OF FIGURES

3.1 Beam Cross-Section of L0RX Series 14
3.2 Beam Cross-Section of L4RX Series 15
3.3 Beam Cross-Section of L6RX Series 15
3.4 Debonded Strands Using Split Sheathing 16
3.5 Pretensioning / Casting Bay 17
3.6 Beam Formwork and Concrete Placement 18
3.7 Demec Point Measurement 18
3.8 Concrete Deck Slab Details 20
3.9 Fabrication of Deck Slab 21
3.10 Load Bearing Plates, Rollers and Spreader Beam 21
3.11 Load Frame 22
3.12 Strand End-slip Brackets 24
3.13 Test Geometry 25
3.14 Support and Loading Arrangement 26
4.1 Effect of Smoothing on Strain Profiles 28
4.2 Typical Smoothed Strain Profile for Fully Bonded Strands 29
4.3 Typical Smoothed Strain Profile for 50% Debonded Strands 29
4.4 Typical Smoothed Strain Profile for 60% Debonded Strands 30
4.5 Comparison of Short-Term Transfer Length with Code Values 35
4.6 Comparison of Long-Term Transfer Length with Code Values 35
4.7 Comparison of Short-Term Transfer Length with Buckner Equation 36
4.8 Comparison of Long-Term Transfer Length with Buckner Equation 36
4.9 Comparison of Short-Term Transfer Length with Lane Equation 37
4.10 Comparison of Long-Term Transfer Length with Lane Equation 37
4.11 Effect of Time on Transfer Length 40
4.12 Effect of Debonding on Transfer Length 40
4.13 Load - Deflection Curve of L4R0-1 42
4.14 Load - Deflection curve of L4R0-2 42

CHAPTER I

INTRODUCTION

The use of precast, prestressed concrete I-beams with cast-in-place deck slabs in highway bridge construction in the United States is a common practice. Efficient material utilization and cost effectiveness has lead to the popularity of this construction technique and its wide spread use. Its popularity through the years has lead to many innovations and improvements in the construction process and in the materials used. These include the use of stay-in-place precast concrete panels as bottom forms for the cast-in-place concrete deck slab, the use of low relaxation prestressing strand, the use of high-strength / high-performance concrete, and the use of larger 0.6-inch (15-mm) diameter prestressing strand. The use of these newer and improved materials calls into question several code requirements that were developed from research conducted using older and outdated material properties and sizes. Of specific interest in this study are the code requirements that control the transfer and development lengths of the newer 0.6-inch (15-mm) diameter, low relaxation, prestressing strand.

The use of 0.6-inch (15-mm) diameter prestressing strand became necessary with the development and use of high-strength / high-performance concrete in standard I-beam sections if the standard 2-inch (50-mm) grid spacing was to be maintained and if the higher strength concrete was to be effectively utilized. The use of high-strength / high-performance concrete in this application requires a much larger prestressing force to fully pre-compress the service load tensile zone of the I-beam. However, the number of strands that can be placed in any given I-beam section on a 2-inch (50-mm) grid is limited. The strand limit also limits the amount of prestressing force that can be applied to the section. The cross-sectional area of 0.6-inch (15-mm) diameter strand is over 40% greater than that of 0.5-inch (13-mm) diameter strand, the maximum previously available diameter. This allows for over a 40% increase in prestressing force for the same number of strands and the same level of stress in each strand by simply changing from a 0.5-inch (13-mm) to a 0.6-inch (15-mm) diameter strand.

The Federal Highway Administration (FHWA) placed a moratorium on the use of 0.6-inch (15-mm) diameter prestressing strand for this application in October of 1988. This moratorium was imposed because of some apparent unconservatism in the code requirements addressing transfer and development lengths of 7-wire prestressing strand. The research conducted at Texas Tech University (TTU) and the results reported herein are an integral part of a larger, joint research project conducted with The University of Texas at Austin (UT) designed to provide addition test data for consideration toward lifting the FHWA moratorium. This joint project was to provide additional full scale test data on the transfer and development lengths of 0.6-inch (15-mm) diameter prestressing strand for two key variables. The effects of the two key variables, concrete strength and strand surface condition, on the transfer and development lengths of the 0.6-inch (15-mm) diameter prestressing strand were investigated for fully bonded and various combinations of bonded and debonded strand used in AASHTO Type I (Texas Type A) I-

beams. Specific details and values of the key variables are provided in Chapter 2 of this report. It should be noted that at the time of writing of this report that there has been a partial lifting of the FHWA moratorium on the use of 0.6-inch (15-mm) diameter prestressing strand due to positive results of additional research. In May, 1996, the FHWA lifted its prohibition against the use of 0.6-inch (15-mm) diameter strand in pretensioned concrete I-beams and allowed its use at 2-inch (50-mm) center-to-center spacing. However, the October 1988 FHWA requirement of 1.6 times AASHTO Equation 9-32 for the development length remains intact.

CHAPTER II
BACKGROUND

2.1 Terminology

2.1.1 Transfer Length

During the I-beam fabrication process, the prestressing strands are elongated by the application of axial tensile forces. Prefabricated forms are placed around the strands to form the I-beam cross-section, and concrete is placed into the forms. Once the concrete has attained sufficient strength, typically within 18 to 24 hours, the forms are removed and the tensile forces initially applied to the prestressing strands are released. As the tensile forces are released, the steel strands try to shorten. Where the strands and the concrete are bonded together, the concrete restrains the shortening of the steel strands and compression stresses are developed in the concrete. The transfer of tensile forces from the prestressing strands into the concrete at release of the strands occurs gradually over some distance along the length of the member. The compression stresses in the concrete are zero at the free end of the beam and gradually increase along the length of the member to some maximum value when the full tensile force in the steel strands is transferred by the bond between the steel strands and concrete into the concrete. Beyond this maximum point, the compression stresses in the concrete caused by the tensile forces in the strands remain constant. The length over which the tensile forces are fully transferred from the prestressing strands into the concrete is defined as the transfer length. By determining and plotting the compression strain in the bottom flange of the concrete I-beam along the length of the beam, the transfer length can be determined. It should be noted that the transfer gradient of the tensile force in the strands matches that of the compression stresses in the concrete, in that it is zero at the end of the beam and increases to a maximum at the end of the transfer length.

2.1.2 Bond

The transfer of the forces from the prestressing steel to the concrete is dependent on the bond which occurs at the interface surface between the two materials. The two primary components of bond in the transfer region can be contributed to a wedge/friction action and a mechanical interlock.

At the end of the beam when the tensile force in a strand is released, the strand tries to expand in its radial direction to its original shape, but it is restrained by the concrete. This restrained expansion creates normal forces between the steel and concrete surfaces, which also allows for the development of frictional forces between the two surfaces. Some radial expansion of the strand occurs as the concrete compresses in the radial direction until equilibrium of these radial forces is reached. The equilibrium diameter of the strand and the magnitude of the frictional force between the strand and concrete also vary along the length of the member in the transfer zone. They are maximum at the free end of the beam where the axial tensile force in the steel is zero and

reduce to minimum values at the end of the transfer zone where the axial tensile force in the steel is maximum. This creates a wedge effect in the radial dimensions of the strand and in the frictional forces between the surfaces of the strand and concrete, both of which help to anchor the end of the prestressing strand and transfer the force from the strand into the concrete.

Mechanical interlock is the second primary component of bond that contributes to the transfer of forces between the prestressing strand and the concrete. It occurs between the helical lay of the individual wires in the 7-wire strand and the concrete that is cast around and conforms to the shape of the strand. Mechanical interlock is dependent on the restraint of twisting of the strand about its longitudinal axis as it tries to slip through the concrete. This twisting restraint is provided by the frictional forces developed at the interface between the steel strand and concrete surfaces. A more in-depth discussion of bond is provided by Russell and Burns (1993).

2.1.3 Flexural Bond Length

Tensile forces in the prestressing steel increase with the application of transverse external loads. The application of transverse external loads creates bending or flexural moments in the beam that must be resisted by and be in equilibrium with an internal couple produced by the compression force in the concrete and the tensile force in the steel. As the external loads increase, the flexural moments in the beam increase, and the compression force in the concrete and the tensile force in steel must also increase to maintain equilibrium. The increase in the tensile force in the steel must also be accompanied by an increase in the bond force at the steel/concrete interface that is required to maintain equilibrium of the steel strand in its axial direction. Therefore, the flexural bond length is defined as the length of strand/concrete interface that is required to develop the bond forces necessary to maintain equilibrium of strand tensile force increases caused by external transverse loads.

2.1.4 Development Length

The concept of development length and flexural bond length is very similar but their difference is important when applied to prestressed concrete. In general, concrete members are designed so that their ultimate internal moment resistance is greater than the maximum moment caused by the ultimate transverse external loads. The maximum tensile force in the steel will occur when the ultimate internal moment is attained, and once again, sufficient bond forces at the steel/concrete interface must be developed to maintain equilibrium. Therefore, the development length is the length of strand/concrete interface that is required to develop the bond forces necessary to maintain equilibrium of the total tensile force in the steel at ultimate condition. In prestressed concrete, the total tensile force in the steel at ultimate is the sum of the prestress tensile force and the increase in tensile force due to the maximum externally applied load. Therefore, for prestressed concrete, the development length is the sum of the transfer length and the maximum flexural bond length.

2.1.5 Embedment Length

The embedment length of the prestressing strand in this project is the shortest distance, along the length of the member, between the critical section and the point where bonding between the strand and the concrete stops. The critical section is defined as the location along the length of the member where the maximum moment occurs. The location where the maximum moment occurs is concurrent with the location where the maximum tensile force in the prestressing strand occurs. Because of this, the embedment length of the steel should always be greater than the development length of the steel. Otherwise, the bond force at the steel/concrete interface will be insufficient to maintain equilibrium with the tensile force in the strand, and the strand will pull out of the concrete resulting in a premature failure of the member. This phenomenon is used to experimentally determine the minimum development length required for 0.6-inch (15-mm) diameter prestressing strand by incrementally shortening the embedment length of the strand until there is a transition from a flexural failure mode to a bond slip failure mode in the member.

2.1.6 Strand Surface Condition

Two extreme strand surface conditions, bright and rusty, were used in an effort to bracket and evaluate the effect of surface condition on the transfer and development lengths of 0.6-inch (15-mm) diameter prestressing strand. Within this project, the term "bright" surface condition was defined as the as-received condition. The strand was stored indoors between uses to maintain its original as-received condition through out the project. It had a smooth surface condition and only the occasional light spotting from atmospheric exposure during the fabrication process. The term "rusty" surface condition was defined as having a light, somewhat uniform coating of rust on the strand which was not easily removed. The corrosion was not severe and had not significantly affected the cross-sectional area of the strand. This condition was achieved by exposing the strand to the weather in the precasting yard for a period of several months. No attempt was made to clean or modify the surface condition of either type strand, except by weathering as noted above. The portion of the project conducted at TTU only used the "rusty" strand surface condition.

2.1.7 Fully Bonded & Debonded Strand

One third of the test specimen in this project were fabricated using fully bonded strands. A member designation of "fully bonded" indicates that all of the prestressing strands in the member were allowed to develop bond between the prestressing strand and the concrete along the entire length of the member. Two thirds of the specimens in this project were fabricated with some designated percentage of the total number of strands in the member debonded. The term "debonded" indicates that contact between the concrete and prestressing strand was restricted so that no bond could form at the interface surface of the two materials. Therefore, no forces could be transferred between the strand and the concrete in the debonded regions. Debonding was accomplished by placement of a

plastic jacket or sheathing around the strand in the region of the beam where no bond was desired. Debonding is one method whereby the stresses in the concrete at the ends of the I-beam can be controlled. The prestress forces are typically applied to the beam cross-section below the neutral axis of the beam, and this eccentricity of prestress force causes compression stresses in the lower fibers and tensile stresses in the upper fibers of the concrete beam. The magnitudes of these stresses must be controlled most critically at initial release of the prestress force when the concrete is at its weakest condition. In the mid-region of the beam, flexural stresses caused by self-weight are of the opposite sign of those created by the eccentric prestress force and help to control the prestress force stresses in the concrete. However, at the ends of the members, the self-weight bending stresses go to zero and are not available to control stresses in the concrete caused by the prestress force. Two techniques are currently used to control stresses in the concrete caused by the prestress force at the end of the member. One is to reduce the eccentricity of the prestress force at the ends of the member by draping the strand. The other is to reduce the magnitude of the prestress force that is being transferred to the concrete at the ends of the member by debonding some of the strand in that region. Debonding of strands was included as a part of this research project to provide additional full scale test data for evaluation of current code requirements which address development length of debonded prestressing strand.

2.2 Current Code and Proposed Equations

Three primary codes that provide design guidance for prestressed concrete beams are addressed in this section: *ACI Building Code Requirements for Structural Concrete and Commentary*, ACI 318-95 (1995); *AASHTO Standard Specifications for Highway Bridges*, 16th Edition (1996); and *AASHTO LRFD Bridge Design Specifications* (1997 Interim Revisions). In addition, two reports that contain proposed equations for the determination of transfer and development lengths are also addressed in this section, Buckner (1994) and Lane (1998). Transfer and development lengths determined in this experimental study will be compared, in Chapter 4, to the values predicted by these current code and proposed equations.

2.2.1 Transfer Length

2.2.1.1 Current Code Requirements

ACI 318 provides guidance for the transfer length of prestressing strand in Section 11.4.3 and Section 11.4.4, which address reductions in the shear strength of the concrete section when the critical shear section falls within the prestress force transfer zone of the member. Both sections state that the transfer of the prestress force should be assumed to vary linearly from zero, at the point where bonding begins, to a maximum over a distance equal to 50 strand diameters (d_b). In a discussion on the development length of prestressing strand in the commentary of ACI 318, Section R12.9, an alternate equation is suggested for the determination of the transfer length of prestressing strand. This alternate equation is shown below.

$$l_t = \frac{f_{se} d_b}{3} \tag{2.1}$$

where: f_{se} = The effective prestress after all losses (ksi)
d_b = The diameter of the prestressing strand (inches)

This suggested equation yields transfer lengths in the range of $50d_b$ for typical values of f_{se}.

The AASHTO Standard Specification provides guidance for the transfer length of prestressing strand in Section 9.20.2.4. Its requirements read nearly identical to ACI 318 in that the transfer of prestress force is assumed to vary linearly from zero to a maximum at a distance of $50d_b$. The AASHTO Standard Specification reads as follows:

> *9.20.2.4 For a pretensioned member in which the section at a distance h/2 from the face of support is closer to the end of the member than the transfer length of the prestressing tendons, the reduced prestress shall be considered when computing V_{cw}. The prestress force may be assumed to vary linearly from zero at the end of the tendon to a maximum at a distance from the end of the tendon equal to the transfer length, assumed to be 50 diameters for strand and 100 diameter for single wire.*

The AASHTO LRFD Specification provides guidance for the transfer length of prestressing strand in Section 5.8.2.3. Its requirements read similar to the other two codes except the prestress force transfer takes place linearly over $60d_b$, in lieu of $50d_b$.

2.2.1.2 Buckner Equation

The basic Buckner equation for transfer length came from a best fit linear regression analysis of more current experimental data. The basic Buckner equation for transfer length is shown below.

$$l_t = \frac{1250 \cdot f_{si} d_b}{E_c} \tag{2.2}$$

where: f_{si} = Initial stress in prestressing steel, immediately after release (ksi)
d_b = Diameter of the prestressing steel
E_c = Modulus of Elasticity of the concrete (ksi)

For normal weight concrete and a concrete compressive strength at release of 3,500 psi (24.1 MPa) or greater, the proposed Buckner equation becomes the following equation.

$$l_t = \frac{f_{si} d_b}{3} \tag{2.3}$$

This equation is nearly identical to the ACI 318 equation discussed above. The only difference in the two equations is that f_{si} is used in lieu of f_{se}. The substitution of f_{si} for f_{se} will result in an increase of transfer length. The value of f_{si} in this report will use the initial jacking stress reduced by the short term losses from elastic shortening and from strand relaxation immediately after release.

2.2.1.3 Lane Equation

The initial basis of the proposed Lane equation for transfer length came from a best fit linear regression analysis of Federal Highway Administration (FHWA) experimental data. The initial equation was shown as the following equation.

$$l_t = \left(\frac{3.92 f_{pt} d_b}{f'_c} \right) - 20.67 \tag{2.4}$$

where: f_{pt} = Initial stress in prestressing steel prior to transfer (ksi)
d_b = Diameter of the prestressing steel (inches)
f'_c = Concrete compressive strength at 28 days (ksi)

Since this initial equation was a best fit or mean value, it was modified to provide conservative transfer lengths. In addition, the coefficients were rounded off. The final proposed Lane equation for transfer length that will be evaluated in this report is shown below.

$$l_t = \left(\frac{4 f_{pt} d_b}{f'_c} \right) - 5 \tag{2.5}$$

Since only limited higher strength concrete data was considered, f'_c should be limited to 10 ksi or less.

2.2.2 Development Length

2.2.2.1 Current Code Requirement

ACI 318 provides guidance for the development length of bonded 7-wire prestressing strand in Section 12.9.1. This section states that the development length should be determined by the following equation.

$$l_d = \left[f_{ps} - \left(\frac{2 f_{se}}{3} \right) \right] d_b \tag{2.6}$$

where: f_{ps} = The stress in the prestress strand at nominal strength (ksi)
f_{se} = The effective stress in the prestress strand after all losses (ksi)
d_b = The diameter of the strand (in)

The commentary Section R.12.9 states that this development length equation can be rewritten as the following equation.

$$l_d = \frac{f_{se} d_b}{3} + (f_{ps} - f_{se}) d_b \qquad (2.7)$$

Inspection of this rewritten equation shows that the first term represents the transfer length of the strand and the second term represents the flexural bond length of strand. The form of the equation is consistent with the earlier discussion on development length.

ACI Section 12.9.3 provides guidance for the development length of debonded 7-wire strand. This section states that the development length of debonded strand in members design for tension in the precompressed tensile zone under service load should be twice the development length, as provided in Section 12.9.1, for fully bonded strand.

AASHTO Standard Specification and AASHTO LRFD Specification provide guidance for the development length of bonded prestressing strand in Section 9.28.1 and Section 5.11.4.1, respectively. Both of these codes use equations that are identical to ACI 318 to determine the development length of bonded prestressing strand. The AASHTO Standard Specification reads as follows:

> *9.28.1 Three- or seven-wire pretensioning strand shall be bonded beyond the critical section for a development length in inches not less than*
>
> $$(f_{su}^* - \frac{2}{3} f_{se}) D$$
>
> *where D is the nominal diameter in inches, f_{su}^* and f_{se} are in kips per square inch, and the parenthetical expression is considered to be without units.*

where f_{su}^* is equal to f_{ps} throughout this report.

AASHTO Standard Specification and AASHTO LRFD Specification provide guidance for the development length of unbonded prestressing strand in Section 9.28.3 and Section 5.11.4.2, respectively. Both of these codes have requirements for the development length of unbonded prestressing strand that are identical to ACI 318, where the unbonded strand development length should be twice that of the bond strand. The AASHTO Standard Specification reads as follows:

> *9.28.3 Where strand is debonded at the end of a member and tension at service load is allowed in the precompressed tensile zone, the development length required above shall be doubled.*

2.2.2.2 The Buckner Equation

The development length equation that is recommended by Dr. Buckner is as follows.

$$l_d = \frac{f_{si} d_b}{3} + \lambda\left(f_{ps} - f_{se}\right)d_b \qquad (2.8)$$

The form of Buckner's equation is similar to the current equation in ACI 318, Section R.12.9. However, f_{se} in the first term of the equation is replaced by f_{si}, as in Buckner's transfer length equation. In addition, the constant flexural bond length portion of the ACI equation is modified into a variable flexural bond length by the multiplier λ.

where: $\lambda = (0.6 + 40\varepsilon_{ps})$

ε_{ps} = Strain in prestressing strand corresponding to f_{ps}

f_{ps} = Stress in prestressing strand at nominal strength

Since many applications approximate f_{ps} using ACI 318, Equation (18-3), λ can also be approximate as the following equation.

$$\lambda = 0.72 + 0.102\frac{\beta_1}{\omega_p} \qquad (2.9)$$

where: β_1 = Ratio of depth of equivalent rectangular stress block to the depth of the neutral axis

ω_p = Reinforcement index, $\rho_p f_{ps}/f'_c$

ρ_p = Prestress reinforcement ratio, A_{ps}/bd

Regardless of which equation is used to determine the value of the multiplier λ, the following restriction applies.

$$1.0 \le \lambda \le 2.0$$

2.2.2.3 The Lane Equation

The initial basis of the proposed Lane equation for the flexural bond portion of the development length also came from a best-fit linear regression analysis of FHWA experimental data. The initial equation for flexural bond length was shown as the following equation.

$$l_{fb} = \left[\frac{6.4\left(f_{ps} - f_{se}\right)}{f'_c}\right] + 26 \qquad (2.10)$$

Since this initial equation was a best fit or mean value, it was modified to provide conservative flexural bond lengths, and it was combine with the discussed transfer length equation to yield the following proposed development length equation.

$$l_d = \left[\left(\frac{4f_{pt}d_b}{f'_c}\right) - 5\right] + \left[\frac{6.4\left(f_{ps} - f_{se}\right)}{f'_c} + 15\right] \qquad (2.11)$$

Again, the general form of the equation is consistent with earlier discussions in that the development length is the sum of the transfer length and the flexural bond length.

2.3 Project Overview

The research conducted at Texas Tech University (TTU) and the results reported herein are an integral part of a larger, joint project conducted with The University of Texas at Austin (UT) that was designed to provide additional test data for consideration toward lifting the FHWA moratorium on the use of 0.6-inch (15-mm) diameter prestressing strand with prestressed, precast concrete I-beams. The joint project was designed using standard AASHTO Type I (Texas Type A) I-beams with cast-in-place concrete deck slabs to provide additional full-scale test data on the transfer and development lengths of 0.6-inch (15-mm) diameter prestressing strand. Close coordination and open communication was maintained between the research staff at TTU and UT throughout the project to standardize test procedures and analysis techniques in an effort to minimize any impact on test data and project results that might occur due to testing at the two separate laboratory facilities.

A total of 36 beams were fabricated and tested during this project, all of which were fabricated by the Texas Concrete Company at their plant in Victoria, Texas. The beams were cast in like pairs, with variations, between the pairs, in concrete strength, strand surface condition, and percentage of bonded/debonded strand used. Table 2.1 provides the test matrix and material target values used in this project as well as who was responsible for each test. Each end of each beam was tested separately resulting in the 4 tests per pair of beams shown in Table 2.1. It should be noted that each end of each beam was tested separately for both transfer length and development length. As can be seen in Table 2.1, 6 of the 36 beams, three pairs, were the responsibility of TTU resulting in 12 tests for transfer length and 12 more tests on the same beams for development length.

A four character, alpha/numeric identification code was developed to track and identify the 36 test beams that were cast during the course of this project. The first character of the code was used to identify the target strength of the beam concrete. With reference to the target concrete strengths in Table 2.1, "L" indicates the lowest strength range, "M" indicates the middle strength range, and "H" indicates the highest strength range. The second character of the code was used to identify the number of strands in the section that were debonded and thus were an indicator of the percentage of strands in the section that were debonded. "0" indicates fully bonded, "4" indicates 50% debonded, "6" indicates 60% debonded and "9" indicates 75% debonded. The third character of the

code was used to identify the strand surface condition. Out of the two possible surface conditions used in this project, "R" indicates "rusty" and "B" indicates "bright". The forth character of the code was used to differentiate between the two specimens which were cast in pairs having all other parameters identical. The forth character was either a "0" or a "1". It should be noted that any specimen which had a "1" as its forth character in its code had hairpin H-bars in the lower flange of the beam on one end of the beam. As an example, the specimen that was labeled with the code L0R0 was made with concrete in the lowest strength range, was made with only fully bonded strand, was made using strand with the rusty surface condition, and was the first specimen and did not contain the H-bar. As another example, the specimen that was labeled with the code H4B1 was made with concrete in the highest strength range, was made with 50% of its strand debonded, was made using strand with the bright surface condition, and was the second specimen contained H-bars in one end of the beam.

Table 2.1 Test Matrix and Material Target Values

Concrete Strength, psi	Steel Strand							
	Bright				Rusty			
	Fully Bonded	Debonded			Fully Bonded	Debonded		
		50%	60%	75%		50%	60%	75%
5,000–7,000	4 / UT	4 / UT	4 / UT	---	4 / TTU	4 / TTU	4 / TTU	---
9,500–11,500	4 / UT	4 / UT	---	4 / UT	4 / UT	4 / UT	---	4 / UT
13,000–15,000	4 / UT	4 / UT	---	4 / UT	4 / UT	4 / UT	---	4 / UT

1.0 psi = 6.89×10^{-3} MPa

CHAPTER III

FABRICATION AND TESTING

3.1 Introduction

This joint research project between TTU and UT entailed the fabrication and testing of 36 standard AASHTO Type I prestressed concrete I-beams, all of which were cast by the Texas Concrete Company at their plant in Victoria, Texas. Six of the beams were tested by TTU and 30 of the beams were tested by UT. As an overview, the project can be broken into two basic phases. The first phase was conducted at the precasting yard in Victoria, Texas, and addressed the transfer length of the 0.6-inch (15-mm) diameter prestressing strand. In this phase, mechanical strain gauge points (Demec points) were mounted on the lower flange of the concrete beam once the forms were removed but before the pretensioned strands were released. The Demec points were mounted at the level of the centroid of the bottom row(s) of steel strands on each side of the beam and on each end of beam. Linear measurements were taken, using a Demec mechanical strain gauge device, to determine the distance between the Demec points mounted on the lower flanges of the concrete beams. These measurements were taken before and after the release of the pretensioned strands so that a concrete compression strain profile along the length of the ends of the beams could be determined thus allowing the determination of the transfer lengths.

The second phase of the project addressed the development length of the 0.6-inch (15-mm) diameter prestressing strand. These tests were conducted either at the Ferguson Structural Engineering Laboratory at UT or at the Civil Engineering Structural Laboratory at TTU. In this phase, the precast I-beams were shipped to one of the two laboratories where concrete deck slabs were cast in place, providing composite action between the beams and the slabs. Once the concrete slabs reached sufficient strength, the composite beam sections were loaded in flexure until failure occurred. Failure was defined either as slippage of the strand in the concrete so that no additional transverse load could be carried or as the theoretical ultimate moment capacity of the section being reach where the compression strain in the concrete exceeded 0.003 and/or the total tensile strain in the prestressing strand exceeded 3.5%. Strain in the prestressing strand was estimated by strain compatibility using a measured value of compression strain in the top fiber of the concrete slab and the location of the neutral axis in the concrete section that was estimated by concrete crack development. The location of the transverse load, with respect to the end of the beam, was incrementally shortened trying to change the failure mode from a flexural mode to a bond slip mode, thus bracketing the development length of the prestressing strand.

The general information discussed below about beam fabrication and test procedures is applicable to both TTU's and UT's portion of this project. However, the remainder of this report will be limited to specific data as applicable to TTU's portion of

this project. UT's portion of the testing and associated data will be reported in a separate report.

3.2 Beam Fabrication and Transfer Length Measurements

All of the test specimens in TTU's portion of the project were fabricated using a beam concrete strength in the 5,000 to 7,000 psi (34.5-48.2 MPa) range and prestressing strand with a rusty surface condition. With these conditions, 3 pairs of beams were fabricated with varying levels of bonded/debonded strand: fully bonded, 50% debonded, and 60% debonded. The specific identification codes assigned to the six beams in this portion of the project were L0R0, L0R1, L4R0, L4R1, L6R0, and L6R1. Specific details as to the number and location of strands, levels of initial prestress, and lengths of debonding are provided for these three cases in Figure 3.1, Figure 3.2, and Figure 3.3. Additional details for the placement, shape, and size of the conventional shear and confinement reinforcing steel bars and the lengths of the beams are provided in Appendix A. All of the beams were cast using high early strength concrete to facilitate early removal of forms following casting of concrete sections. In addition, all the prestressing steel used in this project was a 0.6-inch (15-mm) diameter, seven-wire, low relaxation strand with a specified ultimate tensile strength of 270 ksi (1,860.3 MPa) and a nominal cross-sectional area 0.217 in^2 (140-mm^2).

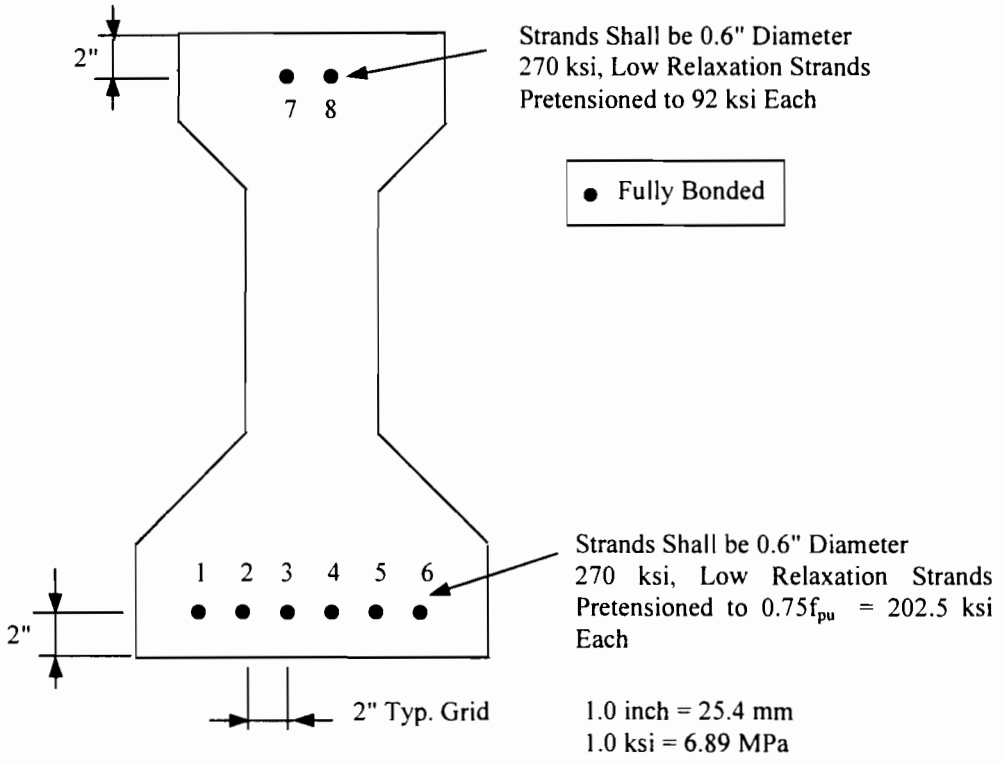

Figure 3.1 Beam Cross-Section of L0RX Series

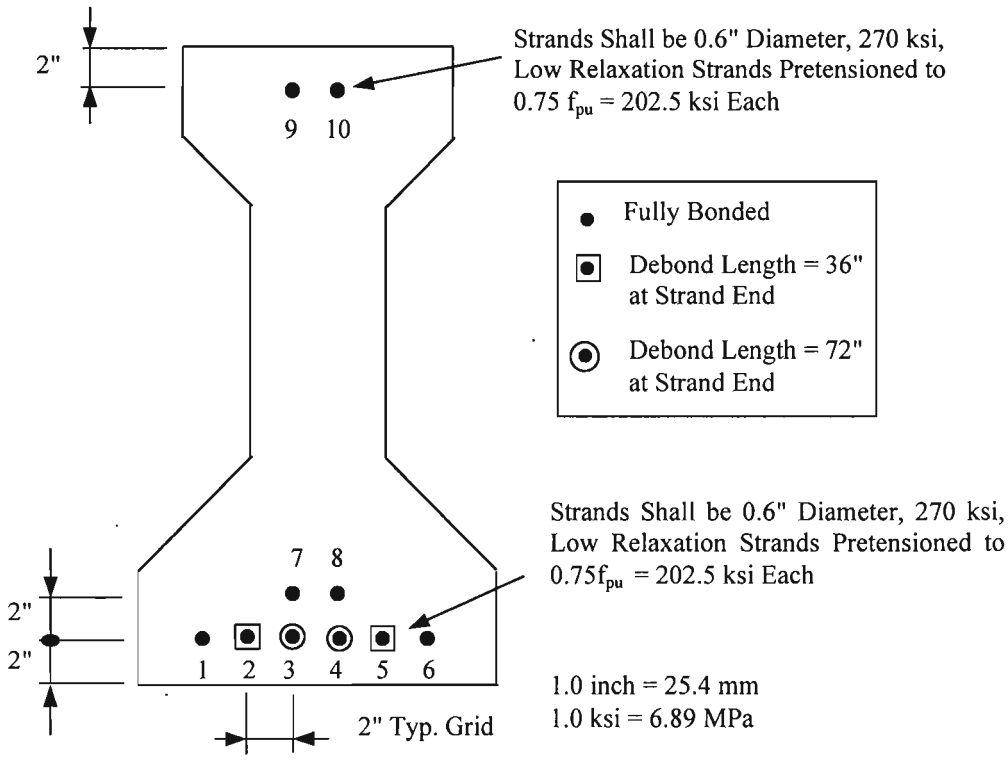

Figure 3.2 Beam Cross-Section of L4RX Series

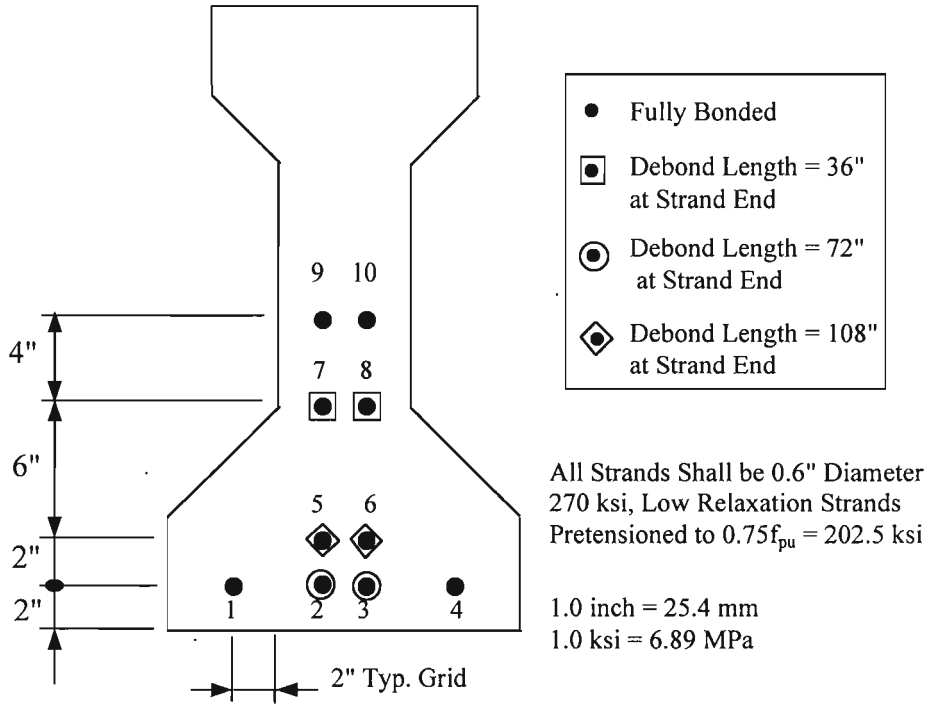

Figure 3.3 Beam Cross-Section of L6RX Series

All of the beams and strand patterns tested in this project were designed by personnel at UT-Austin. Several key issues were considered during the development of the test specimens and strand patterns. First, a full bottom row of strands was used, whenever possible, at a 2-inch (50-mm) grid spacing. This condition would provided a worst case scenario for a weakened horizontal plane in the concrete where a failure could occur. This condition was not always possible without violating one of the other following conditions as in the L6RX series. Second, the sections were proportioned so that the total strain in the bottom row of prestressing strand would equal or exceed 3.5%, the guaranteed minimum fracture strain of the strand. This second condition would fully test the strand for potential bond-slip failure. Third, the sections were proportioned to maintain the levels of stress in the concrete, at release, within the code allowable stress limits. Fourth, the three sections were designed to investigate the effect that debonding some of the prestressing strand would have on the transfer and development lengths of the strand. One section used only fully bonded strands while the two remaining sections used two different percentages of bonded and debonded strands. Fifth, in the L6RX series, debonded strands were placed in the web of the beam to address concerns about web shear cracking occurring where debonded strands were located in the web. Sixth, the lowest outside pair of strands, one on each side of the flange, was always fully bonded.

The split sheathing method of debonding was used in this project to prevent a bond from developing between the concrete and the prestressing strand where specified. A picture of this technique is shown in Figure 3.4. Split sheathing is one of the most commonly used methods. It is very easy to use and install and simply requires slipping the split plastic sheathing over the strand where debonding is desired. The primary disadvantage of this method is that taping of the sheathing joints and ends is required after its installation onto the strand. If it is not taped correctly, concrete can bleed into the sheathing during placement and consolidation, creating unwanted bonding.

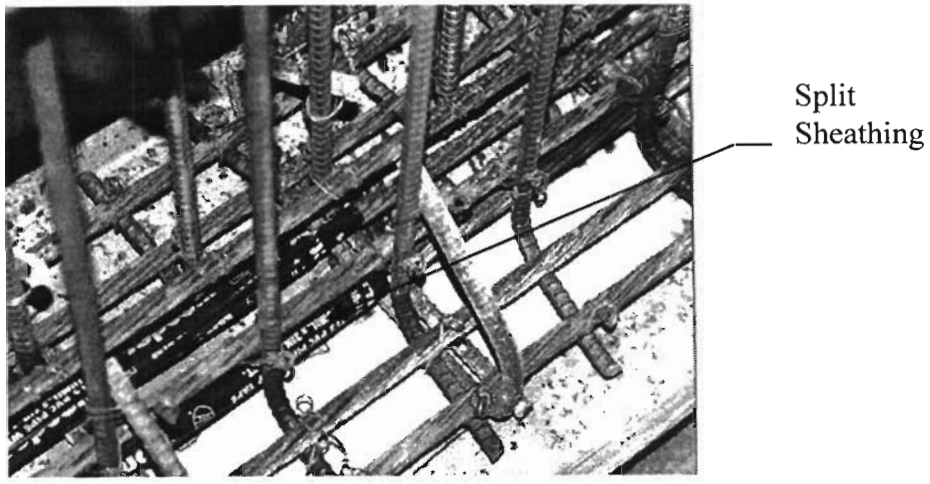

Figure 3.4 Debonded Strands Using Split Sheathing

Each pair of beams in the project having identical concrete strength, strand surface condition, and level of bonded/debonded strand were cast at the same time using the configuration shown in Figure 3.5. The fabrication process included the placement of the prestressing strand in the proper configuration in the steel abutments, the placement of the conventional reinforcing steel in each beam, the placement and securing of the steel forms to the steel casting bed, and the pretensioning of the steel strands to the specified level of initial prestress. To prevent the possibility of damaging the bond characteristics of the strand which would significantly impact the results of this project, form oil was not used.

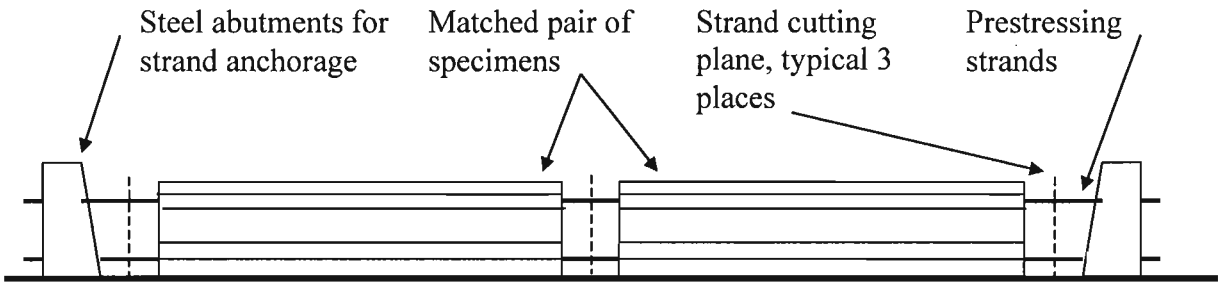

Figure 3.5 Pretensioning / Casting Bay

The concrete was mixed in a batch plant on-site and placed directly into the beam forms as shown in Figure 3.6. The concrete was then consolidated using internal vibrators. The top surface of each beam was left rough to add to the transfer of horizontal shear forces to insure composite action between each beam and its cast-in-place deck slab that would be added during the second phase of testing. During the casting process, standard 6-inch (152-mm) diameter by 12-inch (305-mm) long concrete test cylinders were made for use to determine beam concrete strength prior to prestress release and prior to flexural testing in the laboratory. After casting, the beams and test cylinders were covered with a thick blanket and steam cured for 24 hours. After 24 hours, the blankets and metal forms were removed from the beams and preparations were made for the installation of the Demec points onto the lower flanges of the beams in their end regions.

Prior to the release of the prestress force, the Demec points were epoxied to each side of the lower beam flange on both ends of the beams at the height of the centroid of the prestressing strands in the bottom flange. The mounting heights of the Demec points are provided in Table 3.1. They were placed on an approximate 2-inch (50-mm) center-to-center spacing over a distance greater than the estimated transfer length. The actual distance over which Demec points were placed varied between companion pairs of beams for each test series. These distances are provided in Table 3.1. Once the Demec points were installed and prior to release of the prestressing force, measurements were taken using a Demec mechanical strain gauge device to determine the actual distance between the Demec points, shown in Figure 3.7. These measurements were taken twice along each series of Demec points resulting in two sets of measurements, along any one side of

any flange, that were checked for repeatability. If a significant variation in any of the two sets of measurements was observed, addition measurements were taken until the discrepancy was resolved. This general process was used every time Demec point measurements were taken.

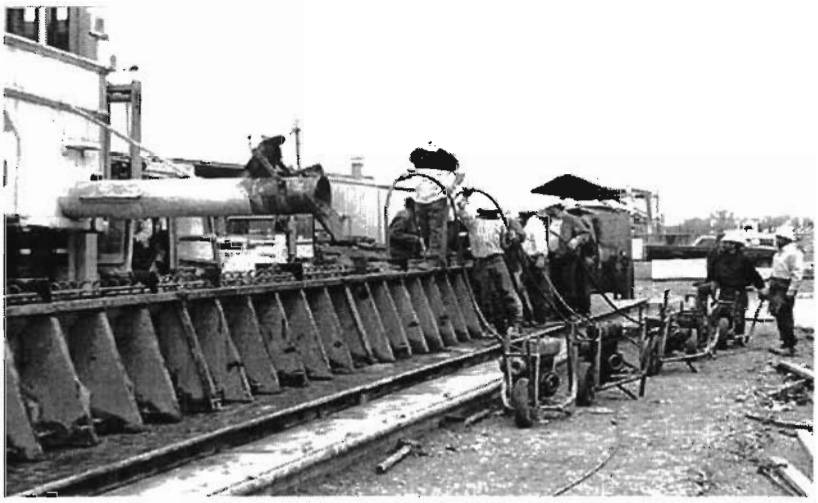

Figure 3.6 Beam Formwork and Concrete Placement

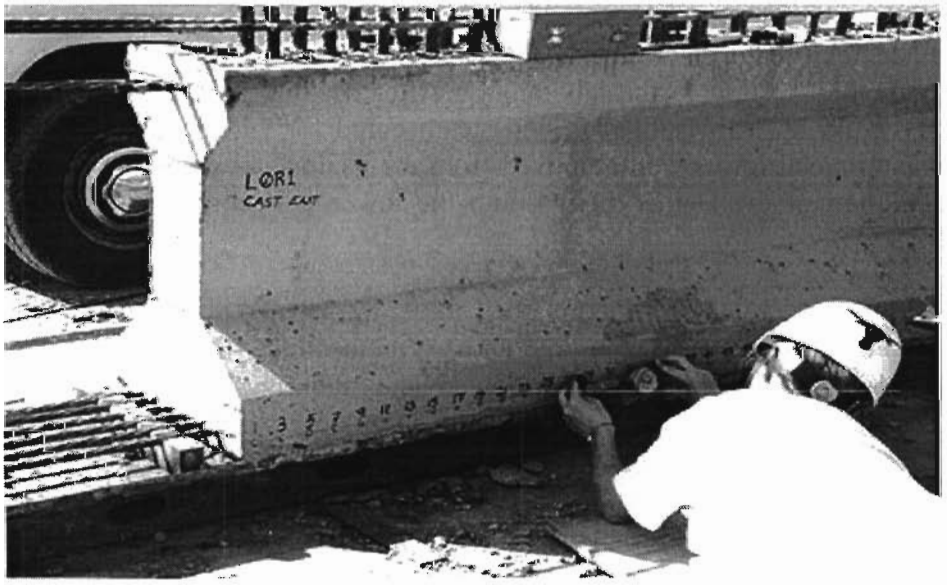

Figure 3.7 Demec Point Measurements

Table 3.1 Length of Mounted Demec Points

Beam Series	Maximum Debonded Length (inches)	Length of Mounted Demec Points (inches)	Demec Points Mounting Height* (inches)
L0RX	0	66	2.00
L4RX	72	137	2.50
L6RX	108	172	2.67

* From bottom of the beam 1.0 inch = 25.4 mm

Concrete test cylinders were also broken prior to the release of the prestressing force to verify adequate concrete strength at release, f'_{ci}. These values are provided in Table 3.2 along with other concrete beam and slab material properties. Release of the prestressing force was accomplished by simultaneous flame cutting of a single strand at the 3 cutting planes shown in Figure 3.5. After release, Demec point measurements were repeated using the general procedure described above. By knowing the distance between any pair of Demec points prior to and after release, the compressive strain between the points caused by the release of the prestress force can be determine. Concrete compression strain profiles along each end of each beam were developed and were used to evaluate the transfer length of strand in each beam. The strain data and profiles are provided in Appendix B and are discussed in Chapter IV of this report. The beams and remaining test cylinders were then moved and stored in the precasting yard in Victoria, Texas, until they were shipped to TTU for additional testing and determination of development length. Additional Demec point measures were taken 4 to 6 weeks after release but prior to shipping to investigate long term effects on transfer lengths. Concrete compression strain profiles were also developed from the delayed Demec point measurements. This strain data and its corresponding strain profiles are also provided in Appendix B and discussed in Chapter 4.

3.3 Deck Slab Fabrication and Composite Beam Set-up

Each of the three like pairs of precast I-beams were then shipped in pairs to the Civil Engineering Structural Laboratory at Texas Tech University for further fabrication and testing. Once each I-beam was positioned on the structural test deck in the laboratory, a 6.5-inch (165-mm) thick by 60-inch (1,524-mm) wide reinforced concrete deck slab was cast-in-place to provide composite action with the I-beam. The deck slab details were selected to model an in-place bridge deck and to provide a compression flange adequate to fully develop the prestressing strands and strain them to a total strain greater than 3.5%, well beyond their yield strain. Specific details of the slabs are shown in Figure 3.8. The concrete deck slabs were cast using prefabricated, reusable forms with adjustable shores as shown in Figure 3.9. High early strength concrete with a target strength value in the 5,000 to 7,000 psi (34.5-48.2 MPa) range was provided by a local batch plant. Standard 6 by 12-inch (152 by 305-mm) concrete test cylinders were cast and match cured with the deck slab. Actual concrete strength and modulus of elasticity values were determined for each I-beam and deck slab at the time of flexural testing.

These values are reported in Table 3.2. Concrete deck slab test cylinders were also used to insure adequate slab strength prior to form and shore removal. This was required to prevent longitudinal cracking of the deck slab at the cantilevered overhang on each side of the I-beam.

Table 3.2 Concrete Material Properties

Beam Series	Precast Beam			Deck Slab	
	f'_{ci} (psi)	f'_c (psi)	E_c (10^6 psi)	f'_c (psi)	E_c (10^6 psi)
L0R0-1	4,540	5,440	4.20	6,500	4.42
L0R0-2	4,540	5,440	4.20	6,500	4.42
L0R1-3	4,540	5,440	4.20	6,120	4.32
L0R1-4	4,540	5,440	4.20	6,120	4.35
L4R0-1	3,790	5,050	3.80	5,835	4.29
L4R0-2	3,790	5,050	3.80	5,700	4.29
L4R1-3	3,790	5,050	3.80	6,070	4.31
L4R1-4	3,790	5,050	3.80	5,700	4.32
L6R0-1	4,630	7,480	5.45	6,850	4.69
L6R0-2	4,630	7,480	5.45	5,360	4.12
L6R1-3	4,630	7,480	5.45	6,360	4.48
L6R1-4	4,630	7,480	5.45	6,360	4.48

1.0 psi = 6.89 x 10^{-3} MPa

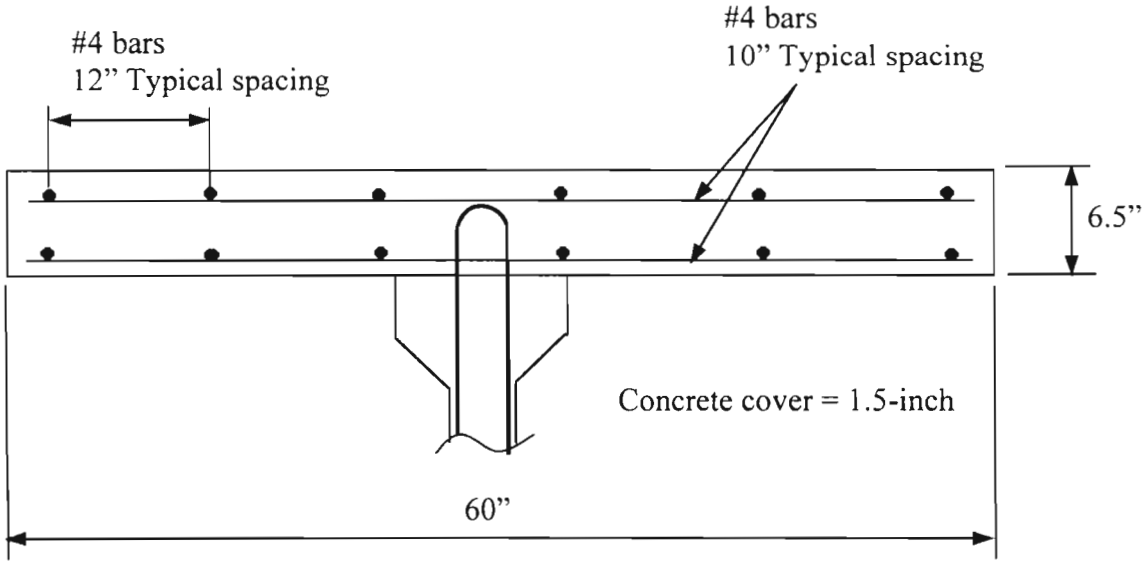

1.0 inch = 25.4 mm

Figure 3.8 Concrete Deck Slab Details

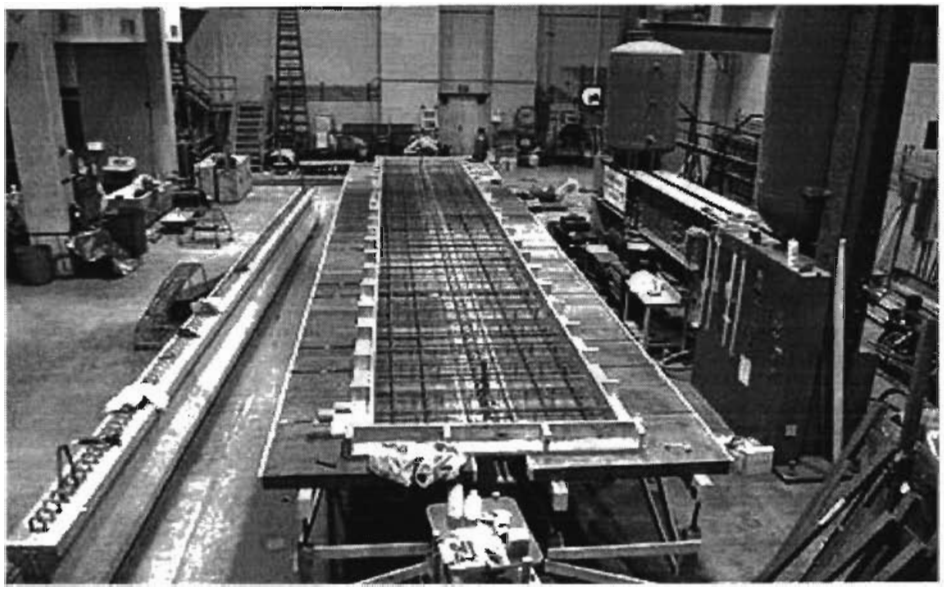

Figure 3.9 Fabrication of Deck Slab

Once the deck slab forms were removed, reinforced concrete beams supports were placed into their final position and 3-inch (76-mm) thick by 11-inch (279-mm) wide, steel reinforced, elastomeric bearing pads were placed between the beam supports and the beam. Load point bearing plates were then positioned and installed on top of the deck slab along with the rollers and load spreader beam, all shown in Figure 3.10. The steel load frame, shown in Figure 3.11, was then set into position and bolted down to the structural test deck. Final positioning of the hydraulic ram along the load frame upper cross-beam was completed to provided a constant moment region in the I-beam and slab.

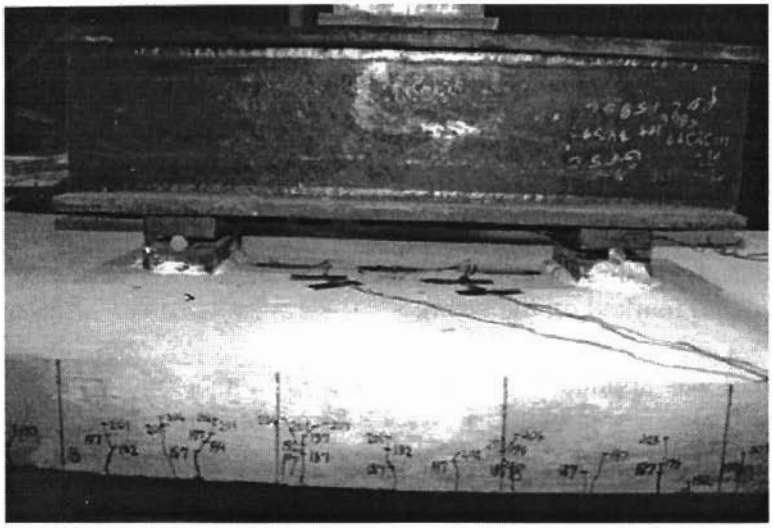

Figure 3.10 Load Bearing Plates, Rollers, and Spreader Beam

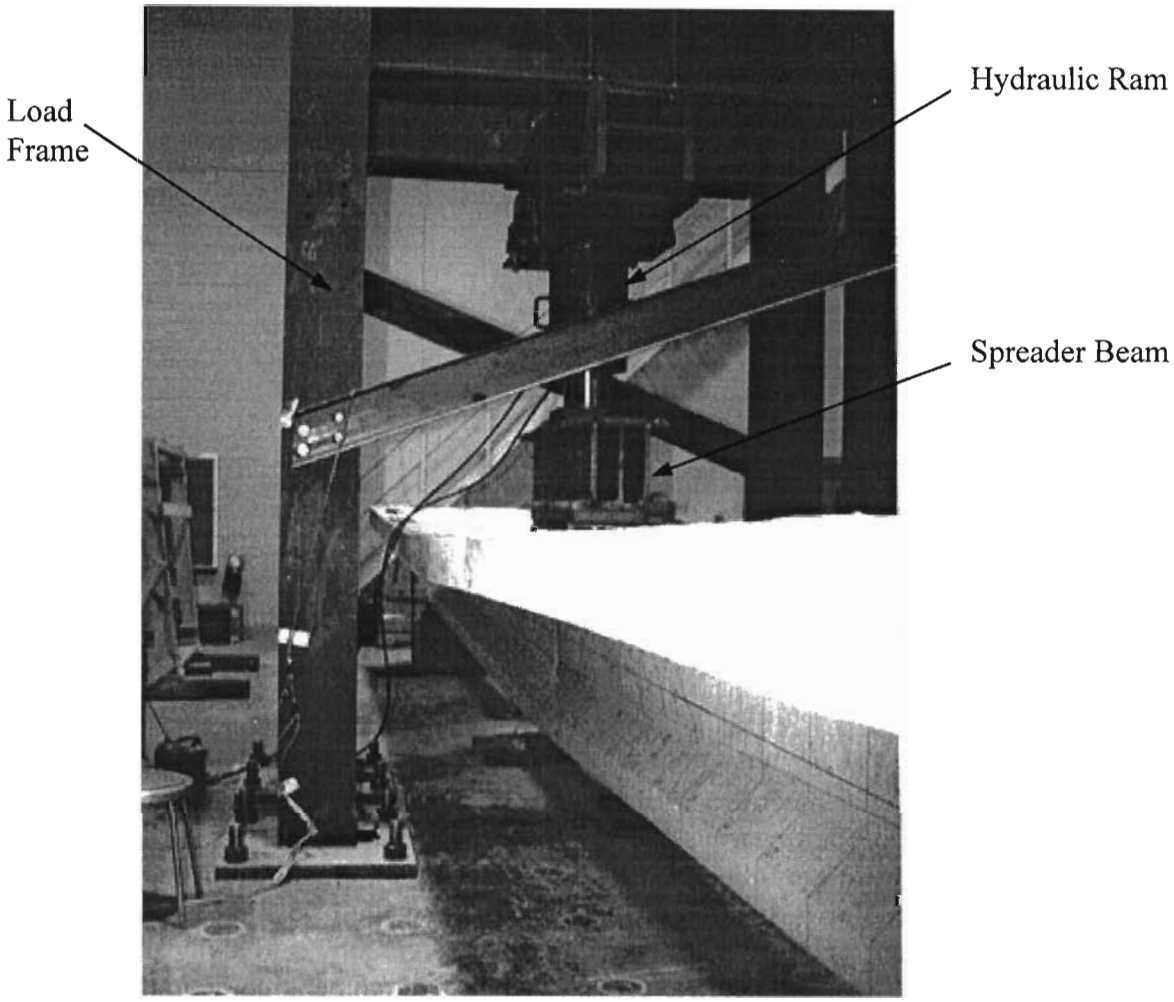

Figure 3.11 Load Frame

3.4 Instrumentation and Test Measurements

Prior to loading, instrumentation was installed for collection of test data. Test data included applied load, beam deflection at the load center point, concrete strain in the top fiber of the deck slab in the constant moment region, and prestressing strand end-slip. Crack development and propagation as a function of the applied load was also monitored and marked on the beam.

The load was applied to the beam by a 400 ton (3,560 N), hydraulic ram with an effective ram piston area of 113 in^2 (72,908-mm^2). The hydraulic pressure that was applied to the ram by a pneumatic actuated hydraulic pump was monitored by a pressure transducer connected to a wheatstone bridge that had a digital readout. By multiplying the pressure and the effective ram piston area, the applied load was obtained. A pressure gage was also used as a secondary source of pressure

monitoring for safety purposes. The applied load was determined and recorded at all stages of each test. The amount of load applied with each increment varied with changes in beam deflections. Changes in beam deflection were limited to approximately ½-inch (12-mm) in the middle stages of loading and to approximately 1-inch (25-mm) in the latter stages of loading.

Beam deflections at the applied load center point were determined by two separate methods. One method used three dial gages at strategic locations along the length of the beam. One dial gage was placed under the beam at the center of the load, and the other two were placed under the top slab at the center line of each beam support to account for elastomeric bearing pad deformations. By subtracting the average of the two end support deformations from the center of load deflection, the true center of load deflection was obtained. The other method used a thin wire stretched between two bolts attached to the web of the beam, one at the centerline of each support. In addition, a metal scale graduated to 0.01-inch (0.25-mm) was mounted to the web of the beam at the center of load, along with a mirror. As the beam deflected, the scale moved with the beam while the wire remained straight and only moved due to support deformation. By taking the difference between two readings, the deflection was determined. The mirror was used to insure a consistent horizontal line of sight while reading the scale. Deflections were determined for each applied load increment. Load-deflection curves were developed from the data of each beam test, and they are provided in Appendix C and are discussed in Chapter 4.

Strain in top fiber of the concrete deck was monitored in the constant moment region of the beam between the two load points. Concrete strains were monitored by two methods. The primary method used three electrical resistance strain gages mounted directly above the longitudinal centerline of the beam and spaced along the constant moment region of the beam as can be seen in Figure 3.10. A secondary method was used incase the bond between the electrical resistance strain gages and the concrete surface failed rendering the electrical strain gages ineffective. A pair of Demec gage points were epoxied to the top surface of the concrete deck slab near the center of the load with an approximate 2-inch (50-mm) gage length. Linear distance measurements were taken between the two Demec points prior to and during testing and were used to calculate the strain in the top fiber of the concrete deck slab.

As the composite beam and deck slab approached its ultimate moment, vertical cracks in the constant moment region of the test specimen moved up into the deck slab as can be seen in Figure 3.10. The distance from the top fiber of the deck slab to the top of the vertical cracks was determined and used as an approximate depth to the neutral axis. Knowing the distance from the top of the concrete slab to the neutral axis and to the bottom row of prestressing strand and knowing the strain in the top fiber of the concrete slab, strain compatibility was used to determine the increase in steel strain in the bottom row of prestressing strand caused by flexure. This increase in strain was then added to the prestress strain to determine the total strain in the prestressing strand. The initial prestress strain was calculated by dividing

the effective prestress by the modulus of elasticity. Knowing the initial prestress applied to prestressing strands, the effective prestress was calculated by deducting the prestress losses from the initial prestress value. These prestress losses are elastic shortening, creep and shrinkage of the concrete, and relaxation of the steel, and they were calculated by the procedure described in PCI Design Handbook (1985). Loading of each specimen was continued until the total strain in the strand exceeded 3.5% unless a bond slip failure mode occurred.

End slip or movement of the prestressing strand with respect to the end of the concrete beam was also monitored at each load increment during flexural testing. Small U-shaped metal brackets were attached to each strand approximately 1.5-inch (38-mm) from the end of the beam as shown in Figure 3.12. Measurements from the outside leg of the metal U-shaped bracket and the end of the concrete beam were taken using a digital caliper at each load test increment to monitor end slip of the strand. A small hole was drilled in each upstanding leg of the U-shaped bracket to assure consistent alignment of the caliper on the sequential measurements. In addition, small square pieces of glass were epoxied to the end of the concrete beam directly above each prestressing strand to provide a smooth, consistent surface to seat the far end of the caliper against. A load-end slip curve was developed for each flexural test, and they are provided in Appendix D and are discussed in Chapter 4.

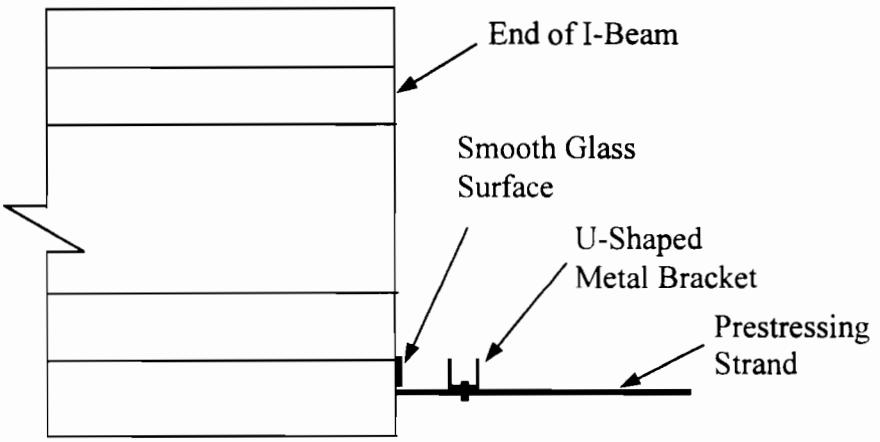

Figure 3.12 Strand End-slip Brackets

3.5 Development Length Tests

The determination of the development length for any given set of parameters requires not a single test but a series of tests. The failure mode of each separate test will either be a flexural, hybrid, or bond slip mode. If the first test fails in a flexural mode, the embedment length of the prestressing strand is greater than the true development length of the strand for the given parameters. If this case occurs, the embedment length of the prestressing strand should be reduced during the next test.

However, if the first test fails in a bond slip mode, the embedment length of the prestressing strand is less than the true development length of the strand for the given parameters. If this case occurs, the embedment length of the prestressing strand should be increased during the next test. From a series of tests, the development length of a prestressing strand for a given set of parameters can be bracketed as the failure mode changes from flexure to hybrid mode or vice-versa.

This procedure of incrementally changing the embedment length of the prestressing strand to determine its development length is the technique that was used during this project. A typical configuration of the test geometry used during this project is shown in Figure 3.13. The distance from the end of the member to the first load point defines the location of the critical section. This distance is equal to the sum of unbonded length and the embedment length of the prestressing strand using the largest unbonded length in the given section and is shown as $l_{ub}+l_e$. The beam span, l_s, was selected large enough to prevent a shear failure but small enough to prevent significant damage to the far end of the beam that would impact the results of the far end test. The dimension "a" controlled where the ram applied the load to the spreader beam. It was selected to provide a constant moment region between the two beam load points. The actual dimensions used during this project are provided in Table 3.3. The total length of the beam, l, was selected long enough so that two tests could be conducted on each beam. The typical load and support configuration used to conduct two tests on each beam is shown in Figure 3.14.

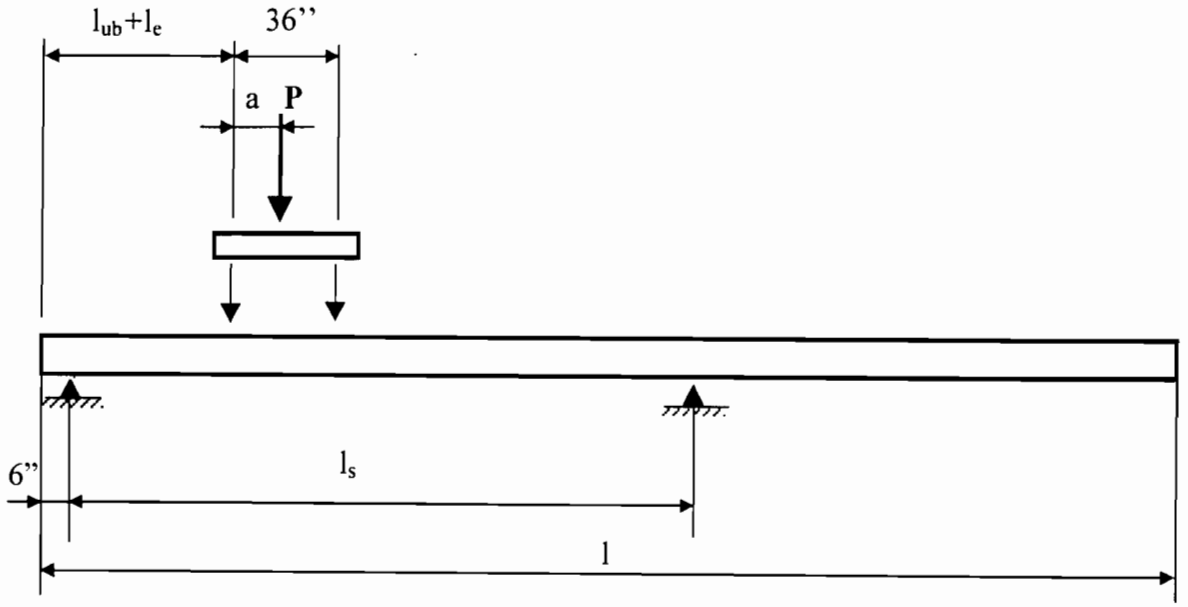

Figure 3.13 Test Geometry

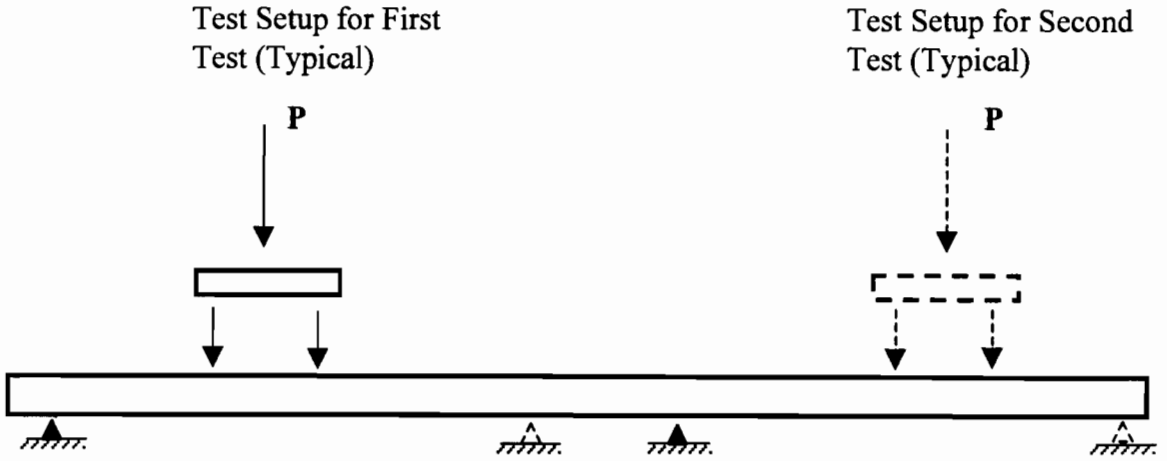

Figure 3.14 Support and Loading Arrangement

Table 3.3 Test Geometry

Beam Series	Beam Length l (in)	Test Span Length l_s (in)	Longest Debonded Length l_{ub} (in)	Embedment Length l_e (in)	$l_{ub} + l_e$ (in)	Ram Location a (in.)
L0R0-1	480	240	0	96	96	16.88
L0R0-2	480	228	0	72	72	12.32
L0R1-3	480	240	0	54	54	8.88
L0R1-4	480	240	0	54	54	8.88
L4R0-1	648	360	72	114	186	21.31
L4R0-2	648	360	72	60	132	14.81
L4R1-3	648	360	72	96	168	19.25
L4R1-4	648	360	72	96	168	19.25
L6R0-1	648	432	108	114	222	18.75
L6R0-2	648	432	108	97	205	18.75
L6R1-3	648	408	108	84	192	18.50
L6R1-4	648	408	108	84	192	18.50

1.0 inch = 25.4 mm

The initial embedment length for the first test in each of the three series, L0RX, L4RX, and L6RX, was chosen as slightly larger than the current AASHTO development length requirement for fully bonded strand. The embedment length for the second and third tests in each of the series was either shortened or lengthened depending on whether or not the previous test in the series had a flexural or bond slip failure mode. The last test of each series always tested the end of the beam that contained the extra hair-pin bars, H-bars, in the lower web, end region of the beam. The embedment length for the last test in each series was set equal to the shortest embedment length of that series in which a flexural failure mode occurred. This was done to determine whether the H-bar had any impact on the response of the beam. Again, all the specific dimensions for the test geometry used during TTU's portion of the project are provided in Table 3.3.

CHAPTER IV

TEST RESULTS

4.1 Transfer Length

Short-term and long-term transfer lengths were determined for each beam using the beam's concrete compression strain profile and the 95% Average Maximum Strain (AMS) Method described below. Short-term strain measurements were taken immediately after release, and long-term strain measurements were taken between 4 and 6 weeks after release but prior to beam shipment. Four sets of strain measurements were taken on each end of each beam and their values averaged to reduce error. The average concrete compression strain values are provided in Appendix B. To further reduce variations in the strain data, the data was smoothed by averaging the strain at a point over three points along the length of the beam. The following equation was used to smooth the strain data, and the effect of smoothing is shown in Figure 4.1.

$$\varepsilon_{i,smoothed} = \frac{\varepsilon_{i-1} + \varepsilon_i + \varepsilon_{i+1}}{3} \tag{4.1}$$

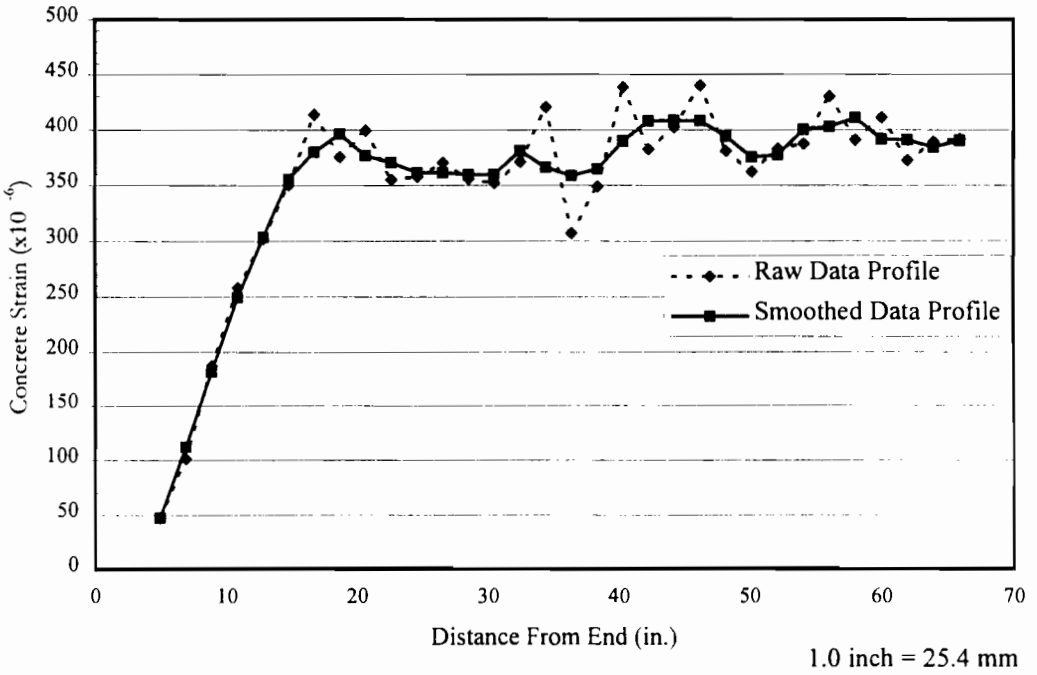

Figure 4.1 Effect of Smoothing on Strain Profiles.

Typical smoothed stain profiles for beams with fully bonded, 50% debonded, and 60% debonded strand are shown in Figures 4.2, 4.3, and 4.4, respectively. While only one transfer region exists at each end of the beam with only fully bonded strand, it should be noted that there are 3 and 4 transfer regions on each end of each beam containing 50% and 60% debonded strand, respectively. A transfer region exists at each location where debonding stops and bonding between the strand and the concrete starts.

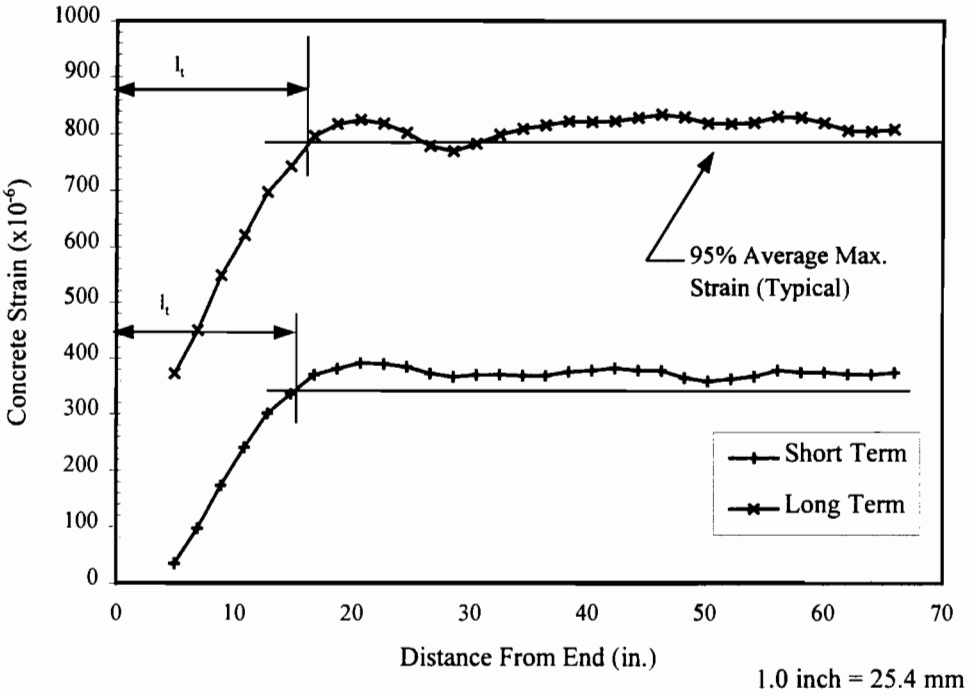

Figure 4.2 Typical Smoothed Strain Profile for Fully Bonded Strands

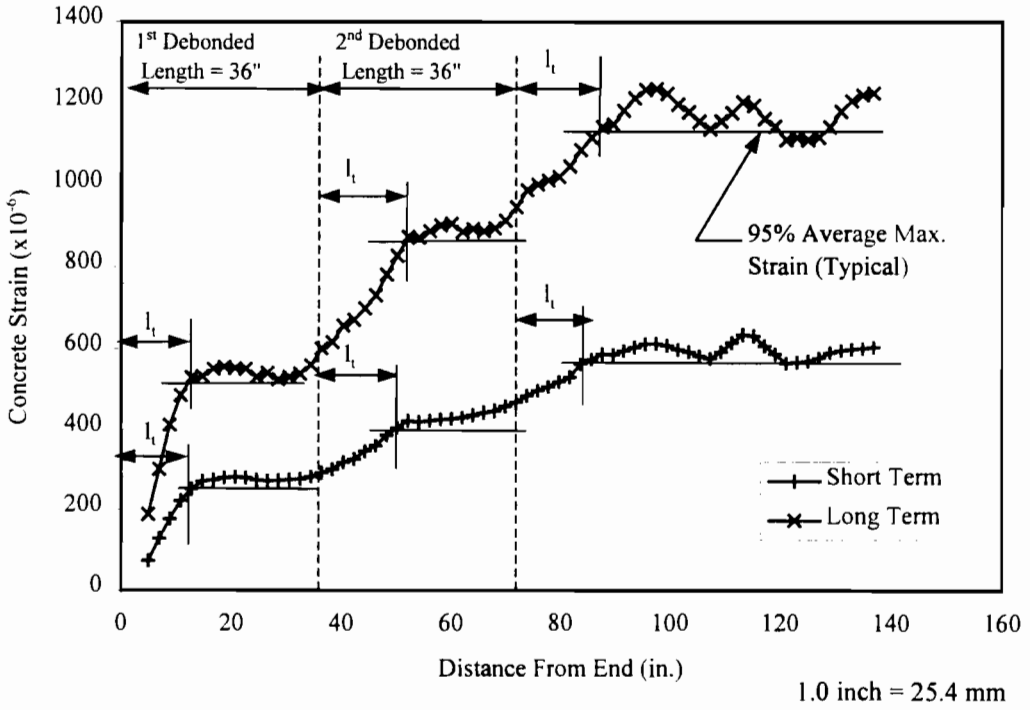

Figure 4.3 Typical Smoothed Strain Profile for 50% Debonded Strands

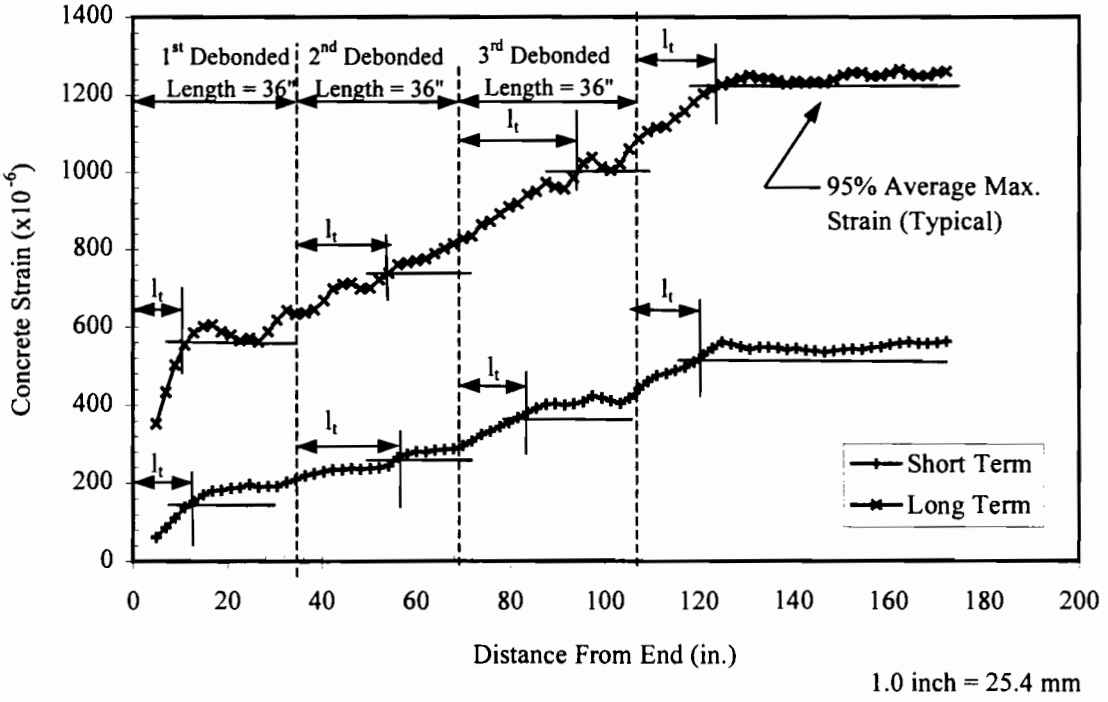

Figure 4.4 Typical Smoothed Strain Profile for 60% Debonded Strands

The 95% AMS method was applied to the smoothed concrete compression strain data to determine the transfer lengths in each transfer region of each beam in this project. The general procedure that was used in this project is described below.

1. The concrete strain values were corrected by deducting flexural tension strains caused by the dead weight of the beam.
2. The corrected values were smoothed as described above. These adjusted strain values were plotted along the length of the beam to produce concrete compressive strain profiles as shown in Figures 4.2, 4.3, and 4.4.
3. Strains values in each maximum strain plateau region were averaged to determine the 100% AMS for that plateau region.
4. The 95% AMS value was calculated and a horizontal line corresponding to this value was drawn on the smoothed strain profile.
5. The transfer length was defined as the distance from the location where bonding started for the strand to the location of the intersection of the strain profile and the 95% AMS line.
6. For the debonded strands, the 100% AMS values were calculated for each strain plateau region. The 95% AMS value was taken as 95% of the difference of the 100% AMS values between adjacent strain plateaus.

7. The above procedure was modified slightly for the determination of the long-term transfer lengths. Since long-term strain values were much higher than the short-term strain values, 95% of the AMS would be larger and would yield shorter transfer lengths. Therefore, 5% of the short-term AMS values were subtracted from the long-term 100% AMS values to get the long-term 95% AMS values.
8. Once the appropriate 95% AMS values were determine for the different cases described above, all the transfer lengths were determine as described in steps 4 and 5 above.

All of the concrete compressive strain profiles, with their corresponding 95% AMS values, for the beams tested in TTU's portion of this project are provided in Appendix B. The corresponding calculated values for the experimental short-term and long-term transfer lengths are provided in Tables 4.1 and 4.2, respectively. It should be noted that the strands in the L0RX beam series were fully bonded with only one transfer region. Also, 50% of the strands in the L4RX beam series were debonded providing three transfer regions, and 60% of the strands in the L6RX beam series were debonded providing four transfer regions.

The values of the short-term and long-term transfer lengths that were experimentally determined in this project are compared to three current code values (ACI 318, AASHTO Standard, and AASHTO LRFD) and to two proposed equations (Buckner and Lane), all of which were identified and discussed in Chapter 2. The comparison of the experimental transfer length values and the predicted transfer length values are provided in Figures 4.5 through 4.10. Transfer length values predicted by ACI 318 and AASHTO-Standard are $50d_b$ and by AASHTO-LRFD are $60d_b$. The transfer length values predicted by the Buckner equation and the Lane equation are provided in Table 4.3. The transfer length values in Tables 4.1, 4.2, and 4.3 were normalized by dividing by d_b, 0.6-inch (15-mm), for similarity with the current code requirements prior to their use in Figure 4.5 through Figure 4.10. The values required by the Buckner and Lane equations are also provided in Table 4.3. The losses from elastic shortening were predicted using the PCI (1985) method, and the losses from strand relaxation were predicted using the following equation from Nawy (1996).

$$\text{R.E.} = f_{pt}\,\frac{\log(t)}{45}\left[\left(\frac{f_{pt}}{f_{py}}\right) - 0.55\right] \qquad (4.2)$$

where: f_{pt} = Initial prestress prior to release (ksi)
t = Time from initial stressing (hours)
f_{py} = Prestressing steel yield (ksi)

The value of time, t, was taken as 48 hours for series L0RX and L4RX and as 72 hours for series L6RX. The value of the prestressing strand yield was taken as $0.90f_{pu}$ = 243 ksi.

Table 4.1 Short-Term Transfer Length

Beam End	Transfer Region				Beam End Average (in)
	First (in)	Second (in)	Third (in)	Fourth (in)	
L0R0 - 1	16.0	N/A	N/A	N/A	16.0
L0R0 - 2	18.0	N/A	N/A	N/A	18.0
L0R1 - 3	16.5	N/A	N/A	N/A	16.5
L0R1 - 4	15.5	N/A	N/A	N/A	15.5
Mean	16.5	N/A	N/A	N/A	16.5
L4R0 - 1	14.0	16.0	14.5	N/A	15.0
L4R0 - 2	15.0	16.5	27.5	N/A	20.0
L4R1 - 3	13.5	20.0	30.5	N/A	21.5
L4R1 - 4	17.0	*	*	N/A	17.0
Mean	15.0	17.5	24.0	N/A	18.5
L6R0 - 1	16.5	17.5	27.5	19.5	20.5
L6R0 - 2	19.5	24.0	21.5	16.0	20.5
L6R1 - 3	17.5	23.5	16.0	14.5	18.0
L6R1 - 4	14.0	21.0	24.5	20.0	20.0
Mean	17.0	21.5	22.5	17.5	19.5

Notes: - 1.0 inch = 25.4 mm
- All the numbers are rounded up to closest half inch.
- "*" indicates that transfer length could not be calculated because of the erratic strain profile for that particular region.
- The value in the shaded area of the table is the average transfer length for that series.

Table 4.2 Long-Term Transfer Length

Beam End	Transfer Region				Beam End Average (in)
	First (in)	Second (in)	Third (in)	Fourth (in)	
L0R0 - 1	16.5	N/A	N/A	N/A	16.5
L0R0 - 2	22.0	N/A	N/A	N/A	22.0
L0R1 - 3	18.5	N/A	N/A	N/A	18.5
L0R1 - 4	18.5	N/A	N/A	N/A	18.5
Mean	19.0	N/A	N/A	N/A	19.0
L4R0 - 1	12.5	19.5	18.0	N/A	16.5
L4R0 - 2	16.0	26.5	29.5	N/A	24.0
L4R1 - 3	15.0	19.5	28.5	N/A	21.0
L4R1 - 4	16.5	*	*	N/A	16.5
Mean	15.0	22.0	25.5	N/A	20.0
L6R0 - 1	15.0	18.5	30.0	18.5	20.5
L6R0 - 2	18.5	24.0	20.5	21.0	21.0
L6R1 - 3	14.5	23.5	19.5	22.0	20.0
L6R1 - 4	16.5	23.0	22.0	20.0	20.5
Mean	15.0	21.0	23.0	20.0	20.5

Notes: - 1.0 inch = 25.4 mm
- All the numbers are rounded up to closest half inch.
- "*" indicates that transfer length could not be calculated because of the erratic strain profile for that particular region.
- The value in the shaded area of the table is the average transfer length for that series.

It can be seen in Table 4.3 that the transfer length values as predicted by both the Buckner equation and the Lane equation varied slightly between the three beam series L0RX, L4RX, and L6RX. For the Buckner equation, this variation in values was caused by differences in the prestress losses from both sources, elastic shortening and relaxation. For the Lane equation, this variation in values was caused by differences in the 28 day strength of the concrete.

Table 4.3 Calculation of Transfer Length Using Buckner and Lane Equations

Beam Series	f_{pt} (ksi)	Losses E.S. (ksi)	Losses R.E. (ksi)	f'_c (ksi)	f_{si}^* (ksi)	Buckner l_t (in)	Lane l_t (in)
L0RX	202.5	11.89	2.15	5.44	188.5	37.7	84.3
L4RX	202.5	13.41	2.15	5.05	187.0	37.4	91.2
L6RX	202.5	14.26	2.37	7.48	185.9	37.2	60.0

* $f_{si} = f_{pt} - E.S. - R.E.$

1.0 inch = 25.4 mm

1.0 ksi = 6.89 MPa

Short-term and long-term experimentally determined transfer lengths are compared to current code values in Figures 4.5 and 4.6, respectively. It can be seen that only one short-term transfer length exceeds the current ACI and AASHTO-Standard code values of $50d_b$. This occurred in the third transfer region of beam L4R1-3 where the transfer length of 30.5-inch (775-mm) exceeds the code requirement by 1.6%. There were two other transfer lengths, one short-term and one long-term, that had values of 30-inch (762-mm) that exactly matches the code requirement of $50d_b$. It can also be seen in Figures 4.5 and 4.6 that no transfer length values, short-term or long-term, exceed or reached the AASHTO-LRFD code requirement of $60d_b$.

Short-term and long-term experimentally determined transfer length values are compared to values predicted by Buckner's equation in Figures 4.7 and 4.8, respectively. No experimentally determined transfer lengths exceed Buckner's predicted values. Also, short-term and long-term experimentally determined transfer length values are compared to values predicted by Lane's equation in Figures 4.9 and 4.10, respectively. It can be seen that no experimentally determined transfer lengths exceed Lane's predicted values. However, the values predicted by Lane's equation are excessively high when compared to this experimental data. For the transfer length data from this portion of the research project, it appears the Buckner equation or the AASHTO-LRFD value would be the best to use, and the AASHTO-LRFD would be better for simplicity.

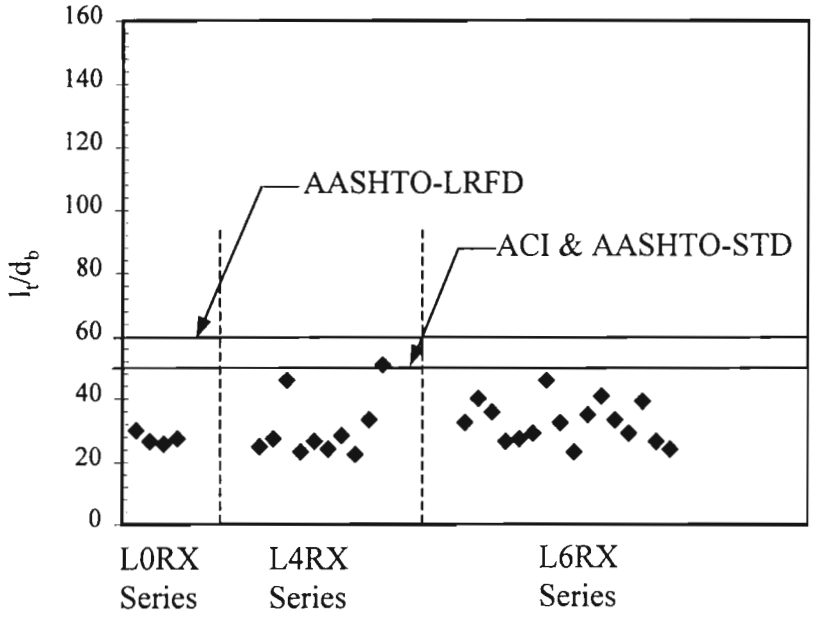

Figure 4.5 Comparison of Short-Term Transfer Length with Code Values

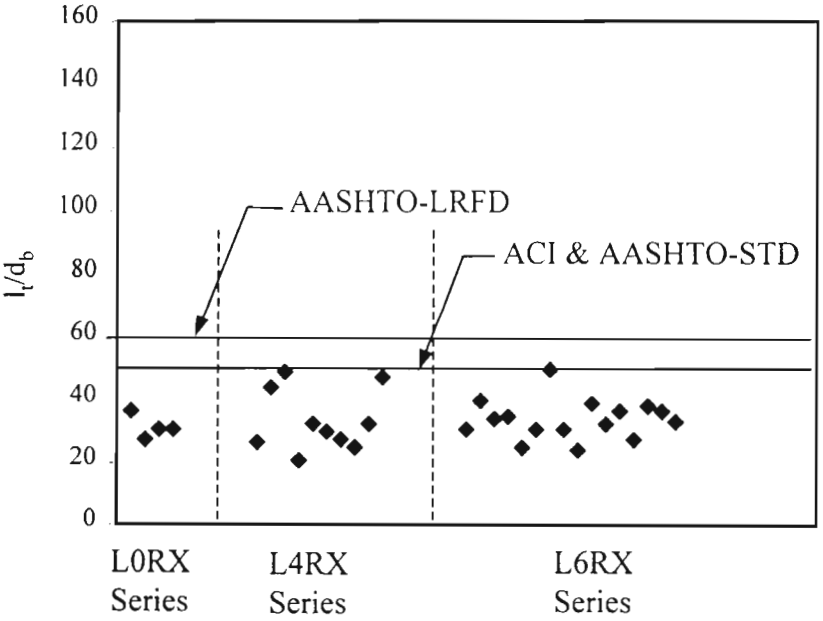

Figure 4.6 Comparison of Long-Term Transfer Length with Code Values

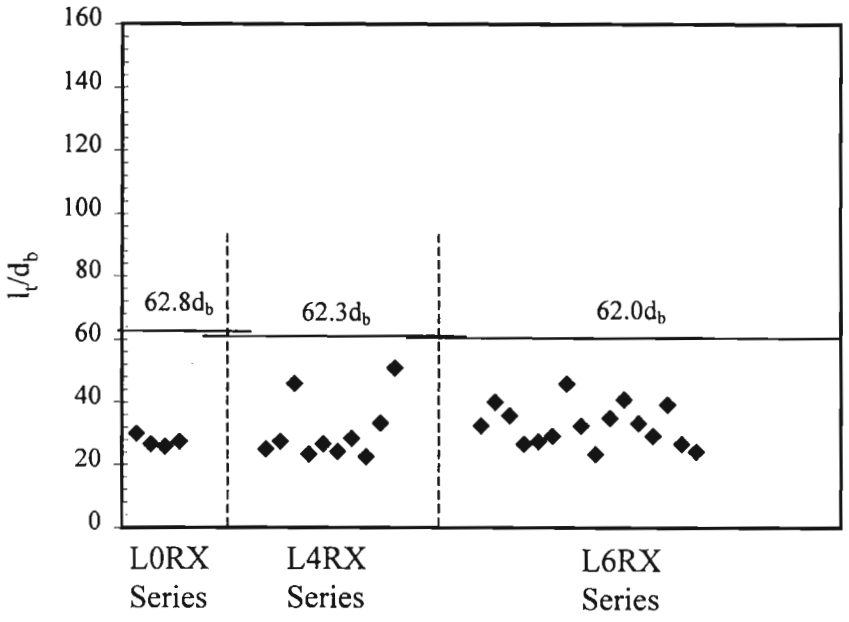

Figure 4.7 Comparison of Short-Term Transfer Length with Buckner Equation

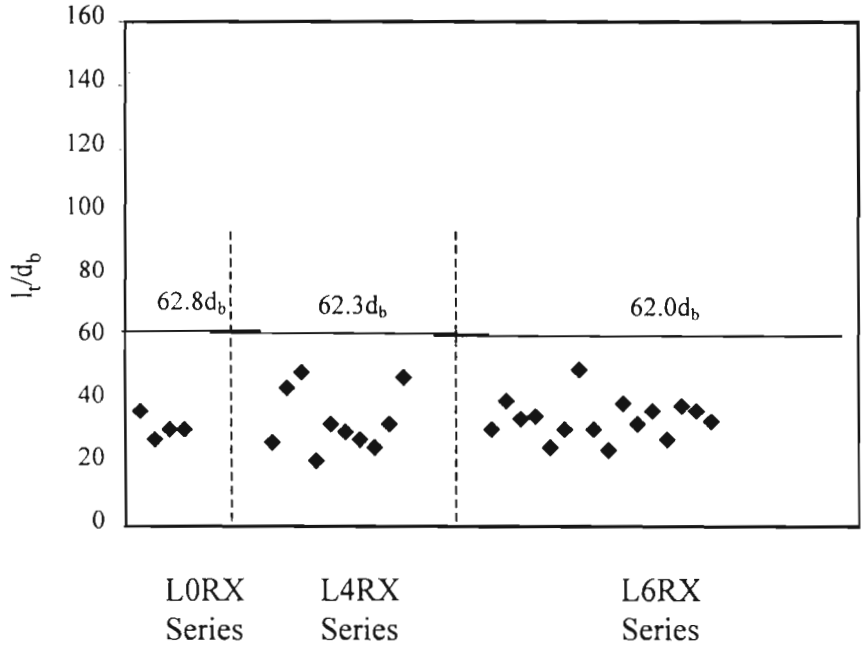

Figure 4.8 Comparison of Long-Term Transfer Length with Buckner Equation

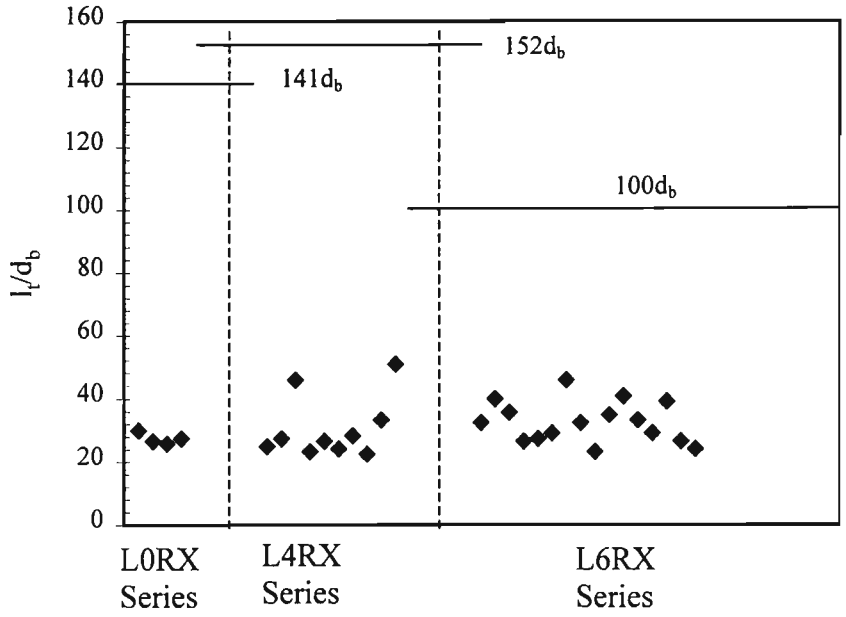

Figure 4.9 Comparison of Short-Term Transfer Length with Lane Equation

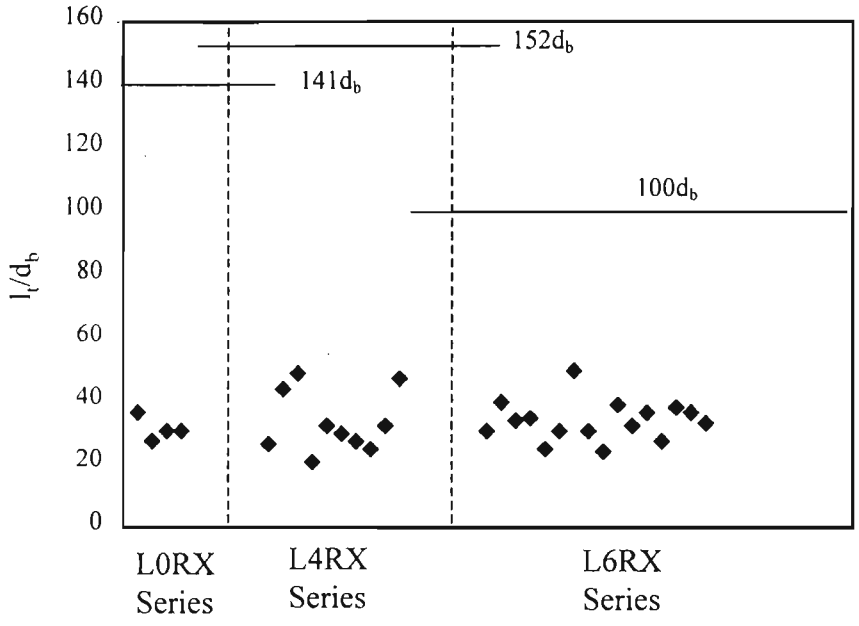

Figure 4.10 Comparison of Long-Term Transfer Length with Lane Equation

The effect that time and debonding of strand have on the transfer length was also considered. Because of the variability or scatter of data typically associated with experimental work, average or mean values were used to look at the effect of time and debonding. Mean transfer length values, short-term and long-term, are provided in Tables 4.1 and 4.2, respectively. The effect of time on the transfer length is shown in Figure 4.11. It can be seen that the transfer length increases with time, but it decreases with increases in levels of debonding. Increases in transfer length with time range from 8% to 12%. The effect of debonding on the transfer length is shown in Figure 4.12. It can be seen that the transfer length is longer in beams with debonded strand. Short-term transfer lengths for fully bonded strands increase by 12% when 60% of the strands are debonded. Long-term transfer lengths for fully bonded strands increase by 8% when 60% of the strands are debonded.

4.2 Development Length

The development length, in this project, was determine for each given beam series (L0RX, L4RX, or L6RX) by testing each of the 4 beam ends from each series with incrementally modified strand embedment lengths. When the failure mode changed from a flexural mode to a hybrid or a bond slip mode, the development length had been bracketed. Beam test geometries and dimensions for TTU's portion of this project are provided in Figure 3.13 and Table 3.3. Material properties and development test results are summarized in Table 4.4. The development length for each beam series was taken as the shortest strand embedment length for which a flexural failure mode occurred. From this definition, the development length for each of the three beam series was determined to be 54, 96, and 114 inches (1,372, 2,438, and 2,896-mm) from tests L0R1-3, L4R1-3, and L6R0-1, respectively. It can be seen in Table 4.4 that only one bond slip failure mode occurred for the test conducted at TTU, beam test L4R0-2. It can also be seen in Table 4.4 that three beams (L6R0-2, L6R1-3 and L6R1-4) fail in a hybrid mode. The hybrid mode is characterized by an end slip in the order of 0.1-inch (0.25-mm) and by the theoretical moment capacity of the section being reached. It should be noted again that the strand embedment length for the fourth beam end tested in each series was a repeated value from a previous test because this beam end contained the additional hair-pin reinforcing bar(s) denoted as a H-bar.

Each beam in this portion of the project was loaded until the total strain in the prestressing steel exceeded 3.5% or until there was significant end slip in one or more of the prestressing strands with an associated loss of load carrying capability. The value of the total strain in the prestressing steel is defined as the sum of the strain in the prestressing strand from the initial prestress, minus losses, and the increase in the strain caused by flexural loading. The flexural strain was estimated using strain compatibility where the strain in the top fiber of the concrete slab was measured, and the depth of the neutral axis was estimated by the measured distance from the top of the slab to the top of the flexural crack in the constant moment region of the beam. Measured concrete strain values and calculated total strand strain values are also provided in Table 4.4. The strain in the bottom row of strands exceed 3.5% in all the tests that failed in a flexural or

Table 4.4 Summary of Development Length Results

Beam Number	f'_c (Beam) (psi)	f'_c (Slab) (psi)	$l_{ub}+l_e$* (in)	Strand Embed., l_e (in)	M_{max} (kip-ft)	M_{th} (kip-ft)	$\frac{M_{max}}{M_{th}}$	Ultimate Concrete Strain	Bottom Strand Strain	Failure Mode
L0R0-1	5,470	6,500	96	96	1,055.2	1,084.5	0.973	0.00258	0.0424	Flexural
L0R0-2	5,470	6,500	72	72	1,146.7	1,086.9	1.055	0.00305	0.0484	Flexural
L0R1-3	5,440	6,120	54	54	1,066.2	1,083.5	0.984	0.00325	0.0489	Flexural
L0R1-4	5,440	6,120	54	54	1,224.7	1,164.0	1.052	0.0031	0.0445	Flexural
L4R0-1	5,050	5,835	186	114	1,471.3	1,368.7	1.075	0.00358	0.0436	Flexural
L4R0-2	5,050	5,700	132	60	1,322.4	1,334.2	0.991	0.0017	0.0218	Bond
L4R1-3	5,050	6,070	168	96	1,408.9	1,366.6	1.031	0.0030	0.0384	Flexural
L4R1-4	5,050	5,700	168	96	1,305.6	1,364.3	0.957	0.0032	0.0395	Flexural
L6R0-1	7,420	5,360	222	114	1,313.7	1,430.8	0.918	0.00307	0.0354	Flexural
L6R0-2	7,420	6,850	204	96	1,450.8	1,440.7	1.007	0.00323	0.0451	Hybrid
L6R1-3	7,420	6,360	192	84	1,525.1	1,438.7	1.060	0.00286	0.0373	Hybrid
L6R1-4	7,420	6,360	192	84	1,501.6	1,439.7	1.043	0.00324	0.0427	Hybrid

* $l_{ub}+l_e$: Location of critical section from end of beam.

M_{max}: Maximum applied moment.

M_{th}: Theoretical moment capacity of the section calculated using strain compatibility.

1.0 inch = 25.4 mm

1.0 psi = 6.89×10^{-3} MPa

1.0 kip-ft = 1.36 kN-m

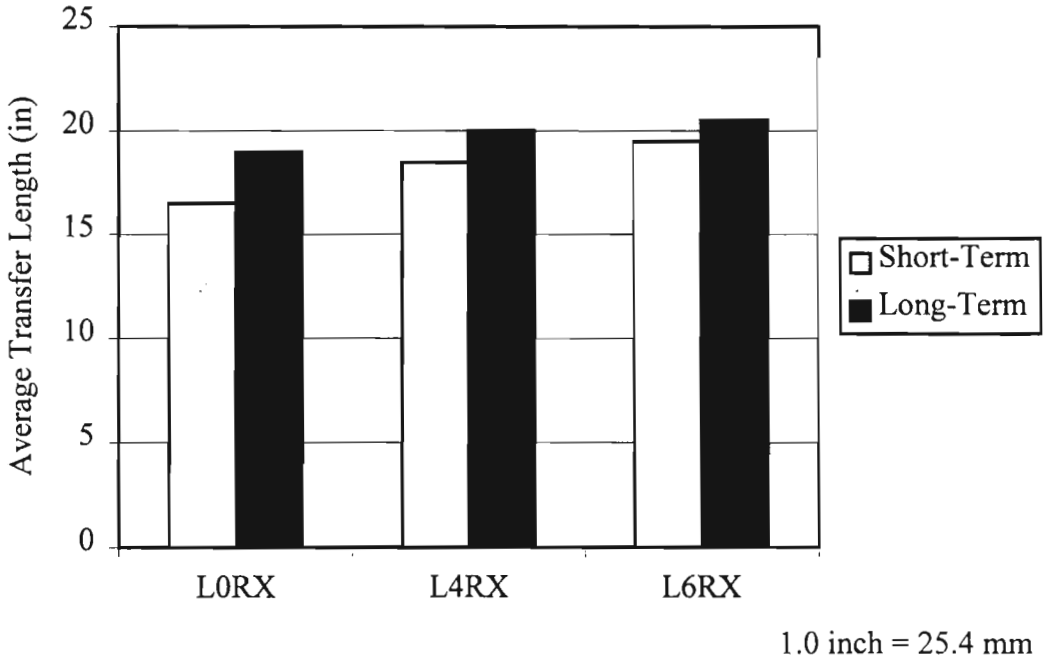

Figures 4.11 Effect of Time on Transfer Length

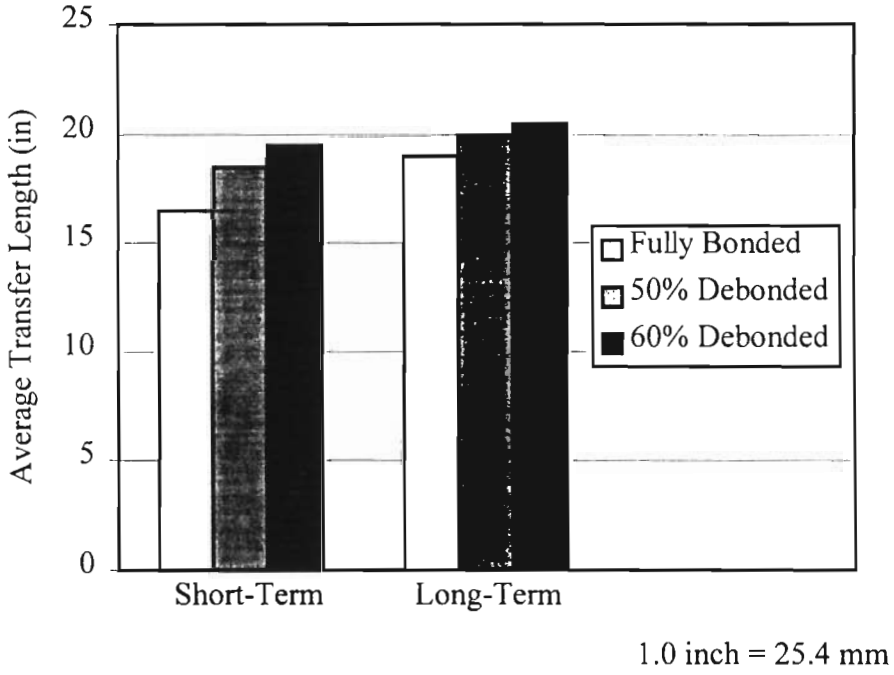

Figure 4.12 Effect of Debonding on Transfer Length

hybrid mode. The only test in which the strand did not exceed the 3.5% value was test L4R0-2 that failed in a bond slip mode.

Load-deflection curves were developed for each beam end tested. These are provided in Appendix C. Figure 4.13 is the load-deflection curve for test L4R0-1 and is a typical load-deflection curve for beams with a flexural failure or hybrid mode. It can be seen in the load-deflection curves that each beam end test that failed in a flexural or hybrid mode was loaded well out into the yield plateau region of the curve. In addition, it should be noted that each of the load-deflection curves associated with a flexural or hybrid failure had a upward slope at the end of the test, indicating additional load carrying capability. Figure 4.14 is the load-deflection curve for test L4R0-2 and is the only beam to fail in a bond slip mode. As can be seen, it shows a loss of load carrying capability at a deflection around 2.5-inch (64-mm), very early in the plateau region.

The value of the maximum moment applied to each beam end test was determined from the measured maximum load applied during each test. These values are also provided in Table 4.4. In addition, the theoretical ultimate moment capacity of each section was calculated using strain compatibility and is provided in Table 4.4. As can be seen in Table 4.4, the ratio of the maximum applied moment to the theoretical ultimate moment capacity for tests L0R1-3 and L4R1-3 were very near or greater than 1.0. Further showing that the beam test which provided the development length for these two series was loaded to its flexural limit without any significant bond slip. Even though the maximum to theoretical moment ratio provided in Table 4.4 for beam test L6R0-1 is only 91%, the values of concrete and strand strains are compatible with a flexural failure.

Strand end slip measurements were taken for each strand at each load increment during testing as described in Chapter 3. Load-end slip curves were developed for each beam in test series L4RX and L6RX and are provided in Appendix D. It should be noted that measurable end slip only occurred in some of the debonded strand, and only those strand's end slip were included in the curves. No measurable end slip occurred during any testing of the fully bonded strand test series, L0RX, so no load-end slip curves were developed for this series. In addition, the maximum value of end slip for each strand from each test is provided in Table 4.5. As seen in Table 4.5, test L4R0-2 had the maximum measured end slip during the test program, 1.2-inch (30-mm). This large end slip was accompanied by a loss of load carrying capability and longitudinal cracking in the concrete on the underside of the bottom flange of the beam in the bonded region of the strand. The combination of all these facts lead to the decision to call this a bond slip failure mode. There were several maximum end slip measurements with values in the 0. 1 -inch (0.25-mm) range in the L6RX series. However, the load-deflection curves associated with these smaller end slip measurements showed no signs of loss of load carrying capability. To the contrary, they all had continuing upward slopes and continued to carry increasing loads even after initial slippage had occurred. In addition, no longitudinal cracking of the concrete in the bottom flange was observed. The

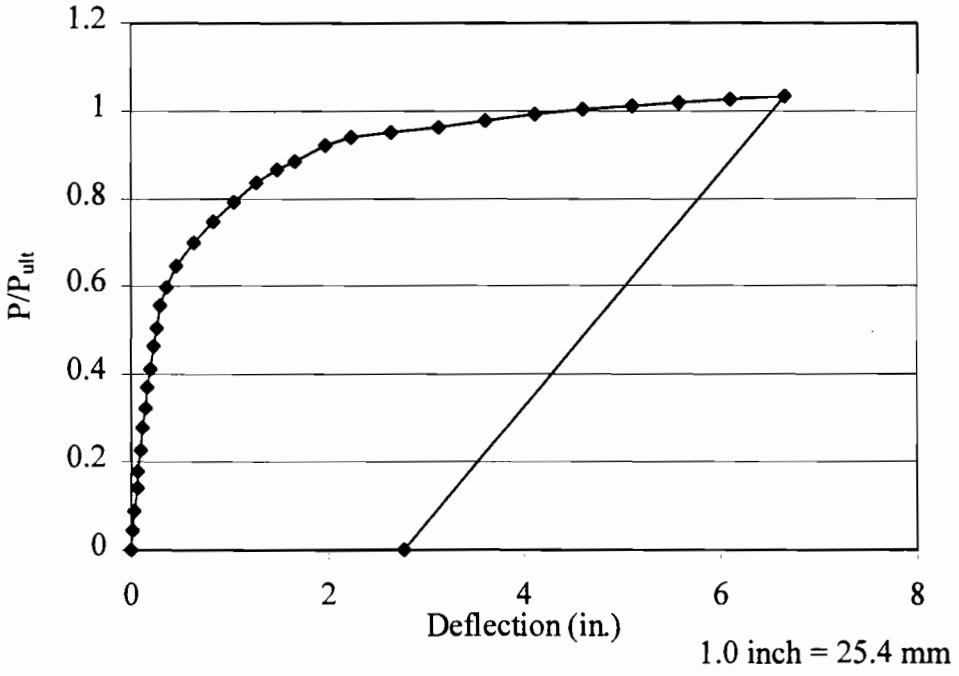

Figure 4.13 Load-Deflection Curve for Test L4R0-1

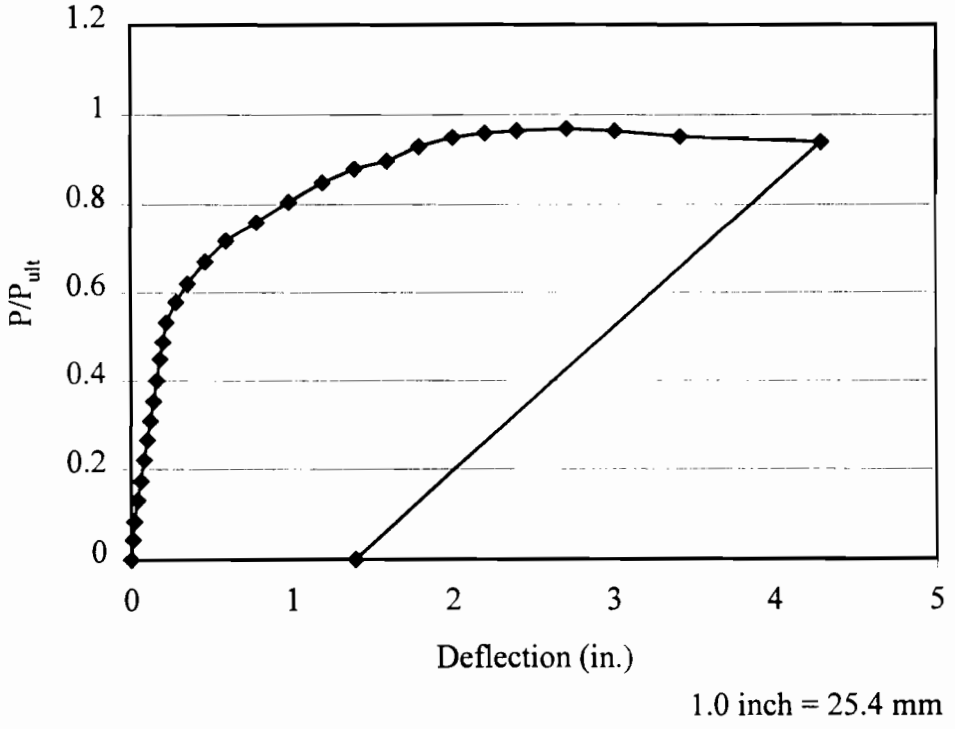

Figure 4.14 Load-Deflection Curve for Test L4R0-2

combination of all these facts lead to the decision to call these intermediate end slip measurements hybrid failure modes. There were three maximum end slip measurements with values less than 0.03-inch (0.76-mm); tests L4R1-3, L4R1-4, and L6R0-1. After considering their moment ratios, load-deflection curves, and maximum concrete and strand strain values, these three beams tests were defined as flexural failures. It is believed that these smaller end slip measurements can be attributed to the movement of the strands in the debonded region of the beam. This movement can be attributed to the increase in the curvature of the beam and to the summation of the crack widths in the debonded region of the strand.

Table 4.5 Maximum End Slip Values (inch)

BEAM ID	Strand No.									
	1	2	3	4	5	6	7	8	9	10
L0R0-1	--	--	--	--	--	--	--	--		
L0R0-2	--	--	--	--	--	--	--	--		
L0R1-3	--	--	--	--	--	--	--	--		
L0R1-4	--	--	--	--	--	--	--	--		
L4R0-1	--	--	--	--	--	--	--	--	--	--
L4R0-2	--	0.039	1.216	1.216	0.055	--	--	--	--	--
L4R1-3	--	0.002	0.028	0.019	0.003	--	--	--	--	--
L4R1-4	--	0.005	0.004	--	--	--	--	--	--	--
L6R0-1	--	0.015	0.015	--	0.015	0.008	--	--	--	--
L6R0-2	--	0.093	0.114	--	0.094	0.098	--	--	--	--
L6R1-3	--	0.120	0.111	--	0.092	0.095	--	--	--	--
L6R1-4	--	0.086	0.104	--	0.109	0.109	--	--	--	--

1.0 inch = 25.4 mm

The development lengths were selected for beam series L0RX, L4RX, and L6RX as 54, 96, and 114 inches (1,372, 2,438, and 2,896-mm), respectively, as discussed earlier. The development length for each beam series as predicted by the current code equations, the Buckner equation, and the Lane equation, as discussed in Chapter 2 of this report, is provided in Table 4.6 along with the values of key equation parameters. It should be noted that the development length as predicted by the current code equations is for fully bonded strands and was not doubled as currently required by code for debonded strands. The experimentally determined and equation predicted values of the development length for each beam series are provided in Table 4.7.

Table 4.6 Calculated Values of Development Lengths

Beam Series	f_{pt} (ksi)	f_{ps} (ksi)	f_{se} (ksi)	f_c' (ksi)	λ^*	Code** l_d (in)	Buckner l_d (in)	Lane l_d (in)
L0RX	202.5	266.8	165.4	5.44	2.0	94	160	171
L4RX	202.5	265.4	163.9	5.05	2.0	94	159	183
L6RX	202.5	267.5	161.7	7.48	2.0	96	164	129

*Actual values of λ exceed 2.0, therefore the upper limit of 2.0 was used.
** ACI, AASHTO-STD, AASHTO-LRFD for fully bonded strand. 1.0 inch = 25.4 mm
1.0 ksi = 6.89 MPa

Table 4.7 Comparison of Development Lengths

Beam Series	Experimental l_d (in)	Code		Buckner		Lane	
		l_d (in)	Ratio*	l_d (in)	Ratio*	l_d (in)	Ratio*
L0RX	54	94	0.57	160	0.34	171	0.32
L4RX	96	94	1.02	159	0.60	183	0.52
L6RX	114	96	1.19	164	0.70	129	0.88

* Ratio = $l_{d,\,exp.} / l_{d,\,predicted}$ 1.0 inch = 25.4 mm

The development lengths for beam series L0RX as predicted by the three equations of interest are significantly longer than the value experimentally determined in this project, as seen in Table 4.7. This shows that all three equations of interest yield fairly conservative predictions with regard to development length for fully bonded strands. The development lengths for the beam series L4RX and L6RX as predicted by the three equations of interest have mixed results when compared to the values experimentally determined in this project. The current code equations for fully bonded strand under predict the development lengths determined in the portion of the project. This is an unconservative scenario. Again, the development length used here as predicted by the current code equations does not include the code requirement to double its value when debonded strands are used. Doubling of the code predicted values would certainly change the values from unconservative to conservative, and the limited data in this portion of the project indicates that debonding some of the strands increases the development length of the strand. However, it appears that the current code factor of 2 is overly conservative. With respect to beam series L4RX and L6RX, both the Buckner and

the Lane equations again yield conservative development length values for beams with some percentage of debonded strands. Both the Buckner and Lane equations yield less conservative results as the percentage of debonded strands increases.

4.3 Effect of H-bars

Two identical tests in each of the 3 beam series were completed to evaluate the effect of the H-bars on the end-slip of the prestressing strands. Since the second beam in each of the 3 series, L0RX, L4RX, L6RX, had the H-bars installed on only one end, the second beam in each of the series was tested with the same embedment length on each end of the beam.

In the L0RX series, the length of the H-bars extended beyond the critical section. Since the H-bars were inside the maximum moment region and had enough flexural bond length beyond the critical section, they increased the beam moment capacity. As seen in Table 4.4, beam L0R1-4 has the highest moment capacity when compared to the other sections in its series. Since there was no end slip in either of the identical test, the effect of the H-bars on end slip for the fully bonded strands was not able to be determined.
In the L4RX and L6RX series, the H-bars did not extend to the critical section as in the L0RX series. Therefore, the H-bars were outside of the maximum moment region and did not effect the beams' moment capacities. In the L4RX series, the effect of the H-bars can be seen by comparing the values of the maximum end slip in Table 4.5. The maximum end slip reduced from 0.028-inch (0.71-mm) in the beam test L4R1-3 to 0.005-inch (0.127-mm) in the beam test L4R1-4 that had the H-bars. No significant end slip effect was observed in the L6RX series between beam tests L6R1-3 and L6R1-4. Another effect of the H-bars that was observed in all of the three beam series was that of reduced crack widths in the H-bar regions.

CHAPTER V

SUMMARY AND OBSERVATIONS

5.1 Summary

The use of 0.6-inch (15-mm) diameter prestressing strand has become necessary with the development and use of high-strength / high-performance concrete in standard I-beam sections if the standard 2-inch (50-mm) grid spacing is to be maintained and if the higher strength concrete is to be effectively utilized. The use of high-strength / high-performance concrete in this application requires a much larger prestressing force to fully pre-compress the service load tensile zone of the I-beam. However, the number of strands that can be placed in any given I-beam section on a 2-inch (50-mm) grid is limited. The strand limit also limits the amount of prestressing force that can be applied to the section. The cross-sectional area of 0.6-inch (15-mm) diameter strand is over 40% greater than that of 0.5-inch (13-mm) diameter strand, the maximum previously available diameter. This allows for over a 40% increase in prestressing force for the same number of strands and the same level of stress in each strand, by simply changing from a 0.5-inch (13-mm) to a 0.6-inch (15-mm) diameter strand.

The Federal Highway Administration (FHWA) placed a moratorium on the use of 0.6-inch (15-mm) diameter prestressing strand in prestressed, precast concrete I-beams in October of 1988. This moratorium was imposed because of some apparent unconservatism in the code requirements addressing transfer and development lengths of 7-wire prestressing strand. The research conducted at Texas Tech University (TTU) is an integral part of a larger, joint research project conducted with The University of Texas at Austin (UT) designed to provide addition test data for consideration toward lifting the FHWA moratorium. This joint project was to provide additional full-scale test data on the transfer and development lengths of 0.6-inch (15-mm) diameter prestressing strand for two key variables. The effects of the two key variables, concrete strength and strand surface condition, on the transfer and development lengths of the 0.6-inch (15-mm) diameter prestressing strand were investigated for fully bonded and various combinations of bonded and debonded strand used in AASHTO Type I (Texas Type A) I-beams.

Concrete strengths in three ranges were investigated in the joint TTU / UT project to evaluate the effect of concrete strength on the transfer and development lengths of 0.6-inch (15-mm) diameter, 7 wire, prestressing strand at a 2-inch (50-mm) grid spacing. The three concrete strength ranges were 5,000-7,000 psi (34.4-48.2 MPa), 9,500-11,500 psi (65.4-79.2 MPa), and 13,000-15,000 psi (89.6-103.4 MPa). These strength ranges were denoted as low, medium, and high strength, respectively. In addition, the effect of the strand surface condition on the transfer and development lengths of the 0.6-inch (15-mm) diameter strand was also investigated. Two extreme surface conditions were used, mill bright and rusty. The mill bright condition was defined as in the as received condition with a smooth, bright, and shiny surface with only very isolated rust spots. The rusty condition was defined as a light surface rusting over the entire surface of the strand

with no significant loss of cross-section area. For each combination of concrete strength and strand surface condition, beams were tested for three other variations in the strand: all strand fully bonded, 50% of the strand debonded, and 60% or 75% of the strand debonded. TTU's portion of the project and the data reported in this report was limited to concrete strength in the 5,000-7,000 psi (34.4-48.2 MPa) range and strand with a rusty surface condition for the each of the three strand variations listed above with a maximum debonded limit of 60%. Two tests were conducted on each beam, one on each end, for both transfer and development length determinations. Six beams and therefore 12 tests for both transfer and development lengths were conducted by TTU and are reported herein.

It should be noted that at the time of the writing of this report that there has been a partial lifting of the FHWA October, 1988, moratorium on the use of 0.6-inch (15-mm) diameter prestressing strand due to positive results of other additional research. This partial lifting allows the use of 0.6-inch (15-mm) diameter strand at a 2-inch (50-mm) grid spacing in pretensioned concrete beam applications. However, the FHWA moratorium still requires a 1.6 increase in the AASHTO-Standard development length as predicted by Equation 9-32.

Transfer and development lengths that were experimental determined during TTU's portion of this project are reported herein. These results are compared to current code requirements for both transfer and development lengths for ACI-318, AASHTO-Standard, and AASHTO-LRFD. In addition, these results are compared to two predictive equations for both transfer and development length: one that was proposed by Buckner and one that was proposed by Lane.

Transfer lengths were determined by constructing concrete compression strain profiles at the level of the prestressing strand for each end of each beam. Concrete compression strain data was collected using Demec mechanical strain gauges and small stainless steel discs that were epoxied to the vertical surfaces of the lower flange of the beam at the center of gravity of the prestressing steel. Measurements between these points were taken before and after release of the prestressing strand, allowing the development of concrete compression strain profiles along the length of the beam. The 95% Average Maximum Strain method was applied to the concrete compression strain profiles to determine transfer lengths. Short-term and long-term transfer lengths were determined. Short-term readings were taken immediately after release, and long-term readings were taken four to six week after release but prior to shipment of beams from the precasting yard to the respective universities for development length testing. A total of 30 short-term transfer length values and 30 long-term transfer length values were determined during this portion of the project due to the multiple transfer regions associated with the beams with debonded strands. All the beams in this project were cast by the Texas Concrete Company in Victoria, Texas.

Development lengths were determined by incrementally changing the embedment length of the strand in three successive flexural beam tests for each set of parameters.

Embedment lengths were incrementally shortened until the failure mode changed from a flexural failure mode to a bond slip mode, thereby bracketing the development length. The development length was then set as the shortest embedment length associated with a flexural failure mode. A fourth flexural test was conducted on one end of one beam in each series that had an additional hairpin reinforcing bar in the lower region of one end of the beam to evaluate the effect of the hairpin bar on the end-slip and development length of the strand. Twelve flexural beam tests were conducted at the Civil Engineering Structural Laboratory at Texas Tech University in Lubbock, Texas.

The beams were transported to the structural laboratory, and concrete deck slabs were cast-in-place to provide composite action with each beam. This was done so that the prestressing steel would be fully yielded if a flexural failure could be achieved in lieu of a bond slip failure. Applied loads, deflections, strand end-slips, and concrete strain in the top fiber of the cast-in-place deck slab were recorded throughout each beam test. The development lengths for the three beam series tested in TTU's portion of the project for beam concrete strengths in the 5,000-7,000 psi (34.4-48.2 MPa) range and a rusty strand surface condition were determined to be 54, 96, and 114 inches (1,372, 2,438, and 2,896-mm) for the fully bonded, 50% debonded, and 60% debonded strand series, respectively.

Three beam failure modes were observed during testing. These were classified as flexural, hybrid, and bond slip. The flexural failure mode was characterized by a maximum concrete compressive strain in the deck slab greater than 0.003 and a total strain in the bottom prestressing strand greater than 3.5%. It was also characterized by a load-deflection curve that extended well out in the yield plateau region and strand end-slip values less than 0.03-inch (0.76-mm). The hybrid failure mode had the same characteristics as the flexural failure mode except that the maximum strand end-slip was in the order of 0.1-inch (0.25-mm). Even though larger values of strand end-slip were observed in the hybrid failure mode, the theoretical ultimate moment capacity of the beam and materials had been reached, and the load-deflection curve still had an upward slope indicating additional load capacity. In addition, there was no observed longitudinal cracking in the concrete on the underside of the bottom flange of the beam that is typically associated with a bond slip failure mode. The bond slip failure mode was characterized by a maximum concrete compressive strain in the deck slab less that 0.003 and a total strain in the bottom prestressing strand less the 3.5%. It was also characterized by a load-deflection curve that peaked very early and had a downward slope indicating a loss of load carrying capability. The bond slip failure also had large strand end-slip values in the order of 1.2-inch (30-mm) and was accompanied by the development of longitudinal cracks in the concrete on the underside of the bottom flange of the beam.

5.2 Observations

The following observations can be made from the test data collected in TTU's portion of this project. Because the data collected in this portion of the project represents a very small percentage of the total data collected in the joint UT / TTU project, any

conclusions drawn from these observations should be weighed carefully against the rest of the data from this project as well as other compatible test data in the literature.

1. Short-term transfer length measurements were made immediately after release of the prestressing force, and long-term transfer length measurements were made 4 to 6 weeks later. Transfer length values were averaged for each beam series to evaluate the effect of time on the transfer length. Average short-term transfer lengths increased by 15%, 8%, and 5% over time for beam series L0RX, L4RX, and L6RX, respectively.

2. Average values of transfer lengths for each beam series increased as the number of debonded strands increased. This was observed for both short-term and long-term values. Average values of short-term transfer lengths for fully bonded strands increased by 12% and 18% as 50% and 60% of the strands were debonded, respectively. Average values of long-term transfer lengths for fully bonded strands increased by 5% and 8% as 50% and 60% of the strands were debonded, respectively.

3. All individual short-term and long-term transfer length values were compared to current code requirements for ACI-318, AASHTO-Standard, and AASHTO-LRFD. These values are $50d_b$, $50d_b$, and $60d_b$, respectively. Only one short-term transfer length value exceeded the $50d_b$ requirement, and this was by less than 2%. None of the short-term transfer length values exceeded the $60d_b$ requirement. Also, none of the long-term transfer length values exceeded either the $50d_b$ or $60d_b$ requirement.

4. All individual short-term and long-term transfer length values were compared to those predicted by the Buckner equation described in Chapter 2 of this report. The transfer length values as predicted by the Buckner equation varied slightly between the three beam series, L0RX, L4RX, and L6RX, due to slight differences in elastic shortening and relaxation losses. The shortest transfer length value as predicted by the Buckner equation was $62d_b$. The longest transfer length, short-term or long-term, determined in this project was $51d_b$, approximately 22% below the Buckner value.

5. All individual short-term and long-term transfer length values were compared to those predicted by the Lane equation described in Chapter 2 of this report. The transfer length values as predicted by the Lane equation varied between the three beam series, L0RX, L4RX, and L6RX, due to differences in the beam concrete strengths. The transfer length values as predicted by the Lane equation were $141d_b$, $152d_b$, and$100d_b$ for beam series L0RX, L4RX, and L6RX, respectively. The longest transfer length, short-term or long-term, determined in this project for each beam series was $37d_b$, $51d_b$, and $50d_b$ for beam series L0RX, L4RX, and L6RX, respectively. All of the experimentally determined values were significantly less than the corresponding Lane values.

6. The development length values determined in this project were 54, 96, and 114 inches (1,372, 2,438, and 2,896-mm) for beam series L0RX, L4RX, and L6RX, respectively.

The development lengths of the two beams series containing debonded strand L4RX and L6RX were approximately two times as long as the beam series containing only fully bonded strand, L0RX.

7. The development lengths from this project were compared to the requirements of the same 3 current codes identified in paragraph three above. All three codes have the same development length requirements that predict values of 94-inch (2,388-mm), 94- inch (2,388-mm), and 96-inch (2,438-mm) for the beam series L0RX, L4RX, and L6RX, respectively. These code predicted values are for fully bonded strand, and the values for the two beam series containing debonded strand were not doubled. Beam series L0RX had a development length that was 57% of the current code requirement. This would indicate that the current code requirement for fully bonded stand is adequate and that the additional FHWA requirement to increase the current code value by 1.6 is not necessary. Beam series L4RX and L6RX had longer development lengths that were 102% and 119% of the current code requirement for fully bonded strand. If code equation development lengths of 94-inch (2,388-mm) and 96-inch (2,438-mm) for beam series L4RX and L6RX, respectively, were doubled as currently required for debonded applications, their code predicted development lengths would be 188-inch (4,775-mm) and 192-inch (4,877-mm), respectively. Using these values, the experimentally determined development lengths are 51% and 59% of their current code requirements, respectively. This indicates that some lengthening of the development length for debonded strand is necessary, but that the current code requirement of doubling may be too conservative.

8. The development lengths determined in this project were compared to values predicted by the Buckner equation. The values predicted by the Buckner equation are 160-inch (4,064-mm), 159-inch (4,039-mm), and 164-inch (4,166-mm) for beam series L0RX, L4RX, and L6RX, respectively. The development length values that were experimental determined in this project are 34%, 60%, and 70% of the values predicted by the Buckner equation, respectively. Indicating that the Buckner equation is very conservative for fully bonded strand and decreasingly conservative for beams containing debonded strand.

9. The development lengths determined in this project were compared to values predicted by the Lane equation. The values predicted by the Lane equation are 171-inch (4,343-mm), 183-inch (4,648-mm), and 129-inch (3,277-mm) for beam series L0RX, L4RX, and L6RX, respectively. The development length values that were experimental determined in this project are 32%, 52%, and 88% of the values predicted by the Lane equation, respectively. Indicating that the Lane equation is very conservative for fully bonded strand and decreasingly conservative for beams containing debonded strand.

10. Two identical tests in each of the three beam series were completed to evaluate the effect of an additional hairpin shaped reinforcing bar, H-bar, that was installed in only one end of the beam in its lower region. In all three beam series, smaller crack widths

were observed in the H-bar region of the beams that contained the H-bar(s). No strand end slip was observed in the L0RX beam series; therefore, no end slip effect was observed. The maximum end slip was reduced from 0.028-inch (0.71-mm) to 0.005-inch (0.127-mm) in the L4RX beam series indicating some possible H-bar benefit. No significant or similar end slip effect was observed in the L6RX beam series.

APPENDIX A

BEAM REINFORCEMENT DETAILS

REINFORCEMENT DETAIL 1 (40' GIRDERS)

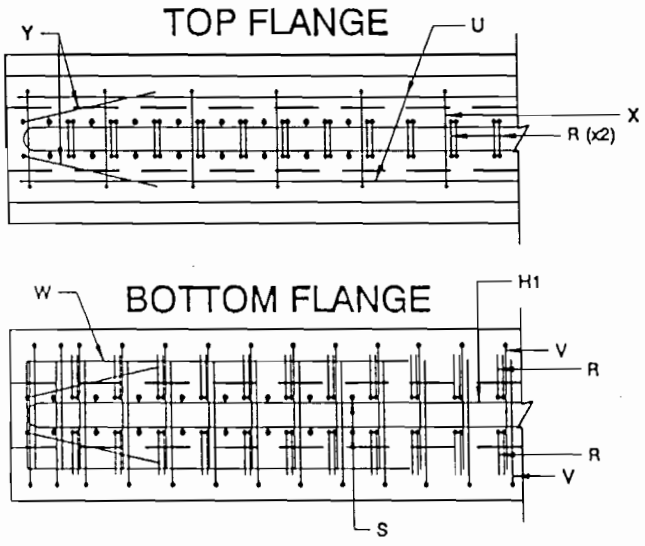

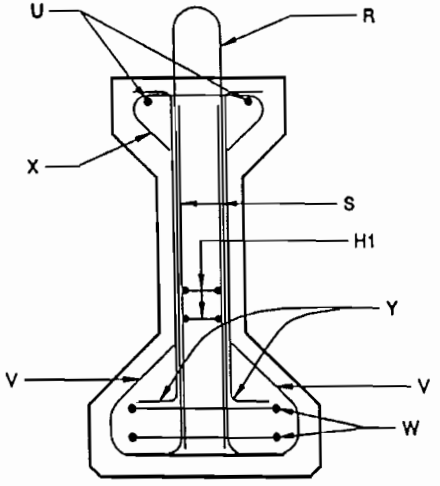

AASHTO TYPE I BEAM

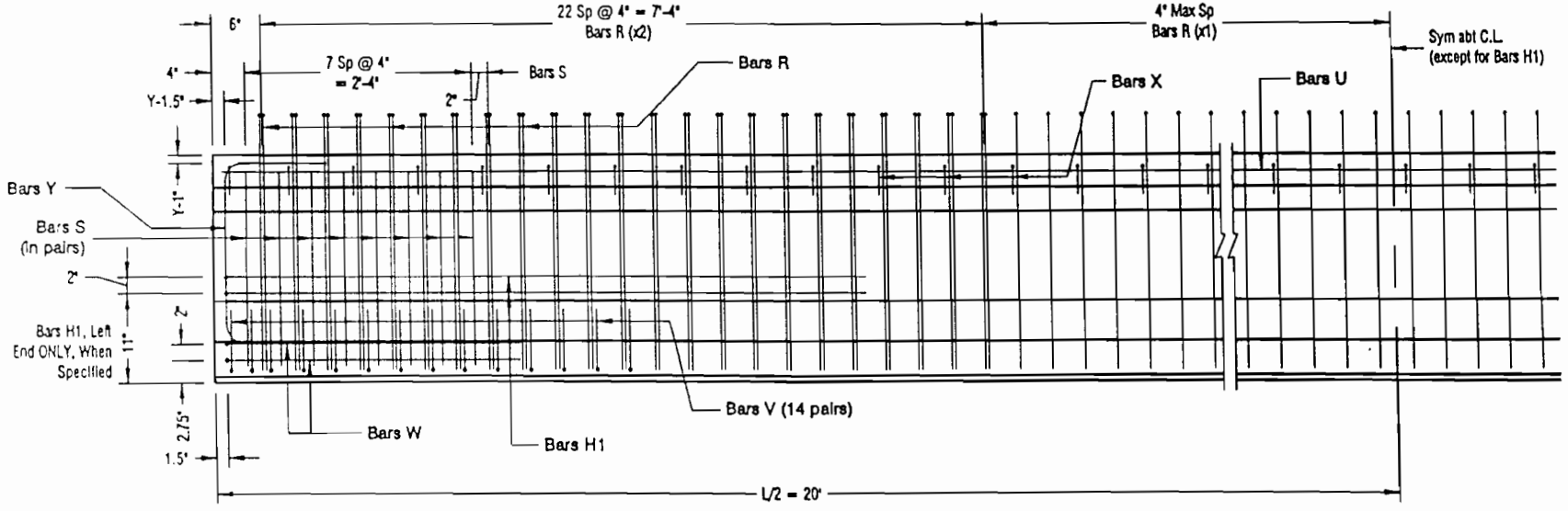

ELEVATION

REINFORCEMENT DETAIL 2 (54' GIRDERS)

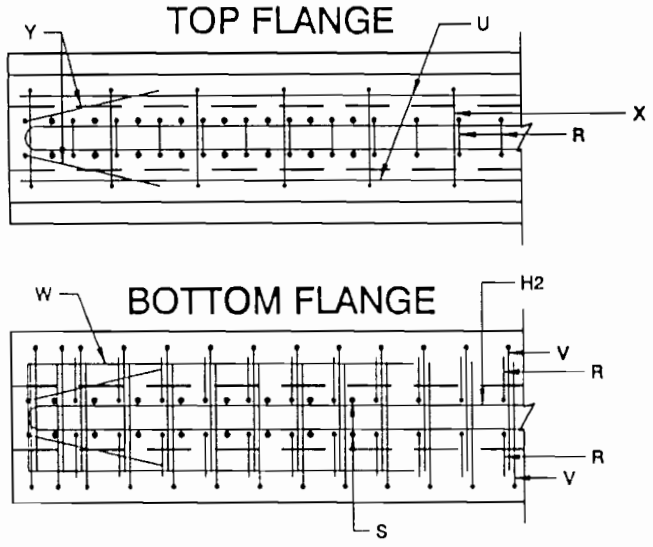

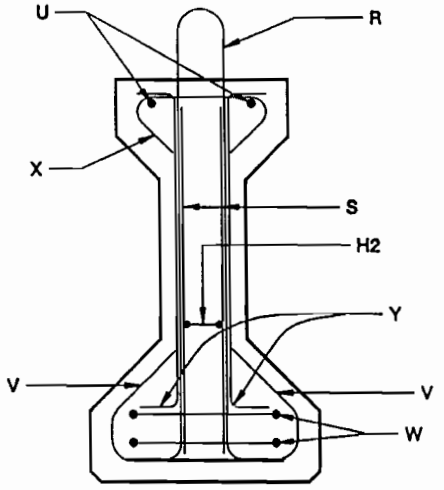

AASHTO TYPE I BEAM

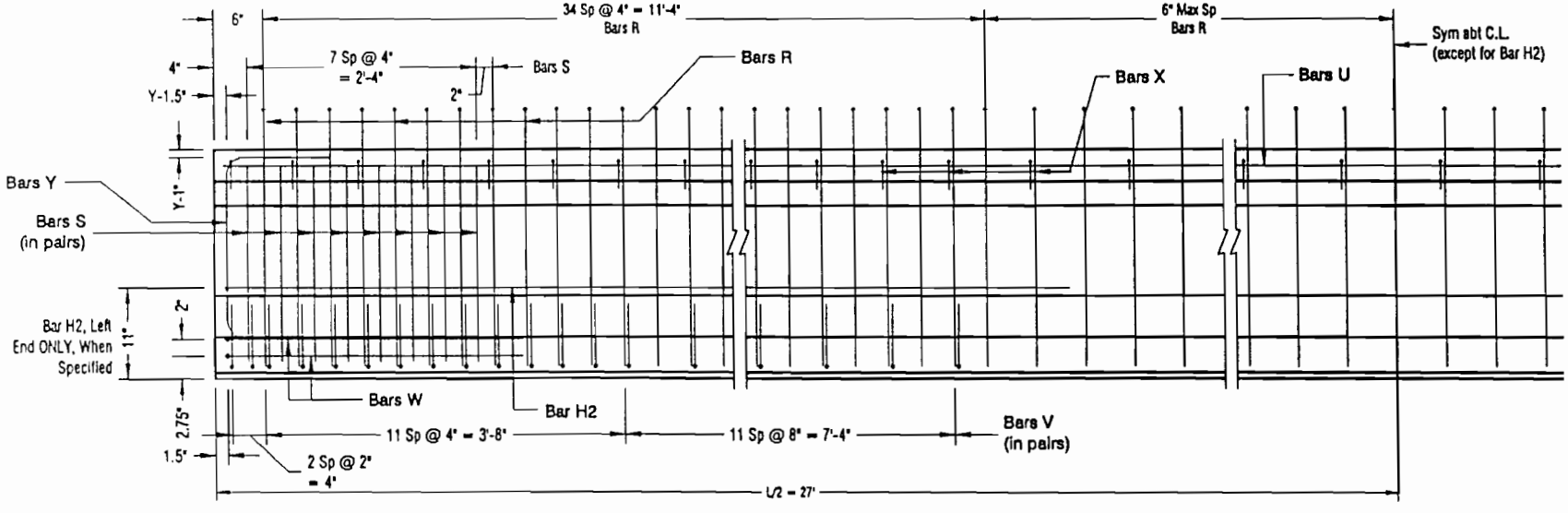

ELEVATION

REINFORCING BAR DETAILS

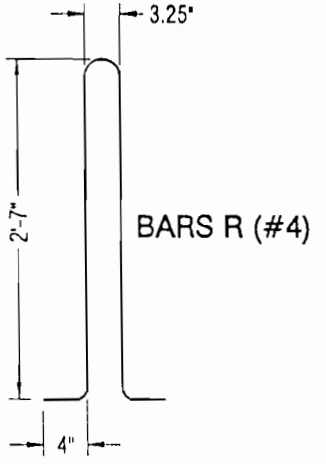

BARS R (#4)

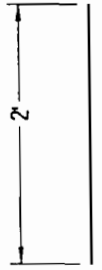

BARS S (#5)

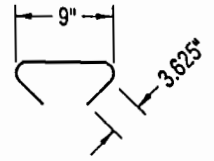

BARS X (#3)

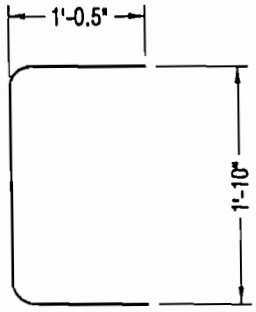

BARS Y (#6)

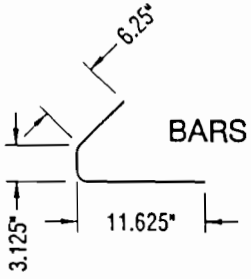

BARS V (#4)

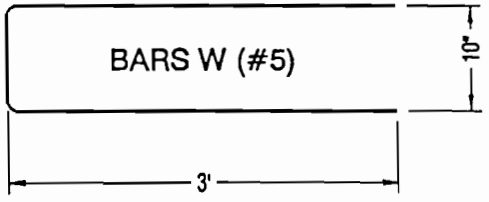

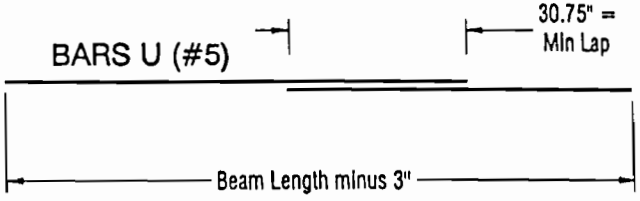

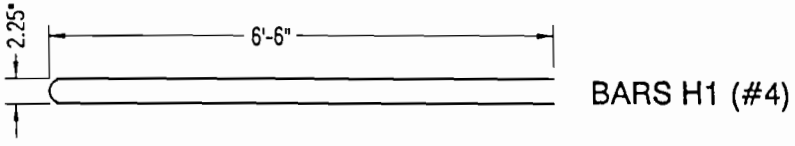

BARS H1 (#4)

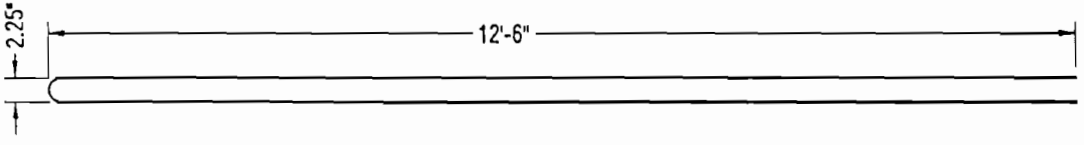

BARS H2 (#4)

APPENDIX B

CONCRETE COMPRESSION STRAIN AND PROFILES

Table B.1 Concrete Compressive Strain, L0R0

Distance* (in.)	L0R0-1		L0R0-2	
	Short Term Strain (10^{-6})	Long Term Strain (10^{-6})	Short Term Strain (10^{-6})	Long Term Strain (10^{-6})
4.9	22	216	34	373
6.9	71	283	89	447
8.9	140	435	166	529
10.8	199	523	266	667
12.8	264	619	290	665
14.8	315	697	347	757
16.7	354	731	370	803
18.7	359	745	395	827
20.7	394	817	380	821
22.6	381	807	401	825
24.6	382	803	390	809
26.6	373	827	365	771
28.5	399	793	365	755
30.5	352	775	372	783
32.5	359	783	375	811
34.5	374	796	368	800
36.4	345	770	367	815
38.4	335	772	375	830
40.4	366	802	388	821
42.3	351	800	373	810
44.3	364	842	388	833
46.3	360	803	376	839
48.2	395	845	371	828
50.2	372	827	350	819
52.2	391	888	357	806
54.1	395	882	383	827
56.1	410	858	364	824
58.1	419	848	389	837
60.0	405	881	373	822
62.0	414	853	364	795
64.0	419	858	379	797
65.9	419	851	371	818

* Distance from end of beam 1.0 inch = 25.4 mm

Table B.2 Concrete Compressive Strain, L0R1

Distance* (in.)	L0R1-3		L0R1-4	
	Short Term Strain (10^{-6})	Long Term Strain (10^{-6})	Short Term Strain (10^{-6})	Long Term Strain (10^{-6})
4.9	18	315	47	302
6.9	85	407	101	386
8.9	150	497	188	509
10.8	230	601	258	624
12.8	267	696	302	686
14.8	323	776	350	733
16.7	347	796	414	836
18.7	376	822	376	824
20.7	362	847	399	841
22.6	374	830	355	795
24.6	362	836	358	766
26.6	373	816	370	793
28.5	353	809	355	815
30.5	323	795	352	809
32.5	392	844	371	846
34.5	352	820	420	855
36.4	359	808	307	746
38.4	355	851	349	816
40.4	375	837	438	911
42.3	375	870	382	865
44.3	389	884	403	866
46.3	385	883	440	909
48.2	374	860	381	859
50.2	381	873	362	873
52.2	377	866	383	878
54.1	368	843	388	872
56.1	344	808	430	913
58.1	339	819	391	847
60.0	376	867	411	882
62.0	371	864	372	868
64.0	376	865	389	876
65.9	345	824	392	846

* Distance from end of beam

1.0 inch = 25.4 mm

Table B.3 Concrete Compressive Strain, L4R0

Distance* (in.)	L4R0-1		L4R0-2	
	Short Term Strain (10^{-6})	Long Term Strain (10^{-6})	Short Term Strain (10^{-6})	Long Term Strain (10^{-6})
4.9	74	189	78	219
6.9	131	287	121	N/R **
8.9	183	421	171	345
10.8	218	525	200	461
12.8	266	503	210	433
14.8	269	554	253	N/R **
16.7	274	535	264	535
18.7	276	557	258	515
20.7	285	569	257	547
22.6	280	525	242	517
24.6	270	551	258	539
26.6	269	511	253	511
28.5	272	553	258	537
30.5	272	505	262	541
32.5	277	529	267	529
34.5	278	579	262	576
36.4	287	567	285	533
38.4	305	642	281	N/R **
40.4	304	643	266	631
42.3	341	688	317	691
44.3	329	684	324	772
46.3	362	727	366	N/R **
48.2	385	782	361	754
50.2	190	373	398	849
52.2	422	875	432	821
54.1	417	846	457	946
56.1	418	897	426	929
58.1	431	923	431	905
60.0	426	888	444	934
62.0	423	908	425	902
64.0	441	865	437	947
65.9	442	909	448	999
67.9	443	892	447	982

* Distance from end of beam 1.0 inch = 25.4 mm

** No Reading due to lost gage point

Table B.3 Concrete Compressive Strain, L4R0 (Continued)

Distance* (in.)	L4R0-1		L4R0-2	
	Short Term Strain (10^{-6})	Long Term Strain (10^{-6})	Short Term Strain (10^{-6})	Long Term Strain (10^{-6})
69.9	454	886	462	960
71.8	473	963	457	925
73.8	474	993	448	947
75.8	501	1012	465	966
77.8	511	1002	454	982
79.7	504	1025	466	976
81.7	541	1039	481	977
83.7	542	1079	514	983
85.6	601	1144	497	1048
87.6	578	1130	562	1102
89.6	585	1154	561	1181
91.5	592	1165	562	1169
93.5	609	1229	575	1175
95.5	612	1245	576	1153
97.4	617	1225	561	1137
99.4	612	1238	580	1186
101.4	597	1210	591	1162
103.4	588	1146	590	1192
105.3	595	1184	593	1238
107.3	564	1140	586	1226
109.3	569	1090	587	1258
111.2	648	1243	622	1244
113.2	631	1199	597	1202
115.2	630	1169	576	1162
117.1	639	1217	627	1218
119.1	556	1102	570	1124
121.1	568	1114	566	1134
123.0	567	1120	559	1120
125.0	564	1118	566	1114
127.0	577	1098	583	1206
128.9	590	1140	584	1184
130.9	605	1192	599	1212
132.9	596	1210	600	1222
134.8	599	1216	599	1224
136.8	611	1233	609	1235

* Distance from end of beam 1.0 inch = 25.4 mm

Table B.4 Concrete Compressive Strain, L4R1

Distance* (in.)	L4R1-3		L4R1-4	
	Short Term Strain (10^{-6})	Long Term Strain (10^{-6})	Short Term Strain (10^{-6})	Long Term Strain (10^{-6})
4.9	11	114	76	183
6.9	55	142	105	241
8.9	104	313	137	323
10.8	144	375	198	397
12.8	171	453	239	501
14.8	199	471	265	561
16.7	192	501	280	582
18.7	193	507	318	630
20.7	197	493	327	616
22.6	196	493	308	597
24.6	189	517	316	631
26.6	173	465	309	593
28.5	176	449	292	605
30.5	185	487	290	573
32.5	175	430	269	535
34.5	180	478	270	564
36.4	193	455	257	501
38.4	198	511	283	546
40.4	222	550	707	1007
42.3	217	567	702	986
44.3	234	636	741	1101
46.3	243	625	893	1300
48.2	271	655	487	906
50.2	288	674	523	977
52.2	305	689	524	986
54.1	330	816	637	1046
56.1	346	814	817	1255
58.1	333	831	808	1272
60.0	338	783	807	1254
62.0	213	416	600	1087
64.0	352	817	471	941
65.9	341	777	476	961
67.9	345	824	497	996
69.9	360	854	621	1141

* Distance from end of beam

1.0 inch = 25.4 mm

Table B.4 Concrete Compressive Strain, L4R1 (Continued)

Distance* (in.)	L4R1-3		L4R1-4	
	Short Term Strain (10^{-6})	Long Term Strain (10^{-6})	Short Term Strain (10^{-6})	Long Term Strain (10^{-6})
71.8	349	764	614	1103
73.8	396	857	627	1150
75.8	391	887	608	1102
77.8	396	866	482	984
79.7	413	940	764	1323
81.7	394	907	759	1289
83.7	417	925	790	1331
85.6	435	943	799	1350
87.6	448	1016	851	1405
89.6	475	1040	862	1453
91.5	482	1064	855	1460
93.5	501	1103	856	1458
95.5	506	1093	560	1181
97.4	507	1157	815	1397
99.4	500	1077	822	1405
101.4	609	1222	801	1390
103.4	584	1182	876	1472
105.3	571	1156	621	1188
107.3	660	1226	654	1242
109.3	575	1118	693	1271
111.2	580	1160	682	1282
113.2	571	1092	663	1278
115.2	598	1184	684	1289
117.1	635	1184	634	1236
119.1	590	1225	582	1204
121.1	590	1208	594	1206
123.0	605	1206	593	1222
125.0	584	1174	594	1198
127.0	587	1130	605	1190
128.9	572	1142	640	1198
130.9	573	1140	617	1244
132.9	568	1150	610	1232
134.8	677	1294	604	1232
136.8	682	1312	652	1290

* Distance from end of beam 1.0 inch = 25.4 mm

Table B.5 Concrete Compressive Strain, L6R0

Distance* (in.)	L6R0-1		L6R0-2	
	Short Term Strain (10^{-6})	Long Term Strain (10^{-6})	Short Term Strain (10^{-6})	Long Term Strain (10^{-6})
4.9	79	373	17	313
6.9	80	429	48	373
8.9	113	471	71	407
10.8	127	503	121	449
12.8	150	572	122	467
14.8	165	588	141	501
16.7	166	598	152	515
18.7	167	624	153	555
20.7	168	582	164	559
22.6	184	601	166	533
24.6	183	577	167	559
26.6	198	613	172	541
28.5	177	587	193	611
30.5	182	599	214	641
32.5	183	639	211	639
34.5	226	651	218	649
36.4	217	691	215	635
38.4	224	734	244	699
40.4	237	706	242	704
42.3	224	722	233	680
44.3	221	728	234	702
46.3	229	760	233	686
48.2	244	758	204	690
50.2	249	726	205	682
52.2	258	748	244	718
54.1	283	792	257	750
56.1	278	804	236	720
58.1	259	786	239	724
60.0	268	766	240	688
62.0	269	776	271	754
64.0	278	786	254	724
65.9	270	792	268	750
67.9	285	820	267	712
69.9	282	808	270	694

* Distance from end of beam

1.0 inch = 25.4 mm

Table B.5 Concrete Compressive Strain, L6R0 (Continued)

Distance* (in.)	L6R0-1		L6R0-2	
	Short Term Strain (10^{-6})	Long Term Strain (10^{-6})	Short Term Strain (10^{-6})	Long Term Strain (10^{-6})
71.8	307	844	301	750
73.8	298	830	276	724
75.8	305	840	299	824
77.8	314	862	304	848
79.7	319	870	295	828
81.7	328	898	342	910
83.7	359	931	351	903
85.6	354	929	374	921
87.6	387	979	383	997
89.6	390	995	390	999
91.5	392	979	399	1041
93.5	427	1052	431	1025
95.5	420	1020	412	1018
97.4	417	998	411	1026
99.4	442	1028	424	932
101.4	431	1063	429	1053
103.4	442	1067	424	1073
105.3	444	1071	441	1109
107.3	457	1112	443	1101
109.3	472	1084	438	1122
111.2	469	1126	471	1110
113.2	470	1121	476	1106
115.2	478	1107	420	1113
117.1	489	1132	483	1181
119.1	510	1172	454	1134
121.1	529	1202	523	1176
123.0	524	1193	562	1213
125.0	524	1211	554	1255
127.0	549	1230	557	1284
128.9	552	1260	540	1242
130.9	567	1199	559	1293
132.9	541	1239	553	1253
134.8	548	1246	554	1238
136.8	545	1237	569	1263

* Distance from end of beam 1.0 inch = 25.4 mm

Table B.5 Concrete Compressive Strain, L6R0 (Continued)

Distance* (in.)	L6R0-1		L6R0-2	
	Short Term Strain (10^{-6})	Long Term Strain (10^{-6})	Short Term Strain (10^{-6})	Long Term Strain (10^{-6})
138.8	543	1211	559	1245
140.8	576	1226	560	1286
142.7	557	1214	591	1346
144.7	541	1203	559	1281
146.7	556	1252	566	1322
148.6	545	1260	583	1334
150.6	549	1239	547	1307
152.6	538	1232	554	1302
154.5	536	1225	551	1276
156.5	533	1205	567	1289
158.5	530	1190	584	1308
160.4	528	1173	567	1265
166.3	531	1150	581	1301
168.3	523	1195	560	1260
170.3	522	1167	528	1259
172.2	529	1190	553	1296
170.28	521	1153	537	1255
172.24	520	1120	536	1250

* Distance from end of beam 1.0 inch = 25.4 mm

Table B.6 Concrete Compressive Strain, L6R1

Distance* (in.)	L6R1-3		L6R1-4	
	Short Term Strain (10^{-6})	Long Term Strain (10^{-6})	Short Term Strain (10^{-6})	Long Term Strain (10^{-6})
4.9	61	352	73	377
6.9	80	423	94	431
8.9	120	524	124	512
10.8	137	556	143	532
12.8	162	582	184	590
14.8	163	616	181	634
16.7	186	606	192	606
18.7	189	600	205	636
20.7	170	559	184	612
22.6	202	581	194	618
24.6	193	555	189	625
26.6	196	577	190	637
28.5	181	549	205	603
30.5	202	639	184	573
32.5	195	665	223	629
34.5	210	627	232	677
36.4	219	607	239	705
38.4	228	668	242	746
40.4	225	662	275	734
42.3	234	678	254	752
44.3	244	754	280	768
46.3	225	700	255	734
48.2	242	686	278	786
50.2	243	708	275	762
52.2	228	704	266	754
54.1	247	752	283	792
56.1	256	760	296	776
58.1	293	766	297	811
60.0	274	769	296	799
62.0	277	777	277	820
64.0	288	778	330	861
65.9	289	811	298	828
67.9	282	816	301	814
69.9	292	814	308	820

* Distance from end of beam

1.0 inch = 25.4 mm

Table B.6 Concrete Compressive Strain, L6R1 (Continued)

Distance* (in.)	L6R1-3		L6R1-4	
	Short Term Strain (10^{-6})	Long Term Strain (10^{-6})	Short Term Strain (10^{-6})	Long Term Strain (10^{-6})
71.8	313	850	321	826
73.8	318	838	314	862
75.8	341	902	333	876
77.8	340	876	344	886
79.7	353	898	357	908
81.7	370	958	362	914
83.7	381	899	377	919
85.6	394	971	392	959
87.6	399	981	409	993
89.6	410	967	420	1029
91.5	401	941	421	1049
93.5	387	962	417	1033
95.5	422	1052	438	1016
97.4	415	1058	439	1050
99.4	432	1006	448	1040
101.4	405	981	439	1041
103.4	396	1029	458	1069
105.3	414	1055	438	1069
107.3	441	1099	483	1090
109.3	468	1110	472	1104
111.2	471	1110	501	1114
113.2	486	1129	480	1123
115.2	482	1119	496	1135
117.1	497	1175	513	1130
119.1	508	1178	524	1190
121.1	523	1192	563	1216
123.0	554	1239	487	1147
125.0	558	1213	532	1213
127.0	571	1228	543	1214
128.9	538	1262	558	1244
130.9	541	1239	565	1285
132.9	551	1253	529	1261
134.8	550	1244	548	1270
136.8	543	1230	553	1268

* Distance from end of beam

1.0 inch = 25.4 mm

Table B.6 Concrete Compressive Strain, L6R1 (Continued)

Distance* (in.)	L6R1-3		L6R1-4	
	Short Term Strain (10^{-6})	Long Term Strain (10^{-6})	Short Term Strain (10^{-6})	Long Term Strain (10^{-6})
138.8	545	1239	567	1303
140.8	536	1218	570	1286
142.7	551	1254	557	1236
144.7	533	1221	565	1269
146.7	530	1230	570	1260
148.6	539	1242	569	1264
150.6	543	1247	565	1265
152.6	542	1264	554	1264
154.5	543	1262	561	1256
156.5	541	1247	585	1265
158.5	556	1236	560	1262
160.4	546	1266	566	1237
166.3	556	1231	568	1245
168.3	553	1252	577	1264
170.3	565	1265	567	1259
172.2	562	1256	534	1220

* Distance from end of beam 1.0 inch = 25.4 mm

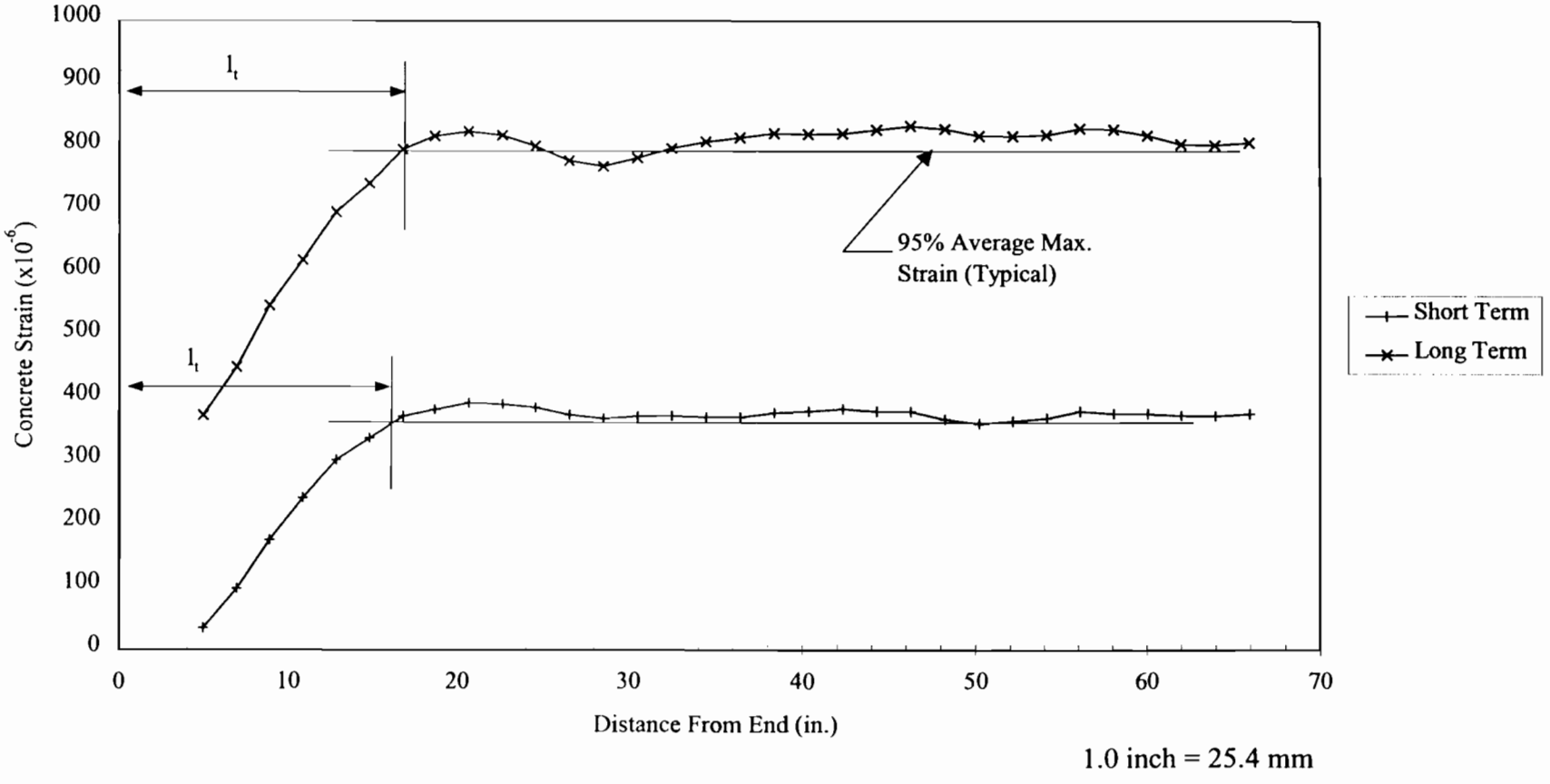

Figure B.1 Transfer Length of L0R0-1

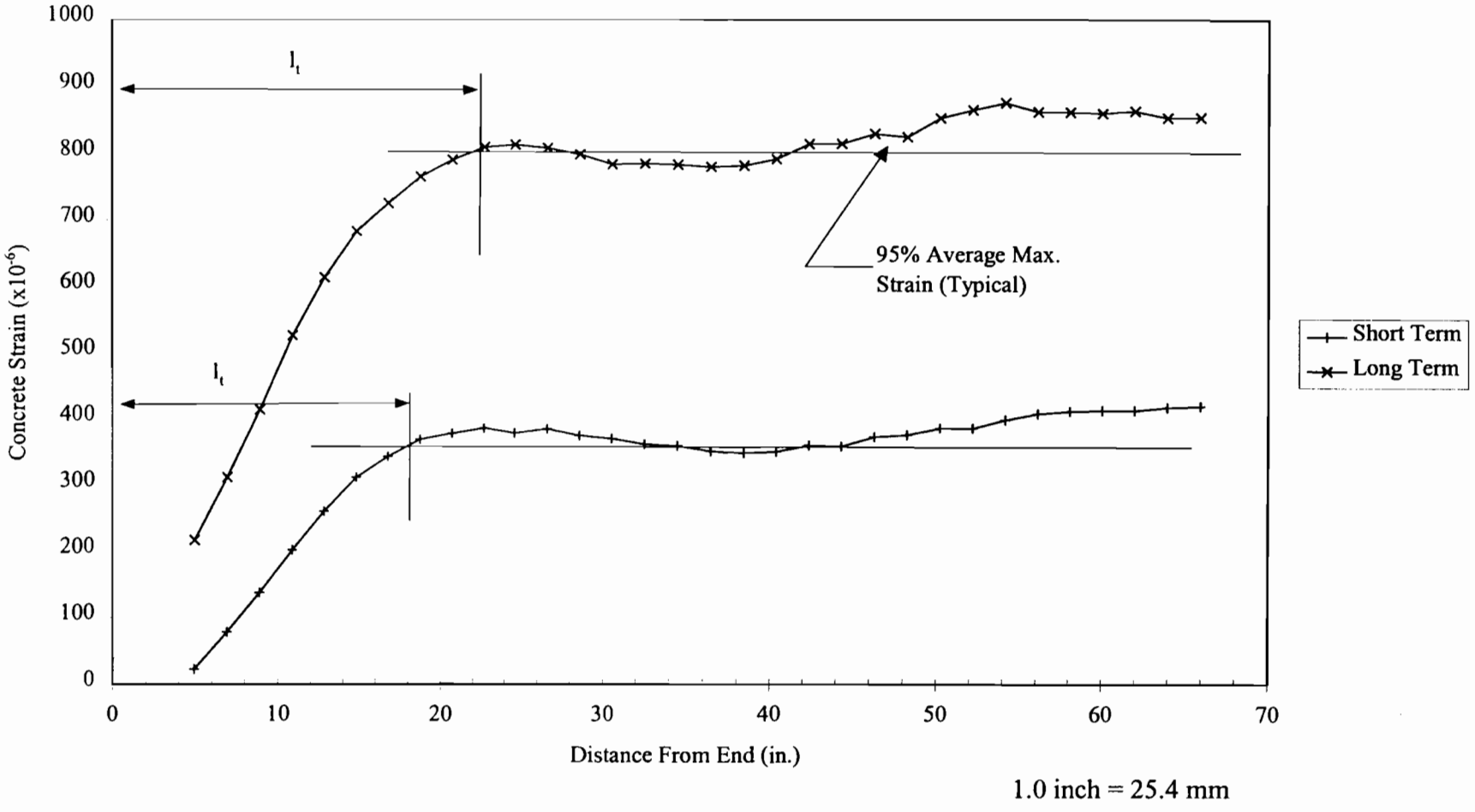

Figure B.2 Transfer Length 0f L0R0-2

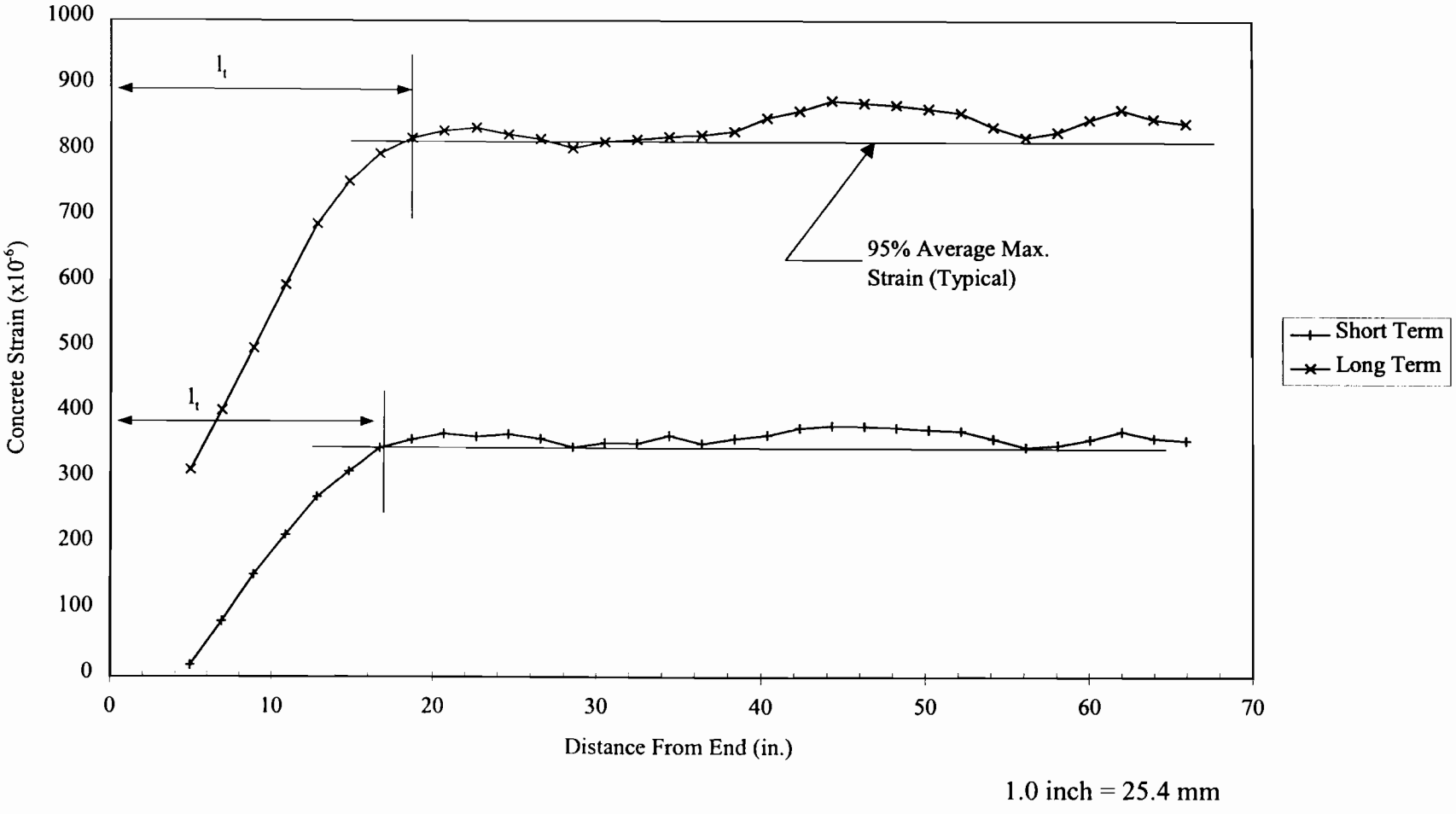

Figure B.3 Transfer Length of L0R1-3

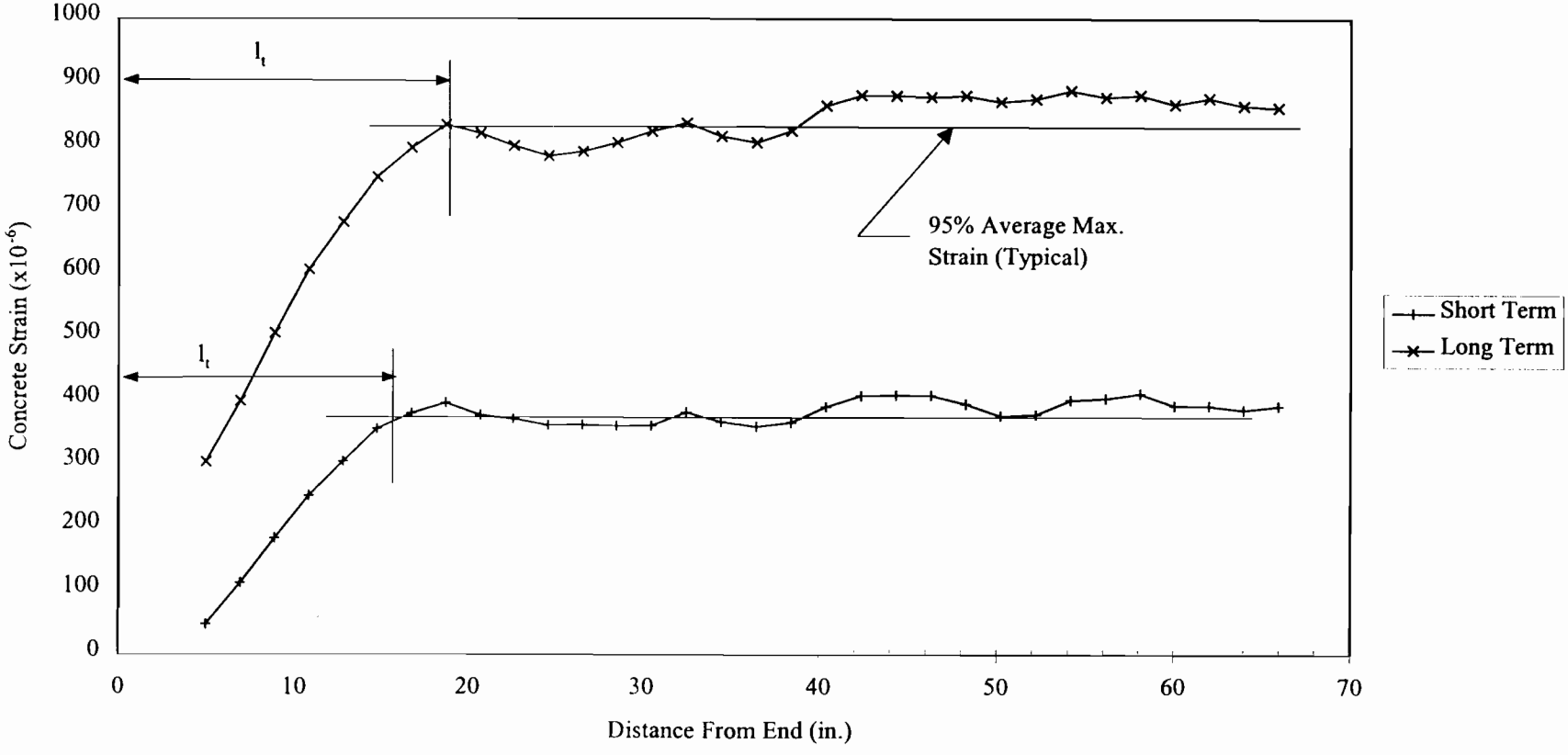

1.0 inch = 25.4 mm

Figure B.4 Transfer Length of L0R1-4

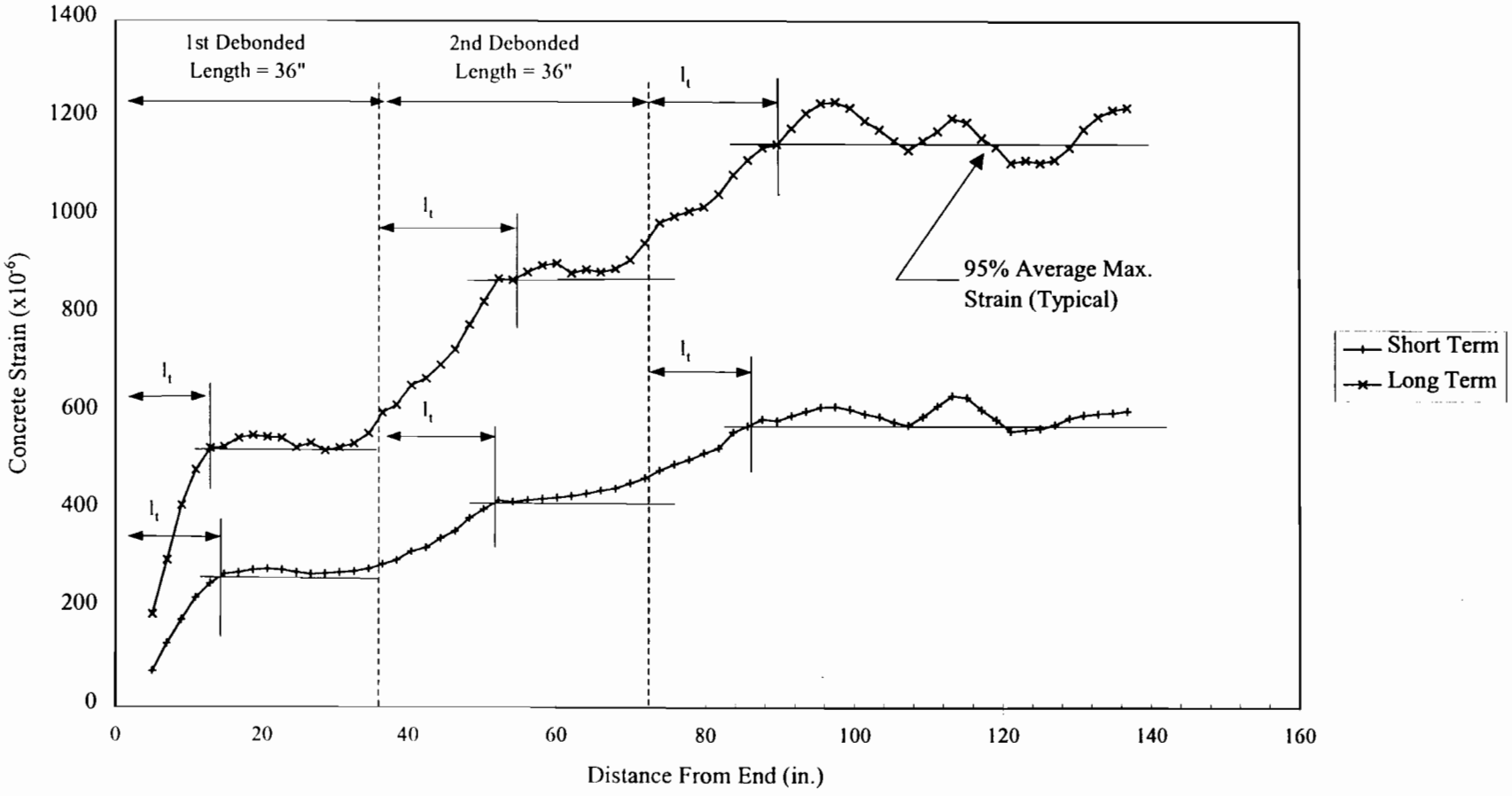

1.0 inch = 25.4 mm

Figure B.5 Transfer Length of L4R0-1

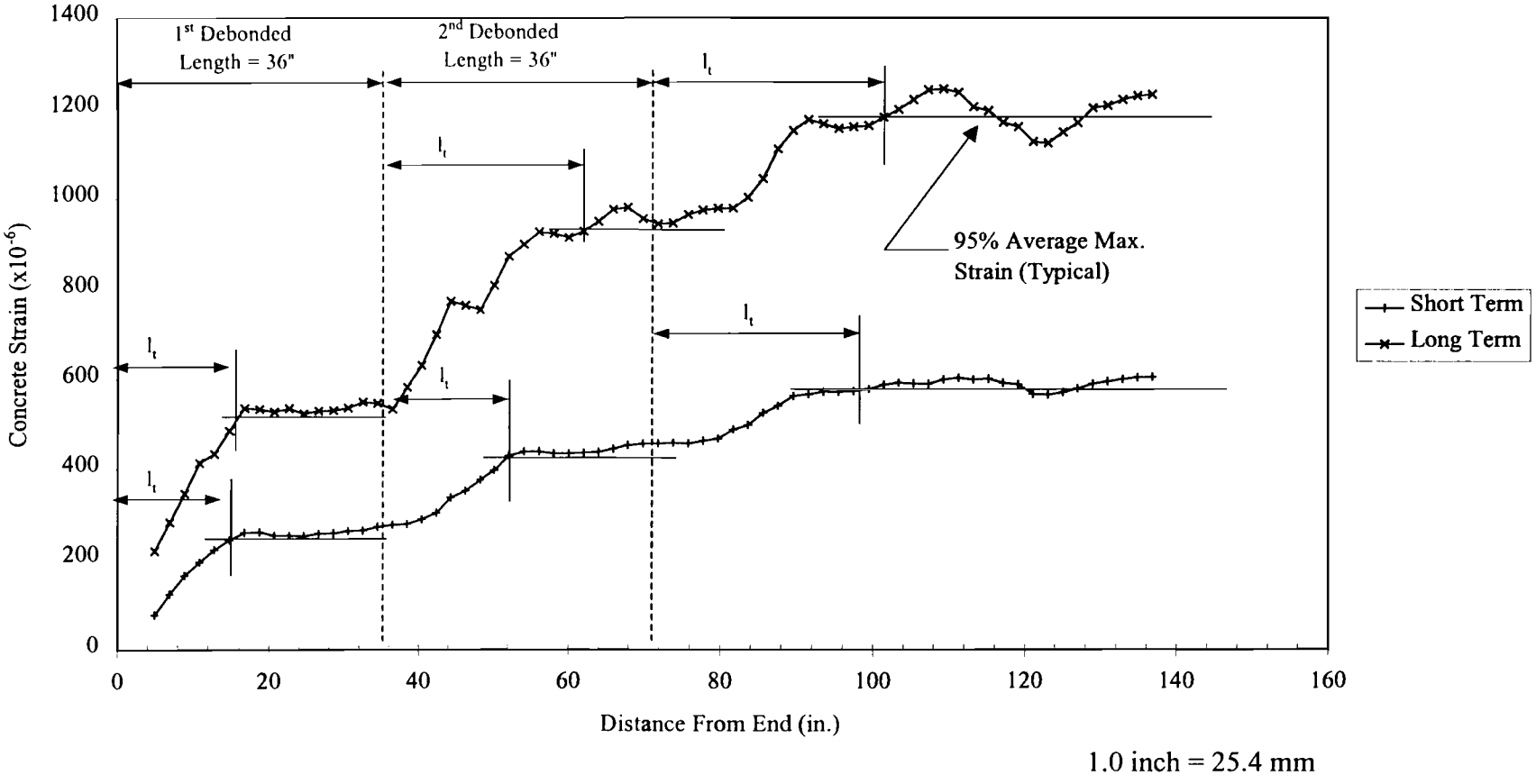

1.0 inch = 25.4 mm

Figure B.6 Transfer Length of L4R0-2

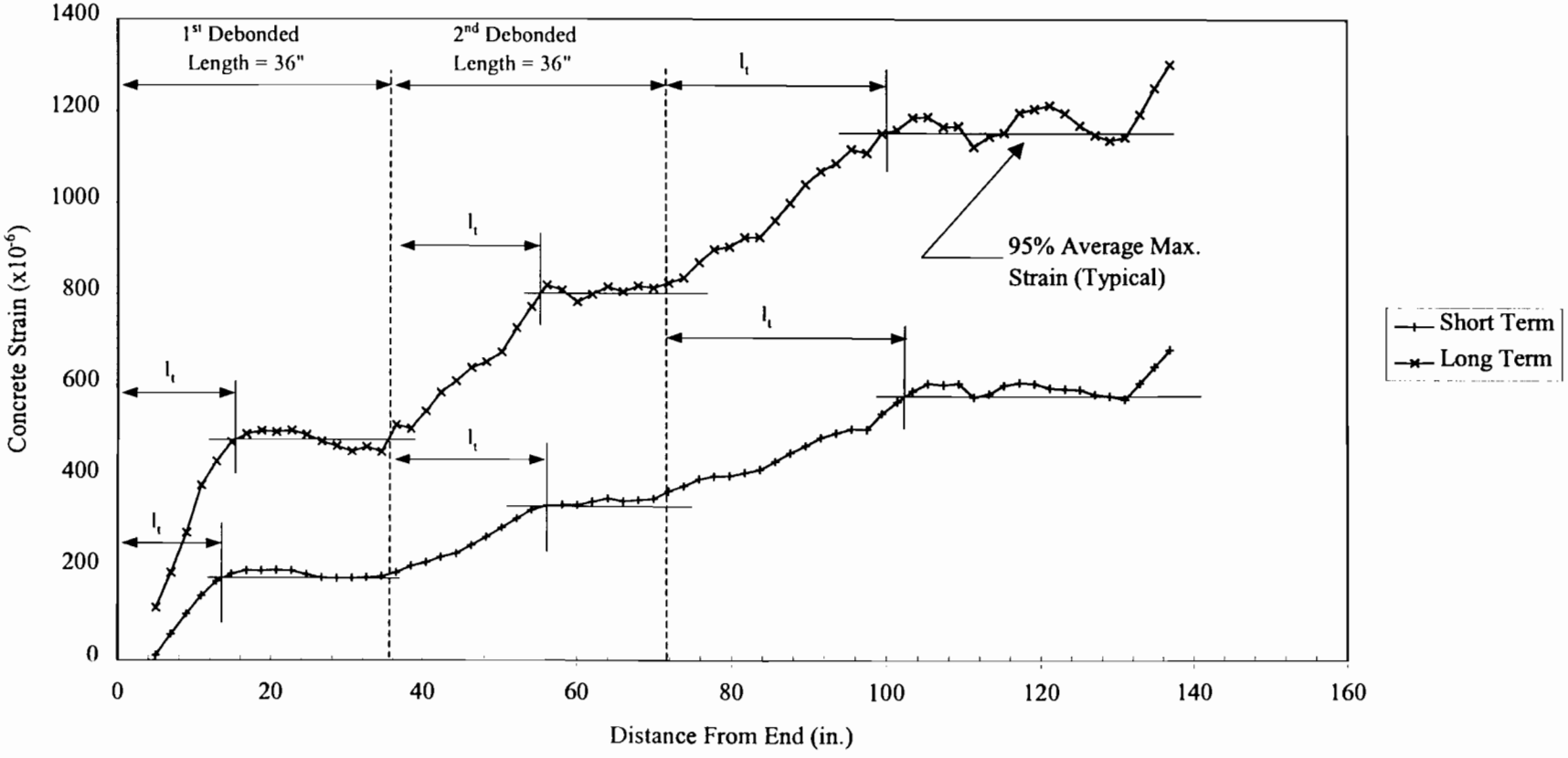

1.0 inch = 25.4 mm

Figure B.7 Transfer Length of L4R1-3

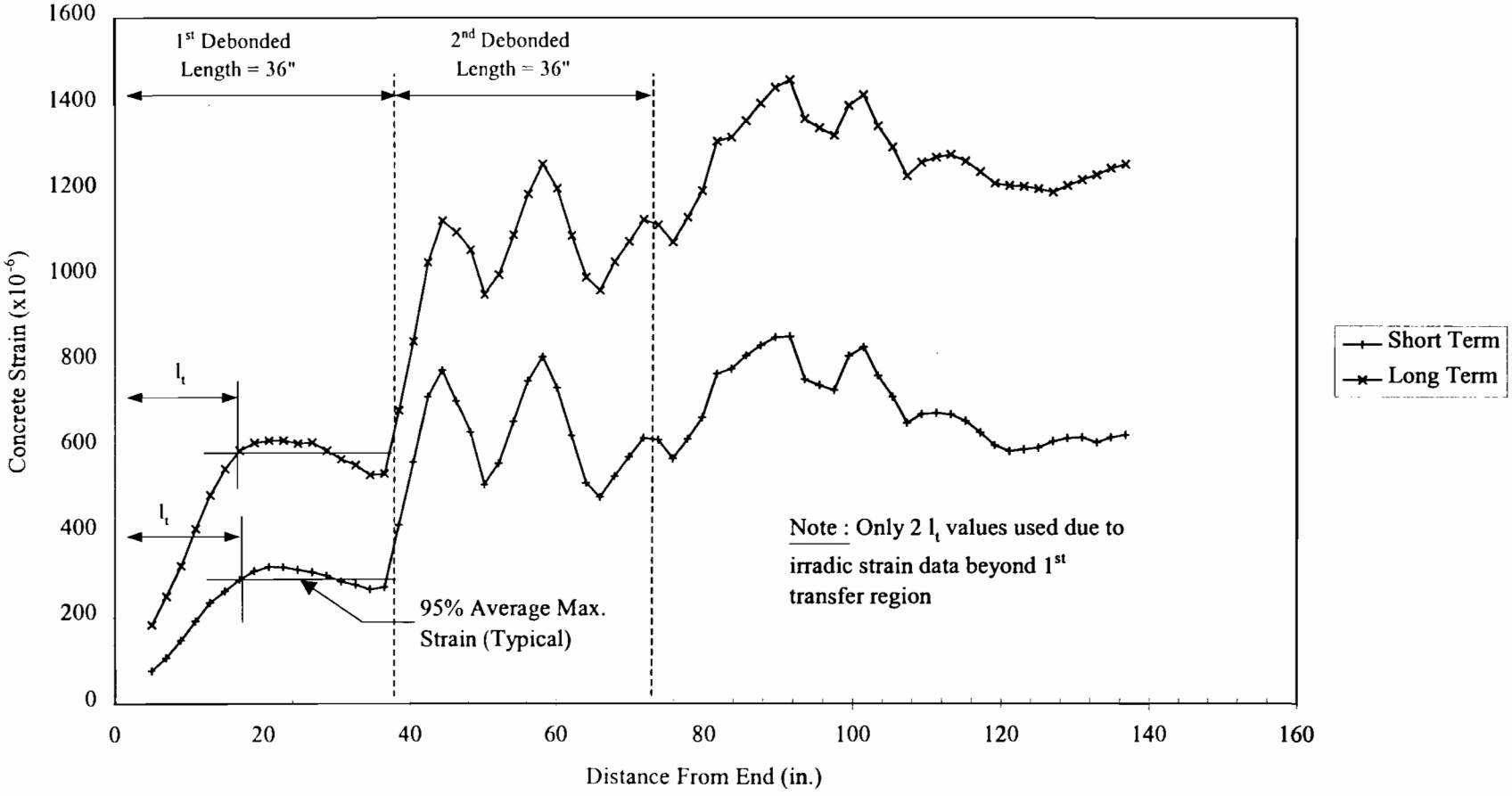

1.0 inch = 25.4 mm

Figure B.8 Transfer Length of L4R1-4

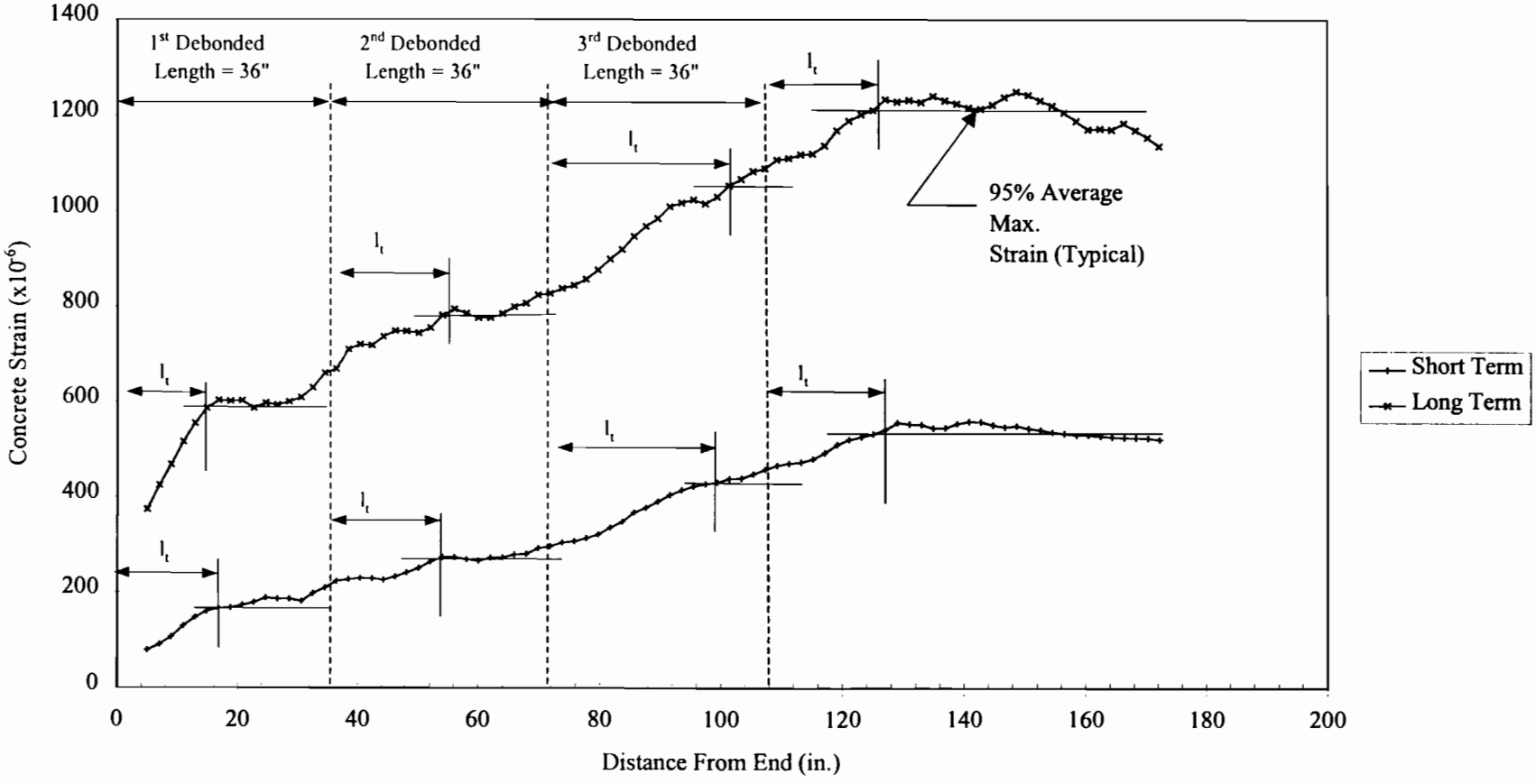

1.0 inch = 25.4 mm

Figure B.9 Transfer Length of L6R0-1

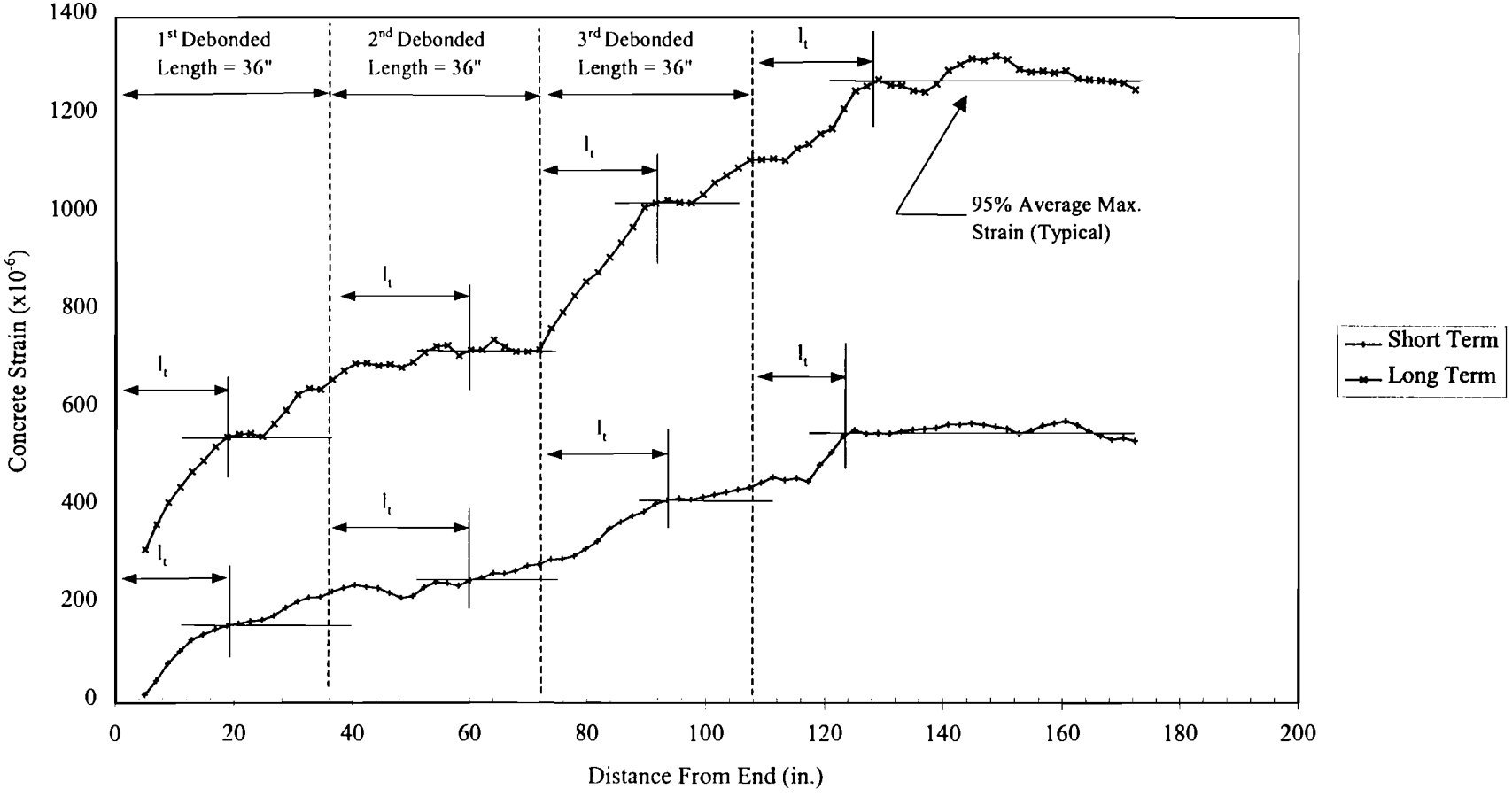

Figure B.10 Transfer Length of L6R0-2

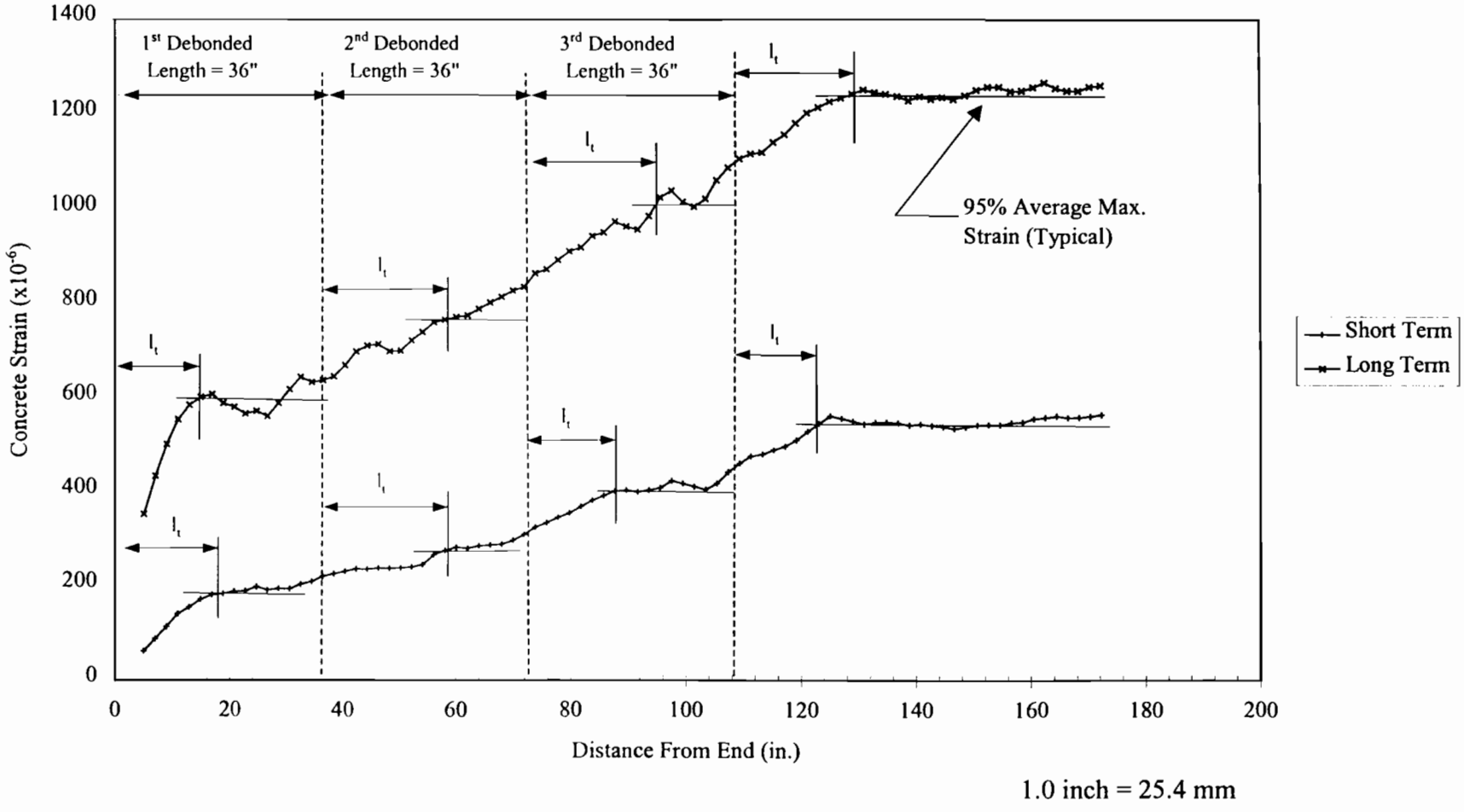

1.0 inch = 25.4 mm

Figure B.11 Transfer Length of L6R1-3

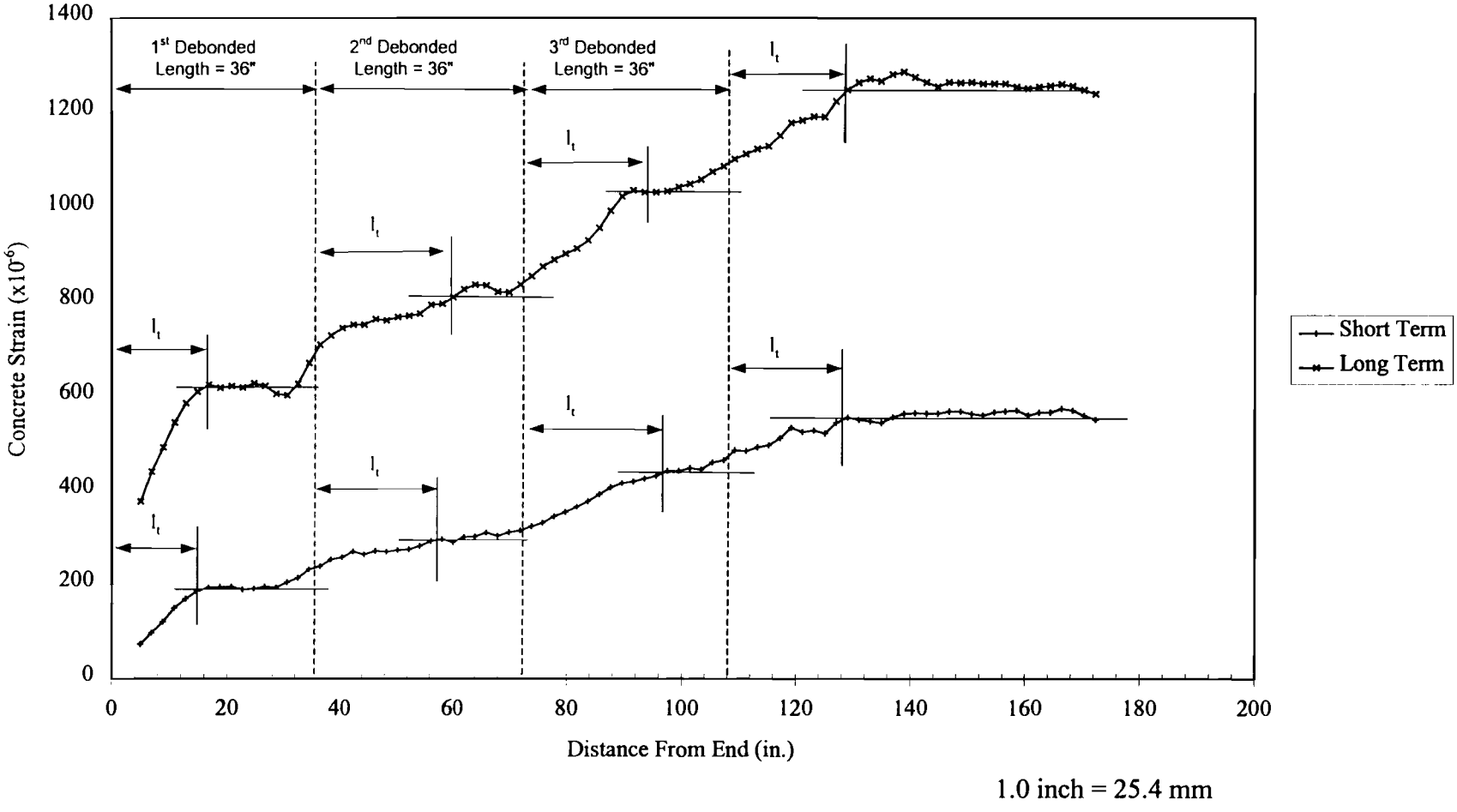

Figure B.12 Transfer Length of L6R1-4

APPENDIX C

LOAD-DEFLECTION CURVES

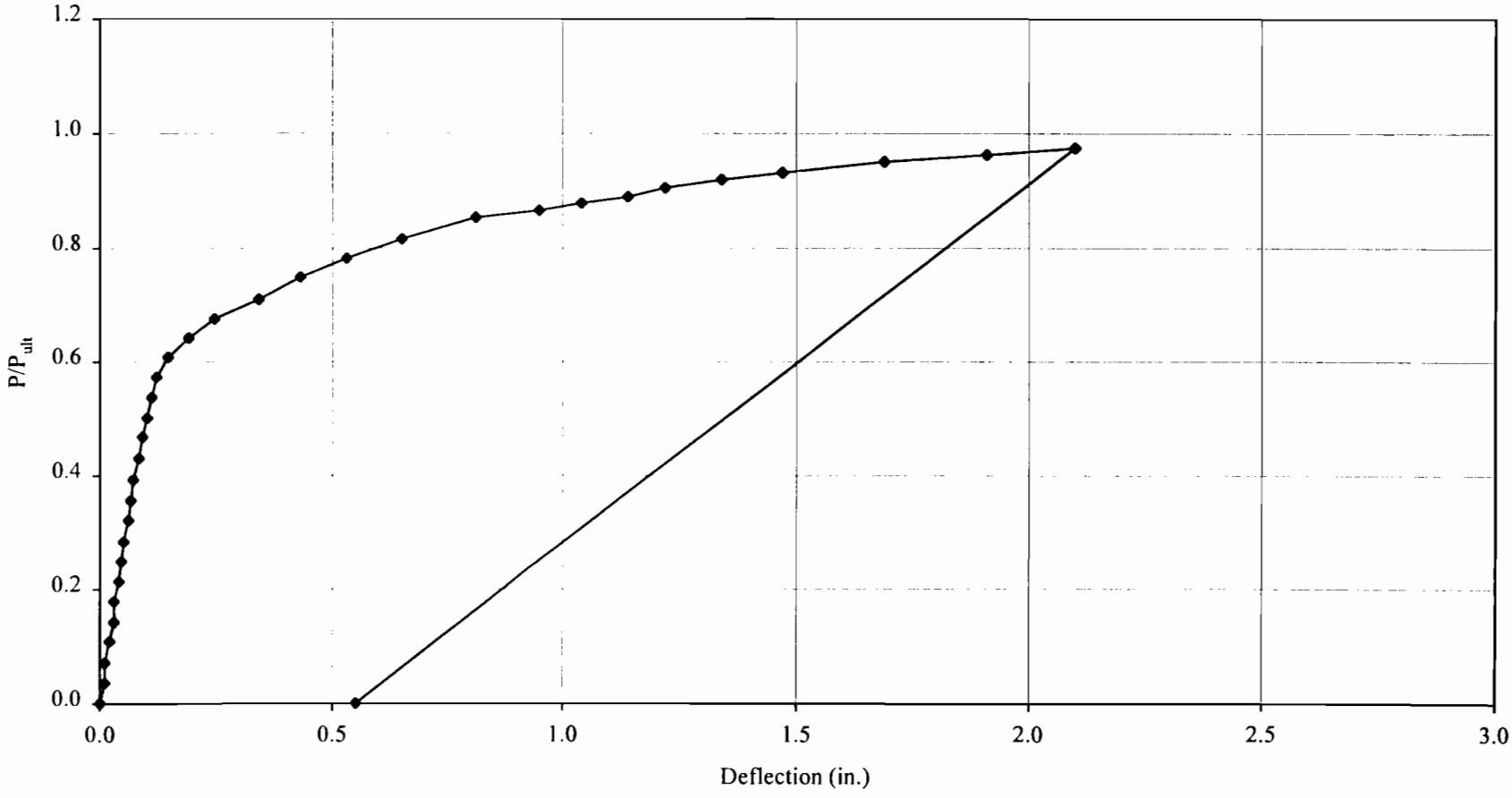

1.0 inch = 25.4 mm

Figure C.1 Load – Deflection Curve of L0R0-1 (P_{ult} = 276.6 kips (1,231 N))

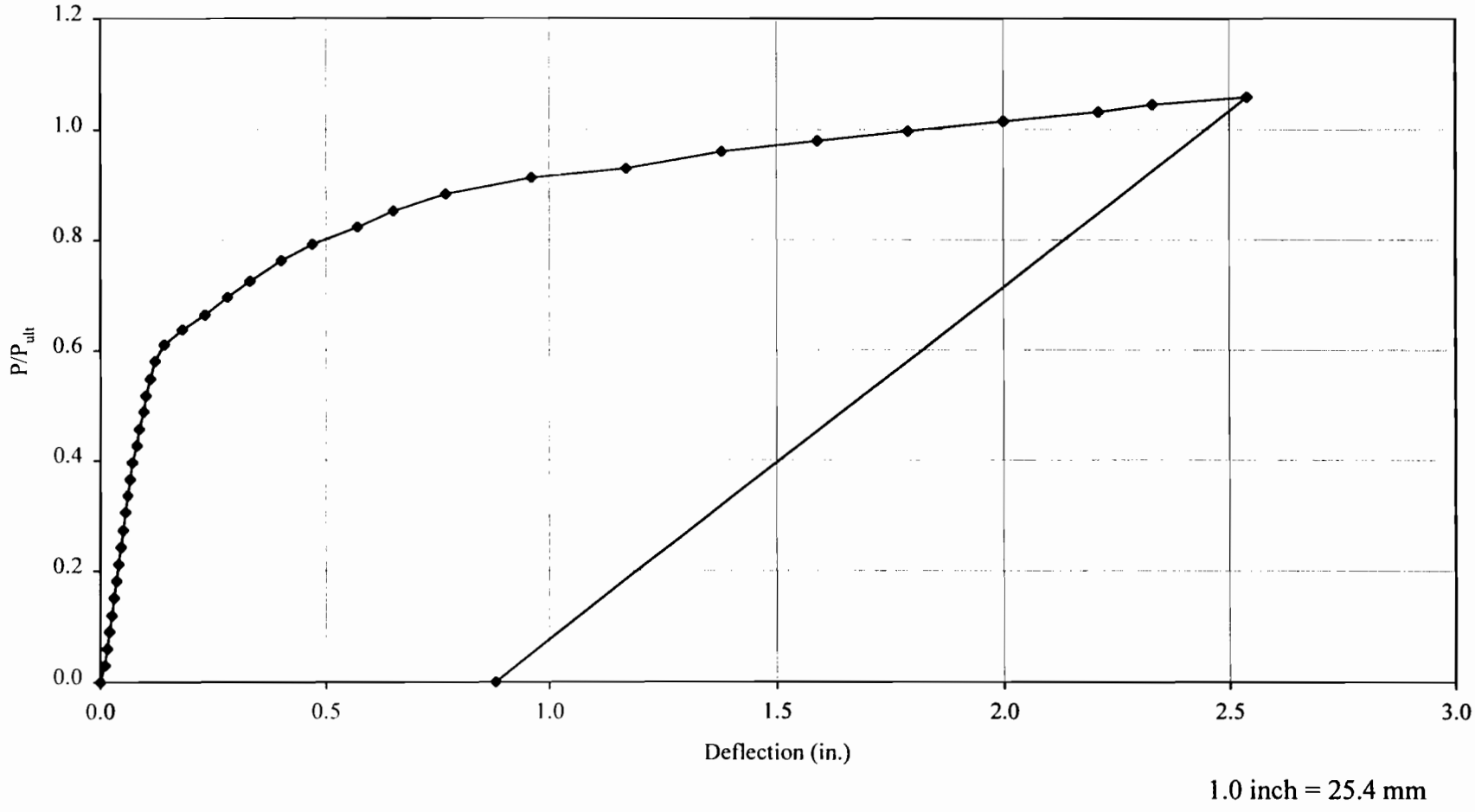

Figure C.2 Load – Deflection Curve of L0R0-2 (P_{ult} = 322.1 kips (1,433 N))

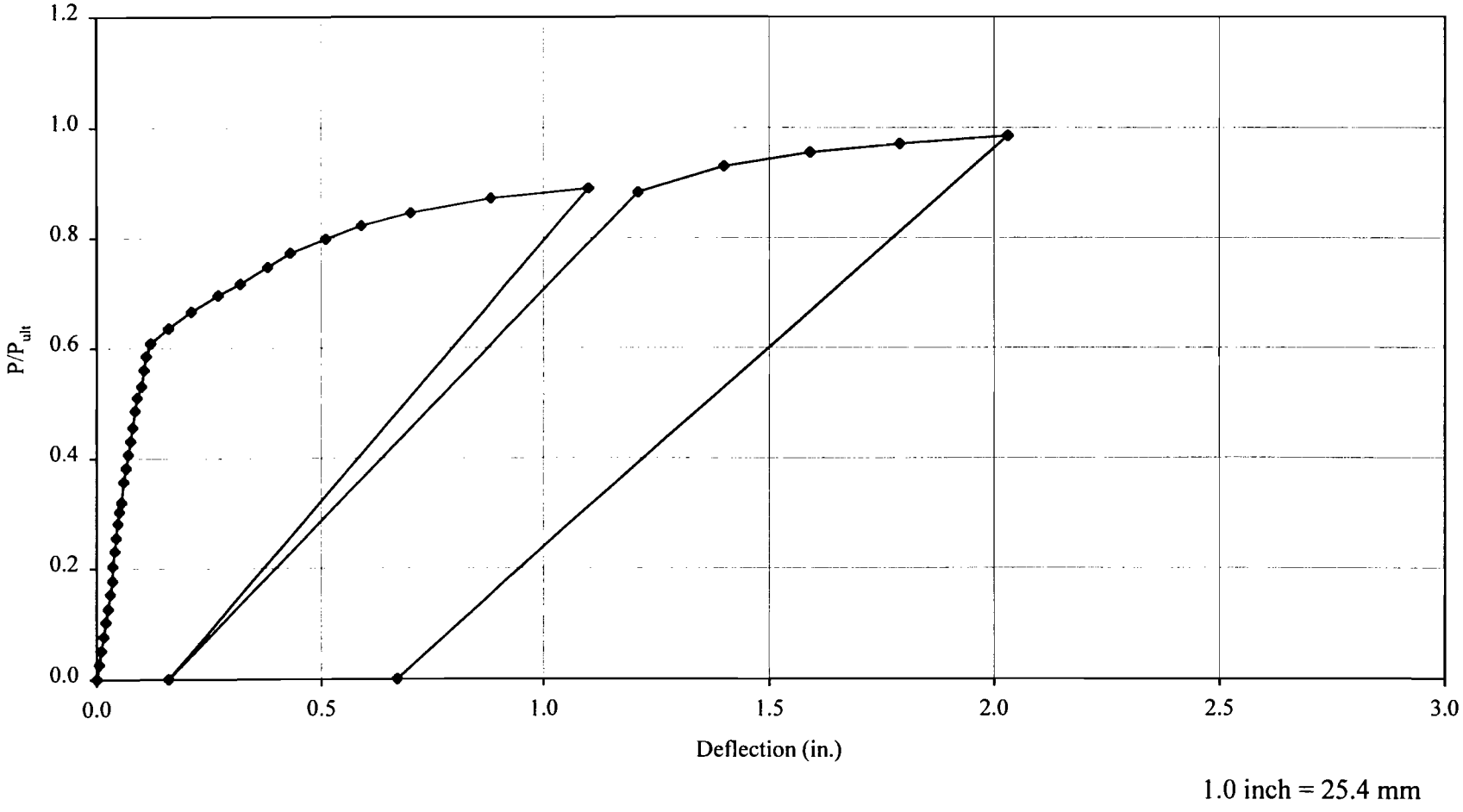

Figure C.3 Load – Deflection Curve of L0R1-3 (P_{ult} = 384.7 kips (1,712 N))

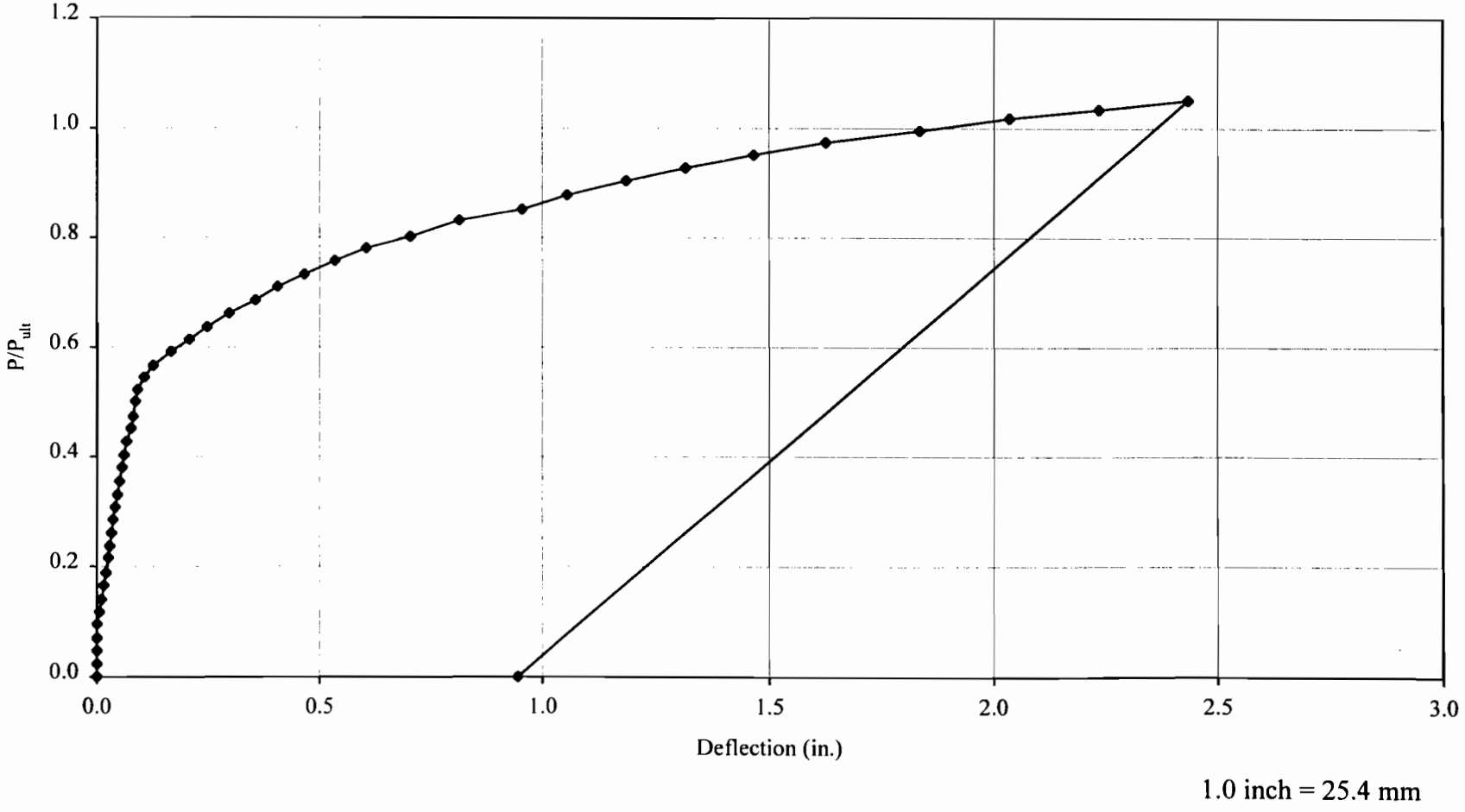

Figure C.4 Load – Deflection Curve of L0R1-4 (P_{ult} = 413.7 kips (1,841 N))

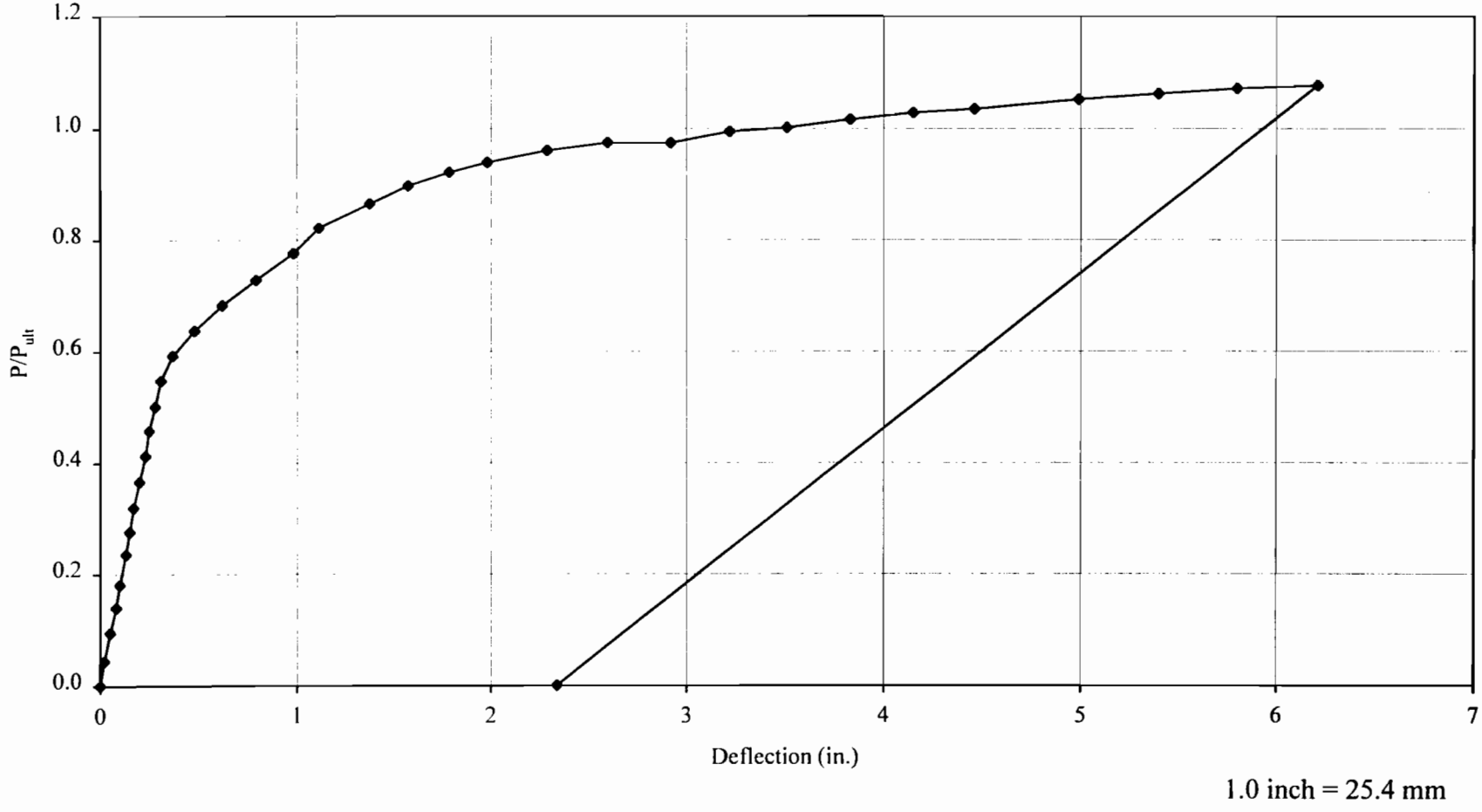

Figure C.5 Load – Deflection Curve of L4R0-1 (P_{ult} = 215.5 kips (959 N))

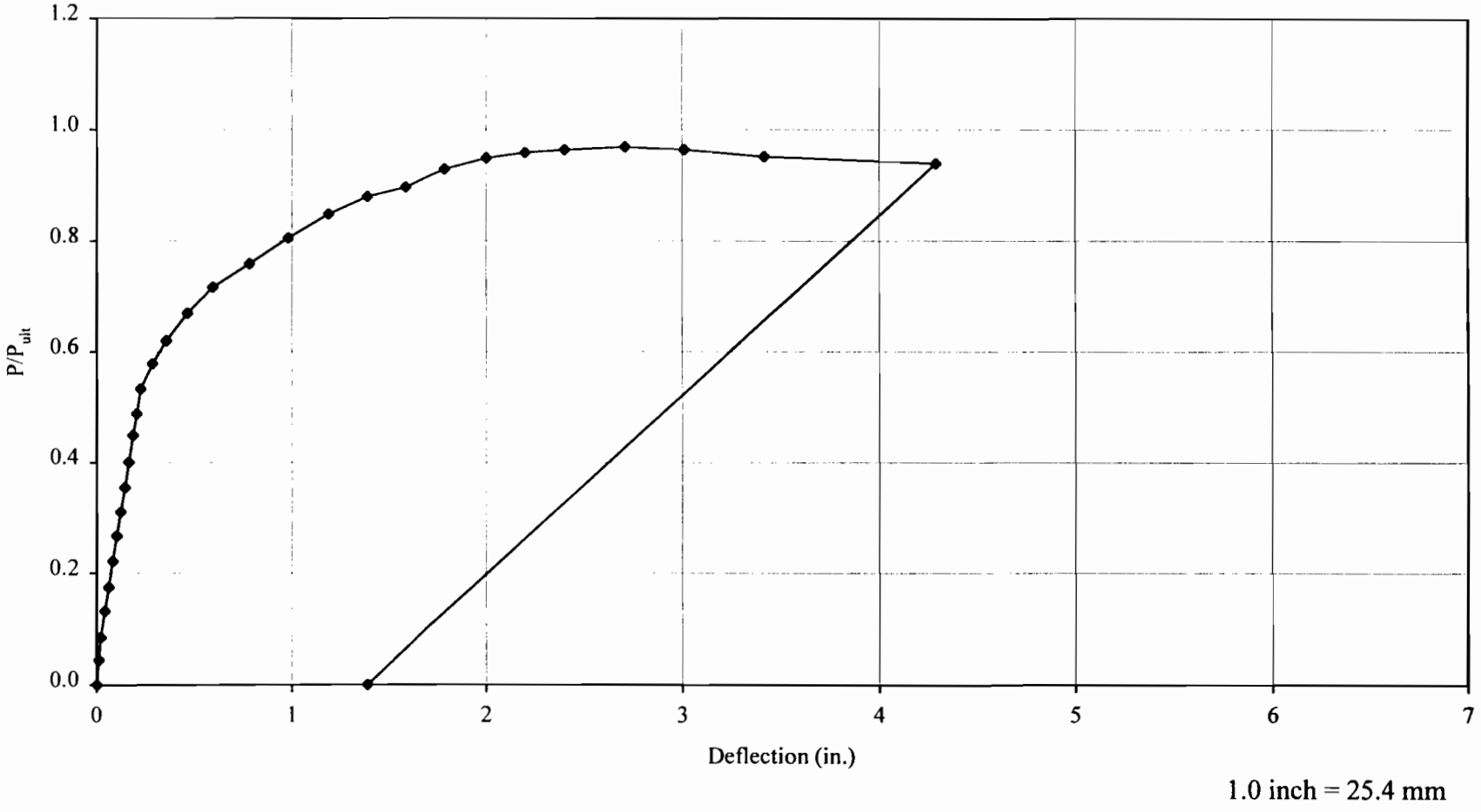

Figure C.6 Load – Deflection Curve of L4R0-2 (P_{ult} = 219.8 kips (978 N))

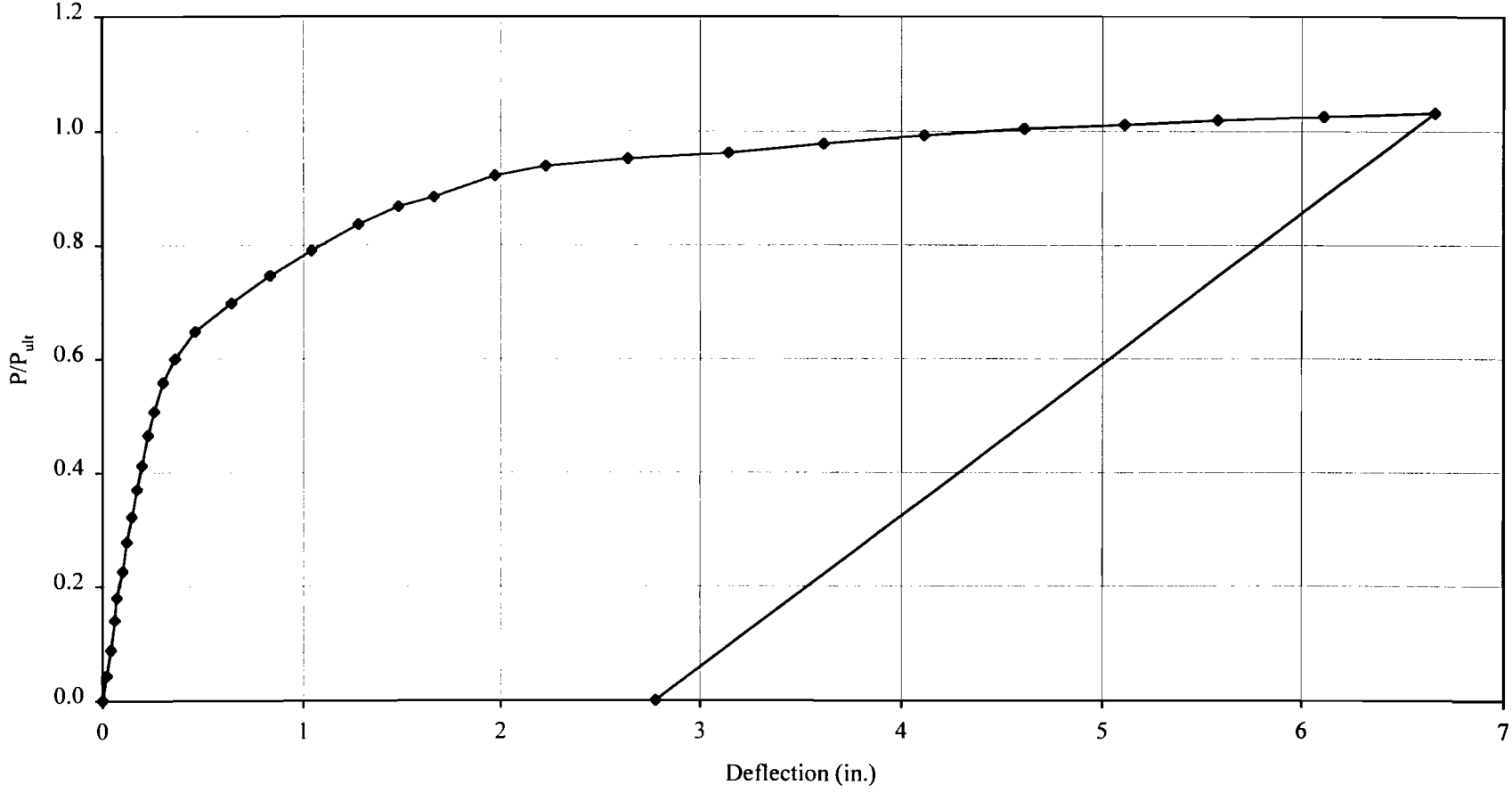

1.0 inch = 25.4 mm

Figure C.7 Load – Deflection Curve of L4R1-3 (P_{ult} = 211.1 kips (939 N))

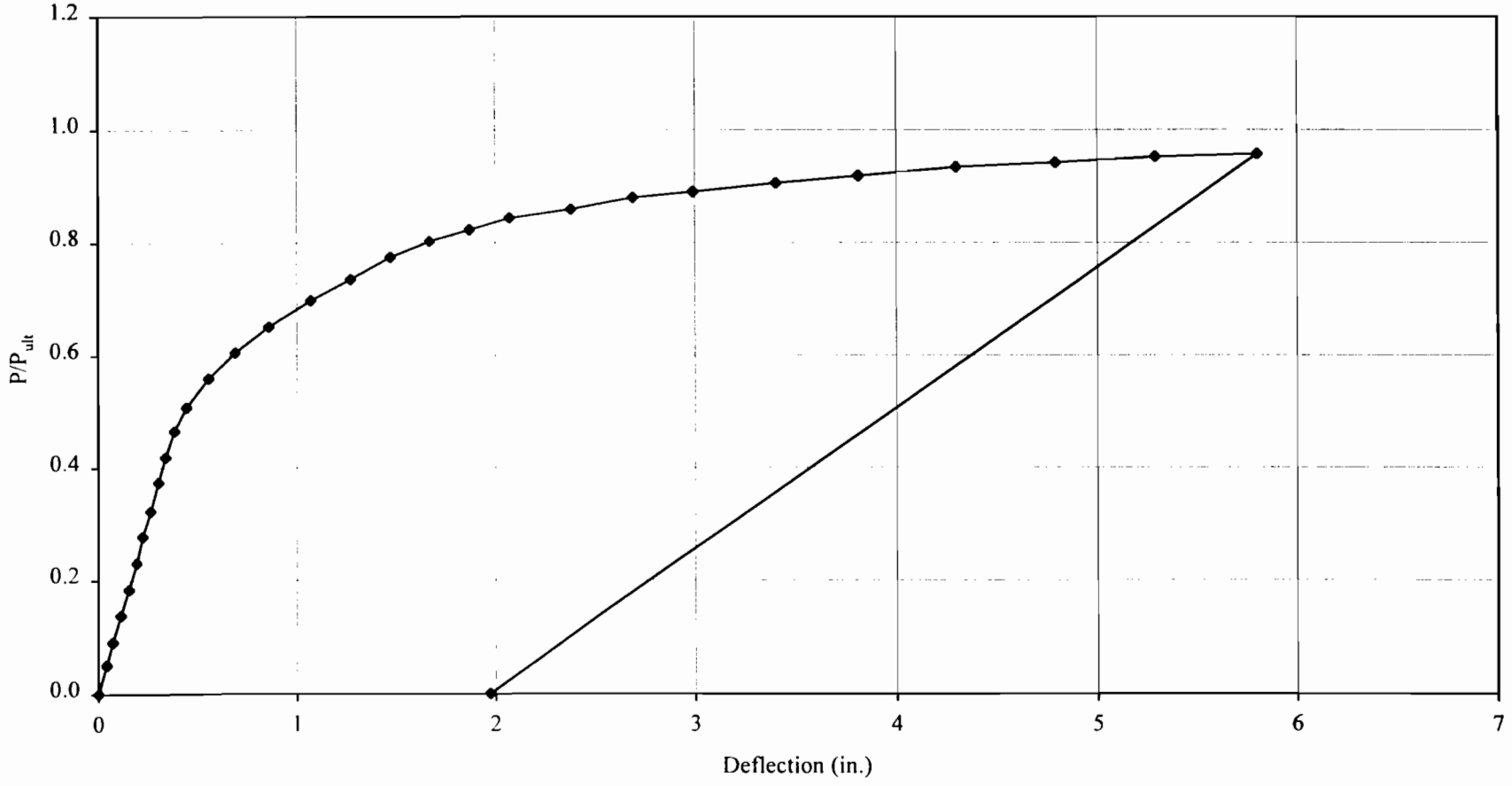

1.0 inch = 25.4 mm

Figure C.8 Load – Deflection Curve of L4R1-4 (P_{ult} = 211.1 kips (939 N))

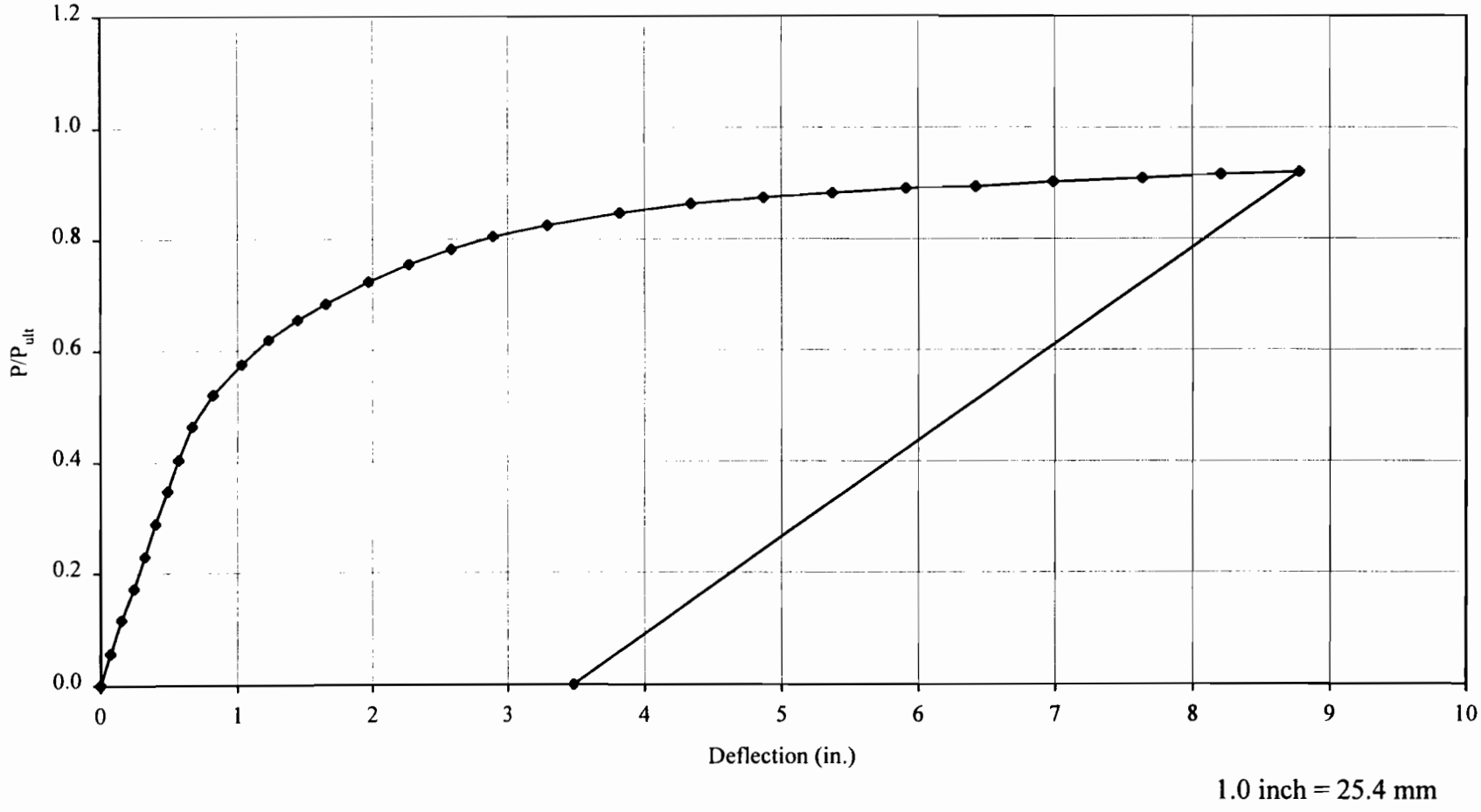

Figure C.9 Load – Deflection Curve of L6R0-1 (P_{ult} = 170.3 kips (758 N))

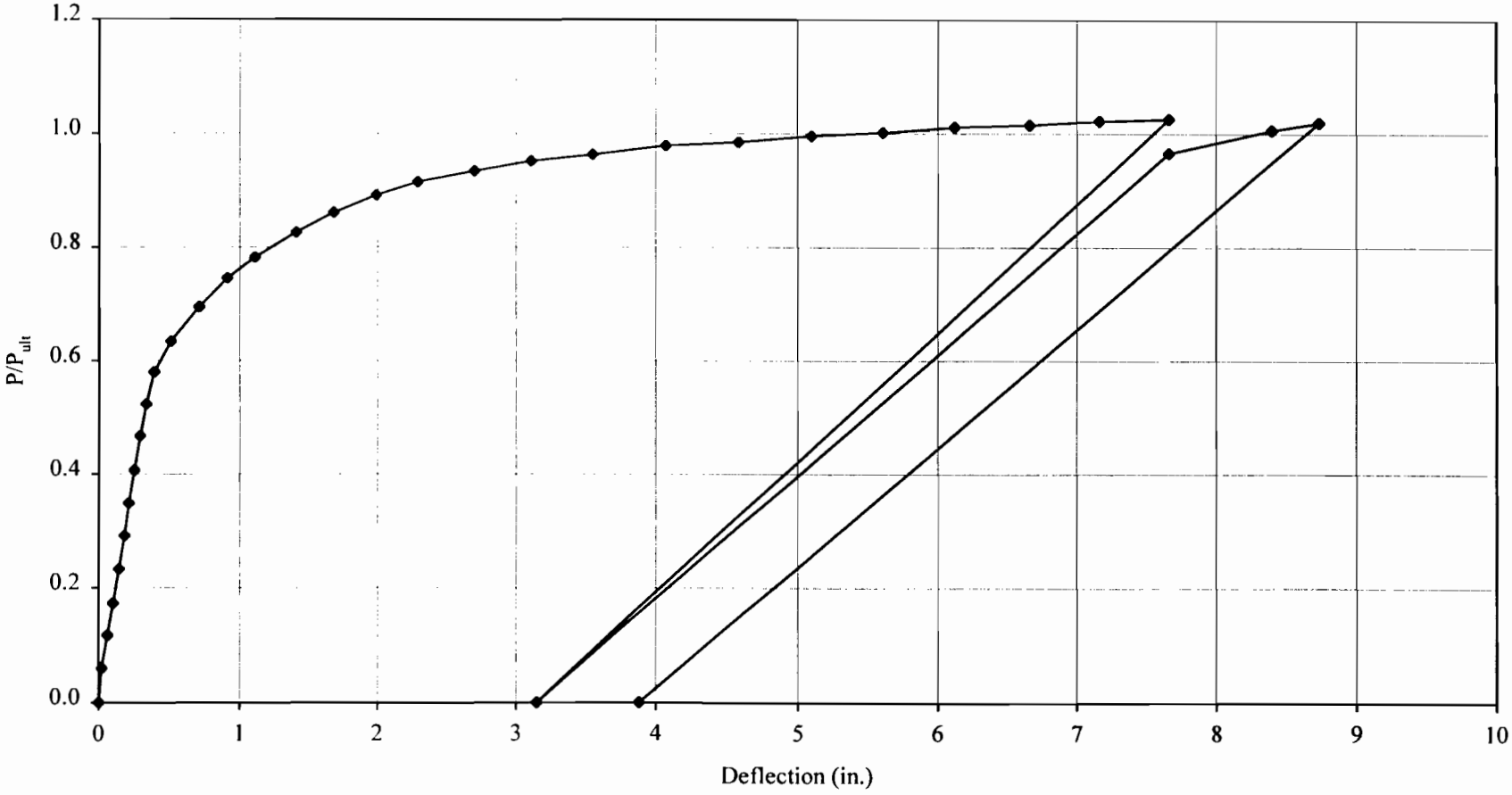

Figure C.10 Load – Deflection Curve of L6R0-2 (P_{ult} = 169.7 kips (755 N))

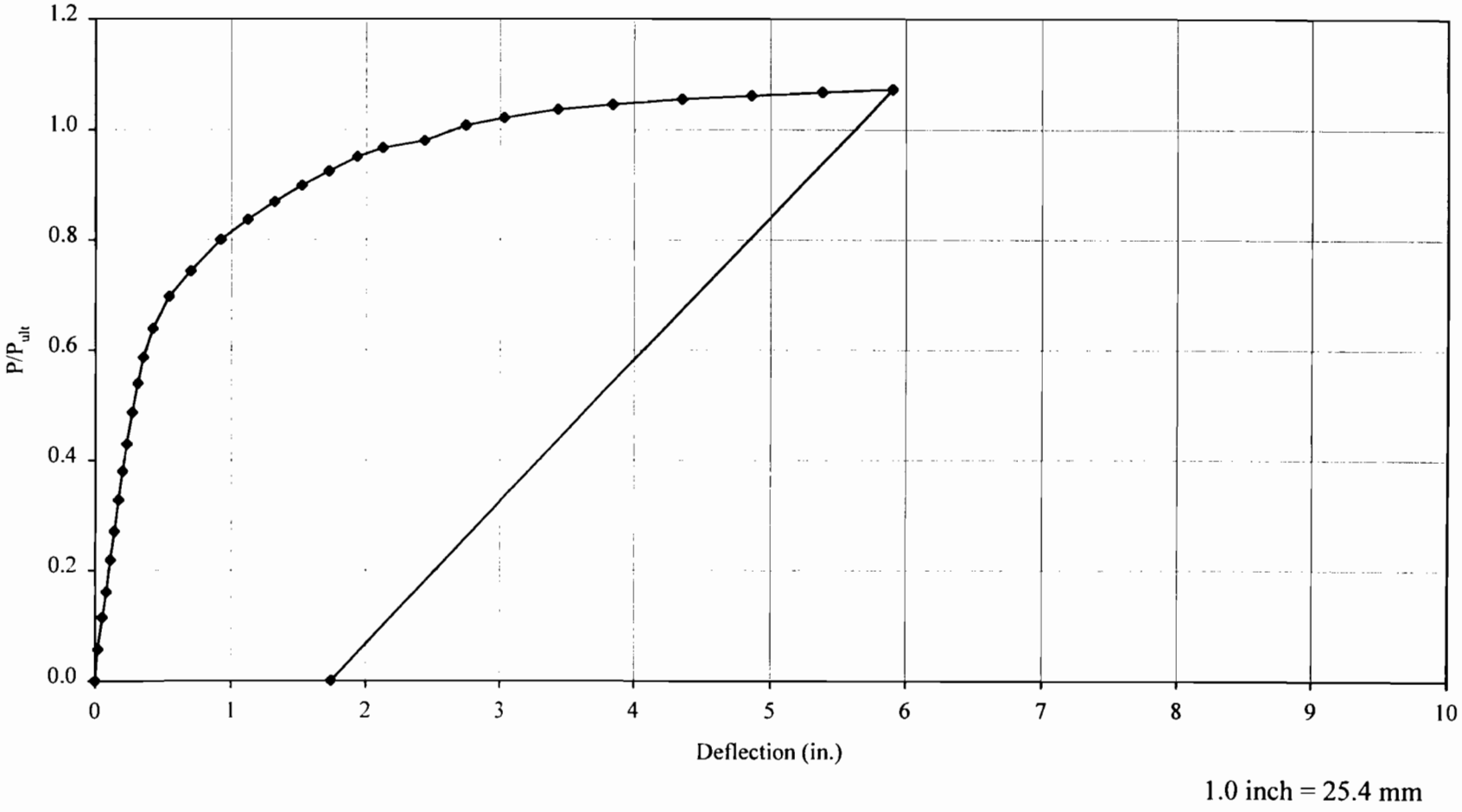

Figure C.11 Load – Deflection Curve of L6R1-3 (P_{ult} = 183.8 kips (818 N))

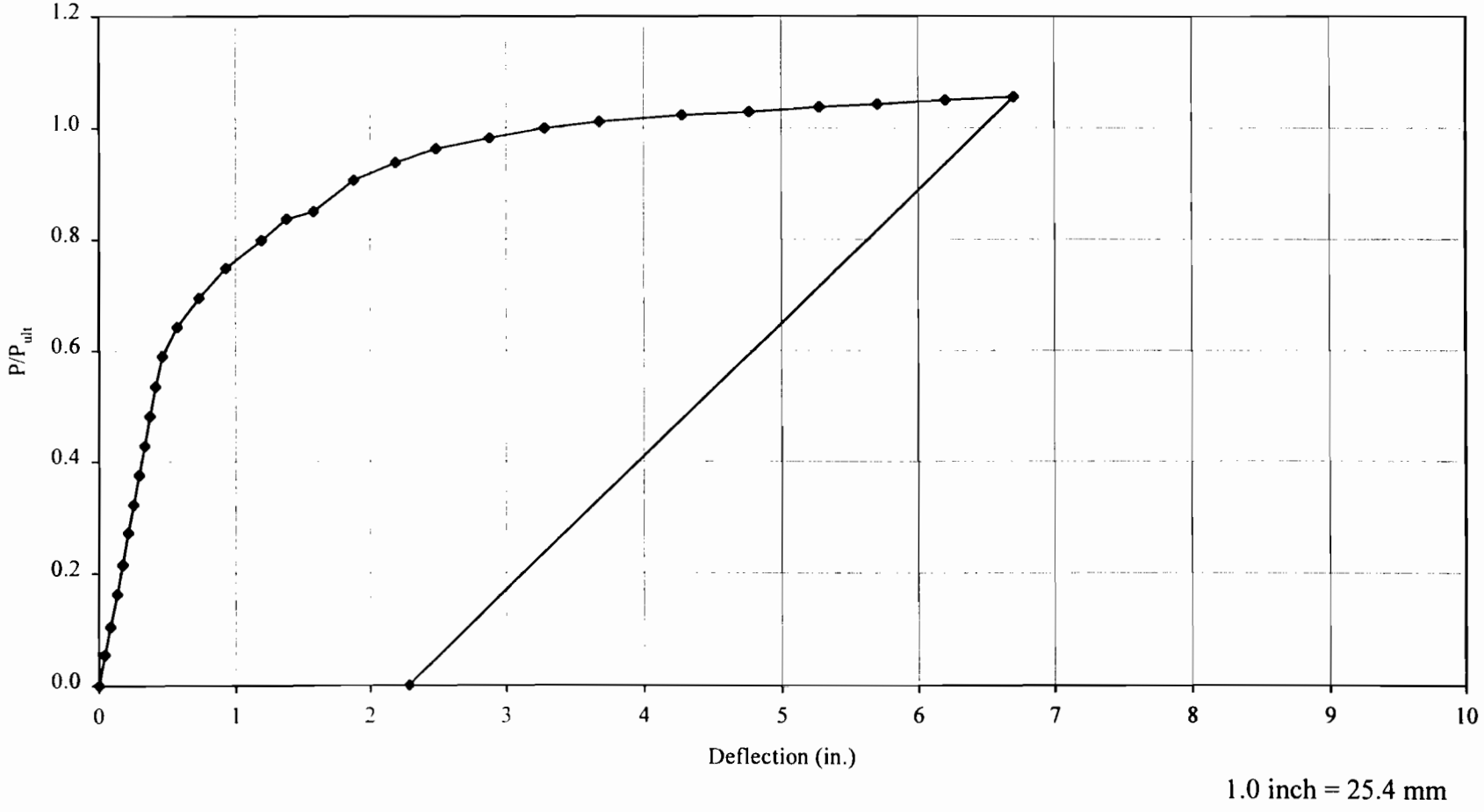

Figure C.12 Load – Deflection Curve of L6R1-4 (P_{ult} = 183.8 kips (818 N))

APPENDIX D

LOAD-END SLIP CURVES

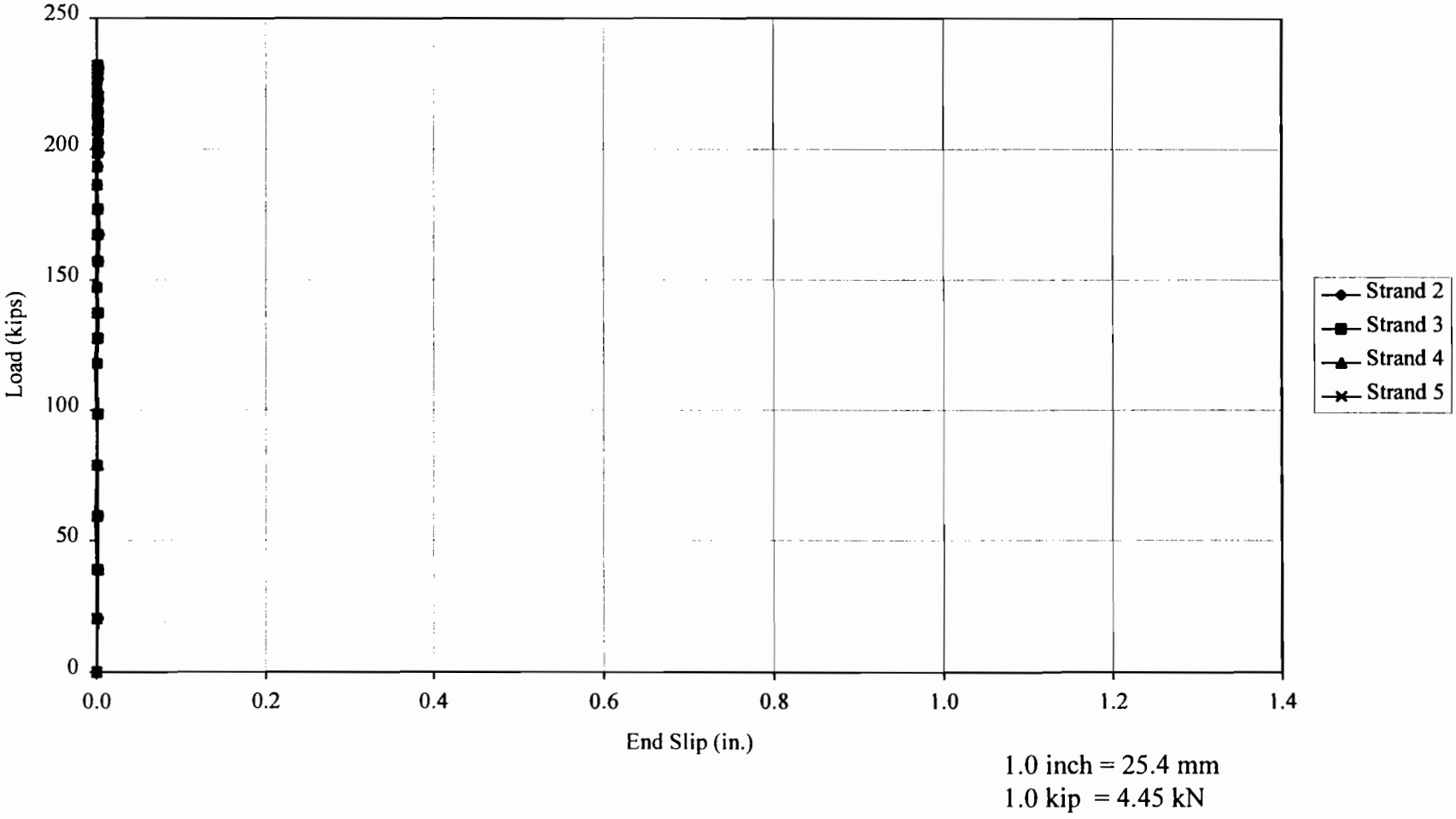

1.0 inch = 25.4 mm
1.0 kip = 4.45 kN

Figure D.1 Load – End Slip Curve of L4R0-1

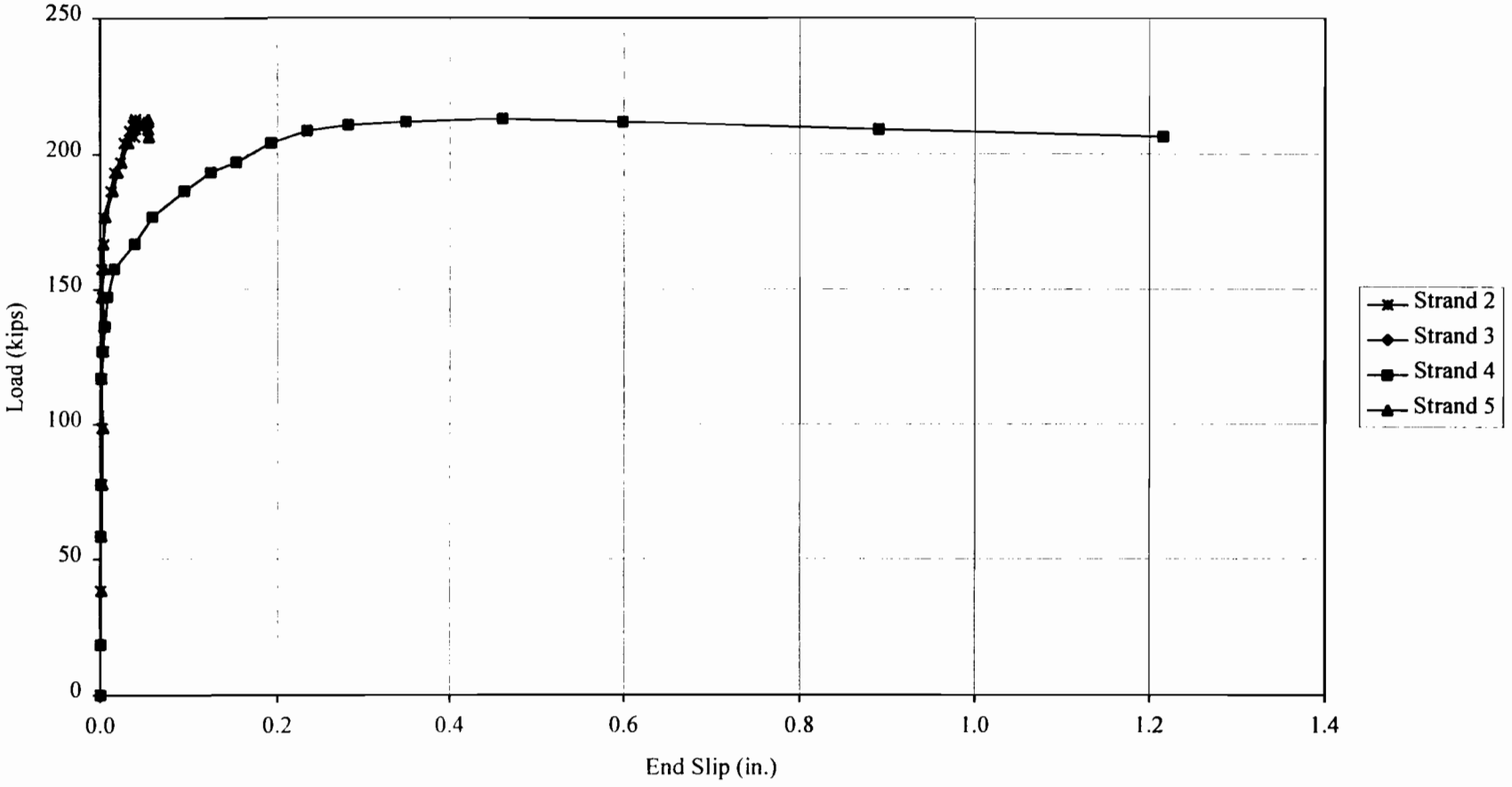

Figure D.2 Load-End Slip Curve of L4R0-2

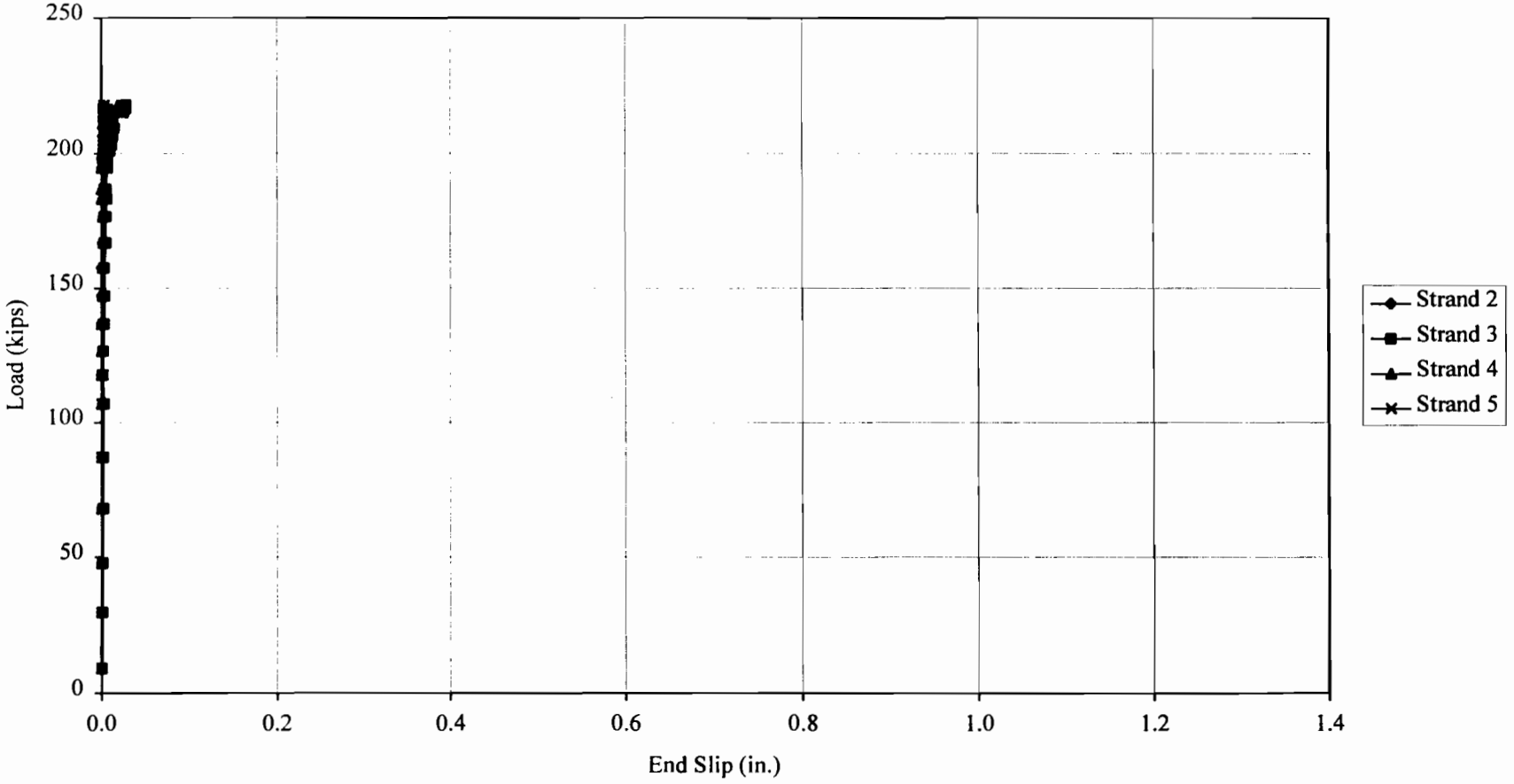

1.0 inch = 25.4 mm
1.0 kip = 4.45 kN

Figure D.3 Load - End Slip Curve of L4R1-3

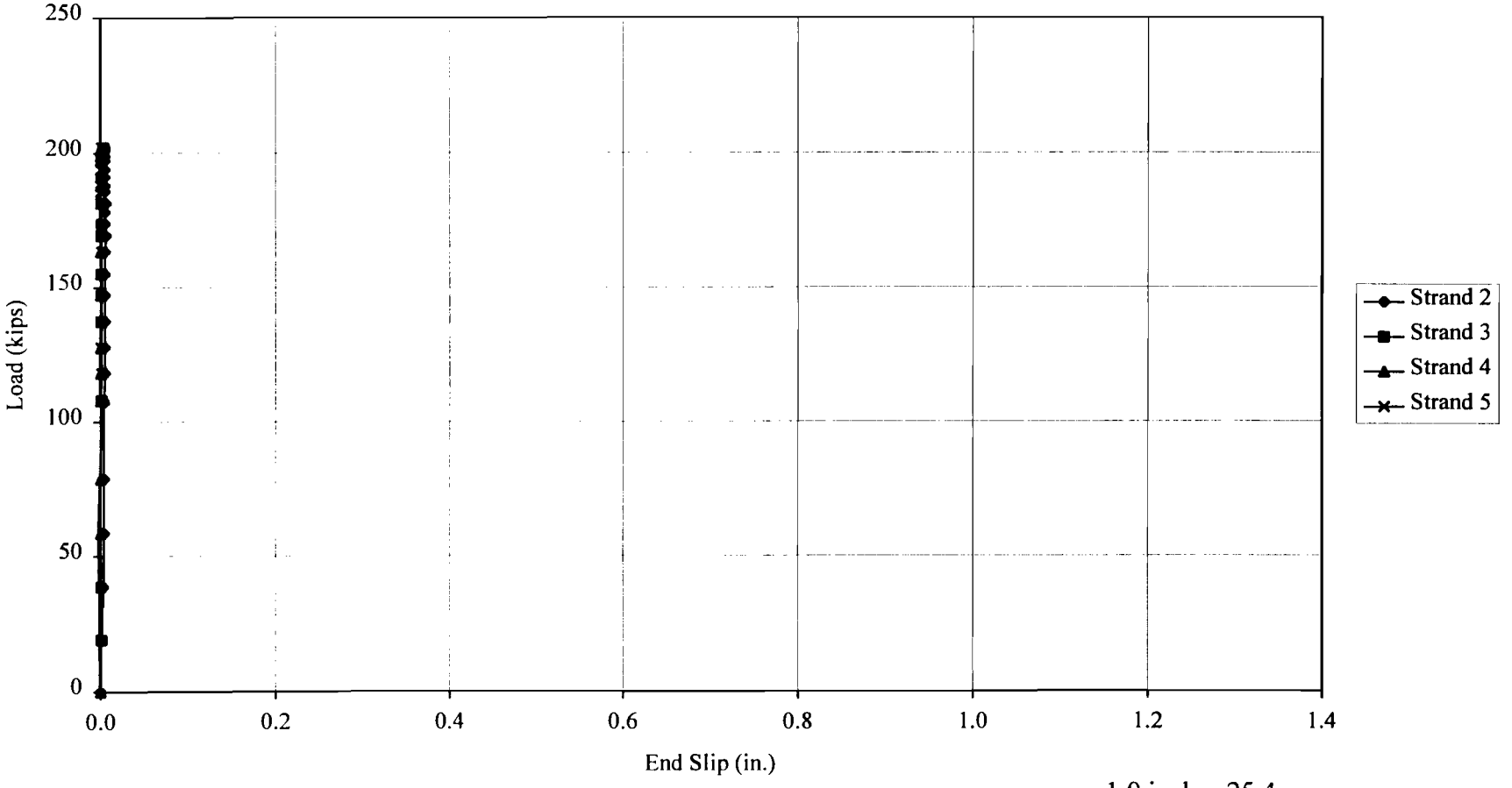

Figure D.4 Load-End Slip Curve of L4R1-4 (H-Bar)

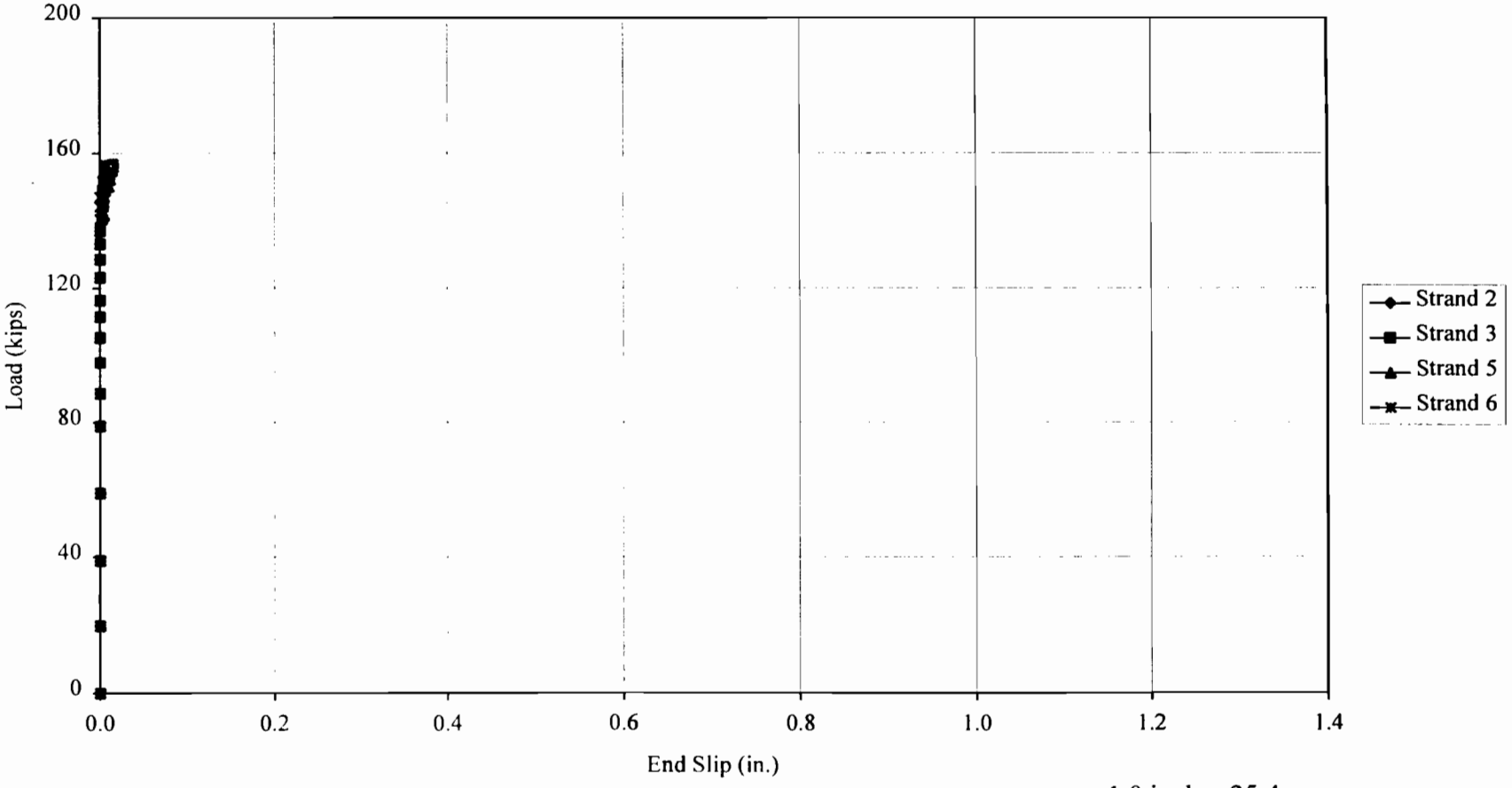

1.0 inch = 25.4 mm
1.0 kip = 4.45 kN

Figure D.5 Load – End Slip Curve of L6R0-1

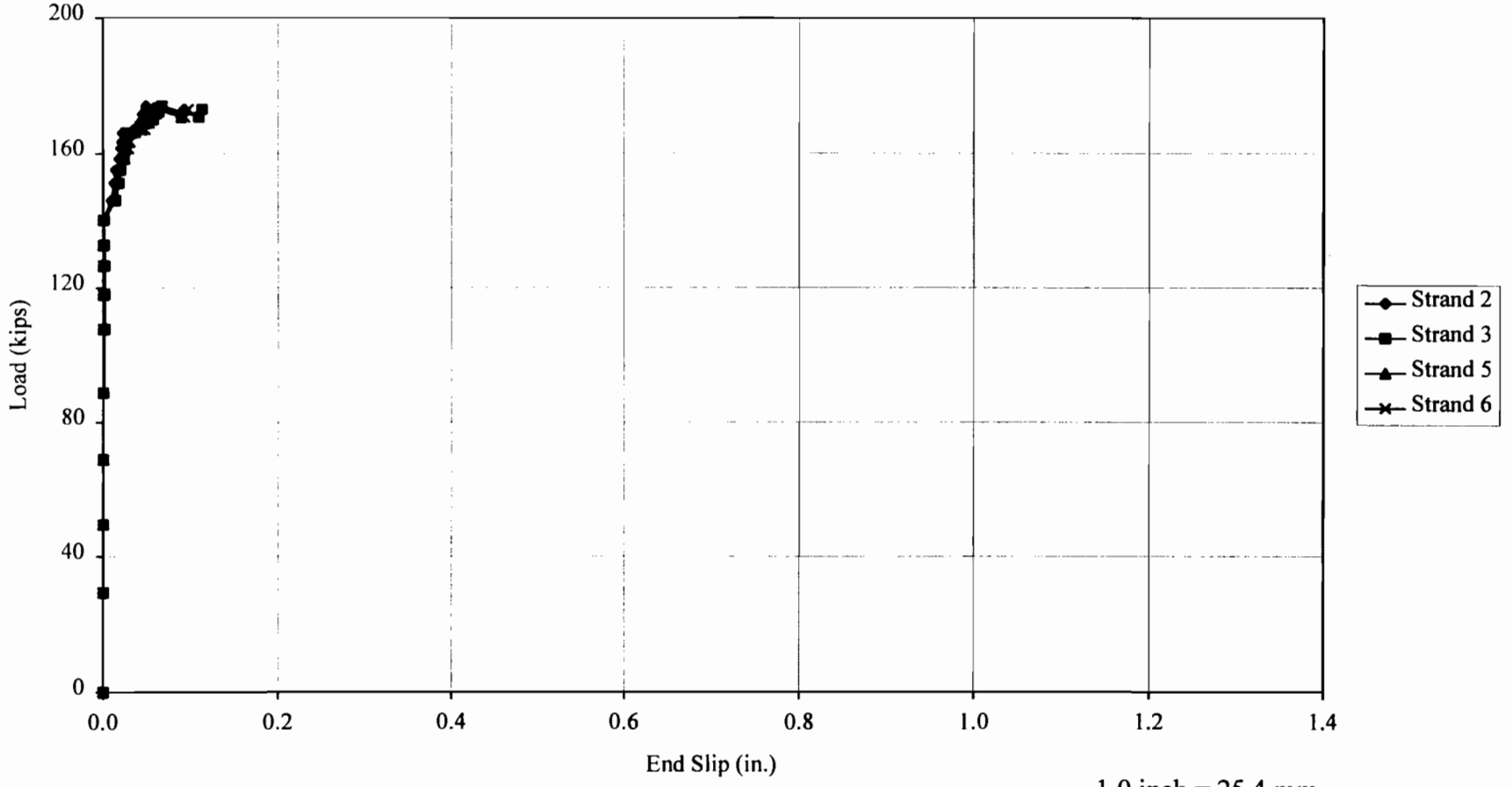

1.0 inch = 25.4 mm
1.0 kip = 4.45 kN

Figure D.6 Load – End Slip Curve of L6R0-2

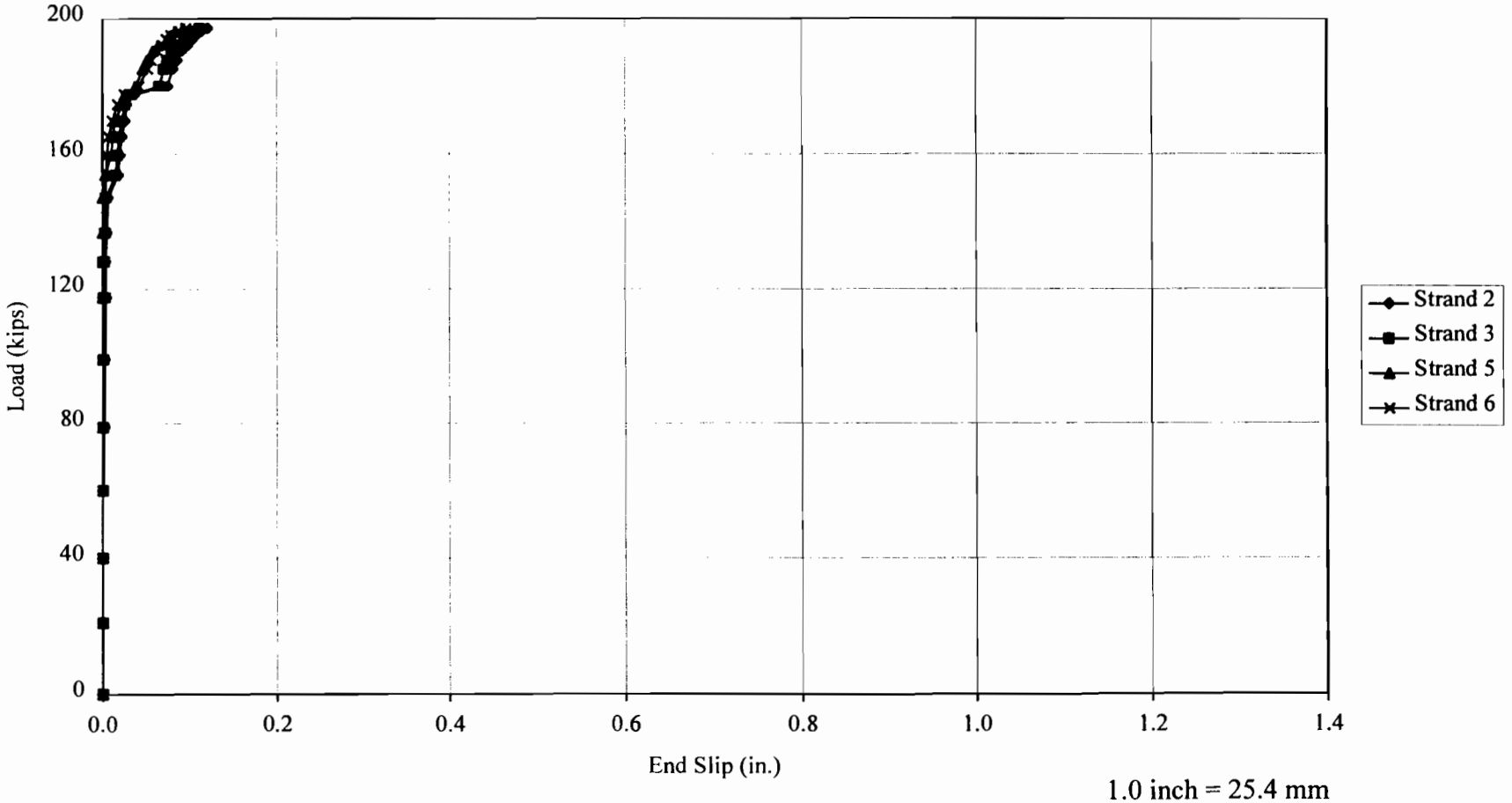

Figure D.7 Load – End Slip Curve of L6R1-3

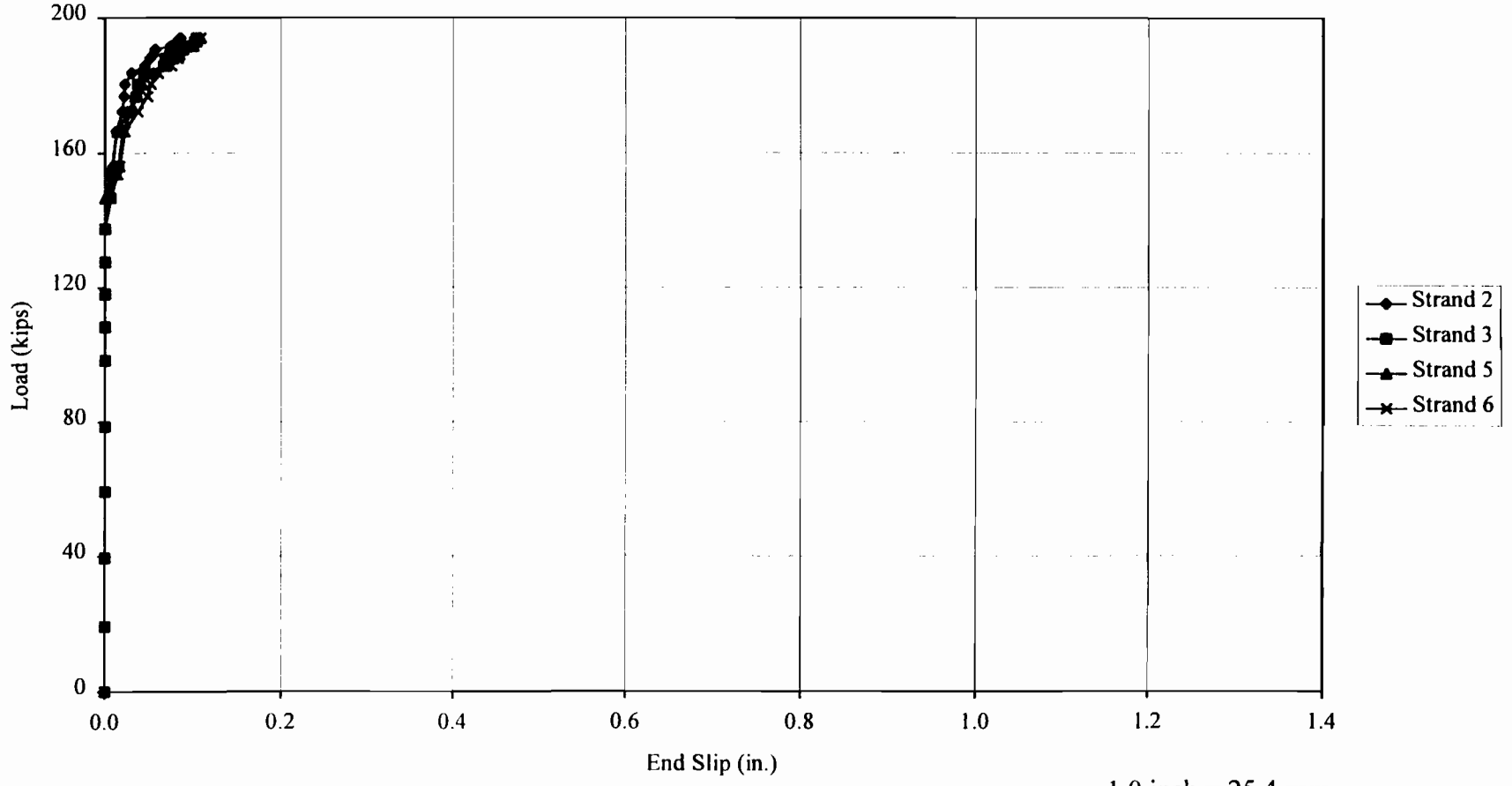

1.0 inch = 25.4 mm
1.0 kip = 4.45 kN

Figure D.8 Load – End Slip Curve of L6R1-4 (H-Bars)

APPENDIX E

NOTATION

Symbol	Description
a	Distance from outside load point to location of hydraulic ram
d_b	Diameter of prestressing strand
E_c	Modulus of elasticity of concrete
f'_c	Concrete compressive strength at 28 days
f'_{ci}	Concrete compressive strength at release of prestress
f_{pt}	Initial prestress in prestressing strand prior to transfer
f_{ps}	Stress in prestressing strand at nominal strength
f_{se}	Effective prestress after all losses
f_{si}	Initial stress in prestressing strand, immediately after release
f_{py}	Yield stress of prestressing strand
l	Beam length
l_d	Development length
l_e	Embedment length
l_{fb}	Flexural bond length
l_s	Test span length
l_t	Transfer length
l_{ub}	Unbonded length of strand
M_{max}	Maximum applied moment
M_{th}	Theoretical moment capacity calculated by strain compatibility
t	time from initial stressing
β_1	Ratio of depth of equivalent rectangular stress block to depth of neutral axis
ε_{ps}	Strain in prestressing strand corresponding to f_{ps}
ρ_p	prestress reinforcement ratio
ω_p	reinforcement index

SI* (MODERN METRIC) CONVERSION FACTORS

APPROXIMATE CONVERSIONS TO SI UNITS

Symbol	When You Know	Multiply By	To Find	Symbol
	LENGTH			
in	inches	25.4	millimeters	mm
ft	feet	0.305	meters	m
yd	yards	0.914	meters	m
mi	miles	1.61	kilometers	km
	AREA			
in^2	square inches	645.2	square millimeters	mm^2
ft^2	square feet	0.093	square meters	m^2
yd^2	square yards	0.836	square meters	m^2
ac	acres	0.405	hectares	ha
mi^2	square miles	2.59	square kilometers	km^2
	VOLUME			
fl oz	fluid ounces	29.57	milliliters	mL
gal	gallons	3.785	liters	L
ft^3	cubic feet	0.028	cubic meters	m^3
yd^3	cubic yards	0.765	cubic meters	m^3
NOTE: Volumes greater than 1000 l shall be shown in m^3.				
	MASS			
oz	ounces	28.35	grams	g
lb	pounds	0.454	kilograms	kg
T	short tons (2000 lb)	0.907	megagrams (or "metric ton")	Mg (or "t")
	TEMPERATURE (exact)			
°F	Fahrenheit temperature	5(F-32)/9 or (F-32)/1.8	Celcius temperature	°C
	ILLUMINATION			
fc	foot-candles	10.76	lux	lx
fl	foot-Lamberts	3.426	candela/m^2	cd/m^2
	FORCE and PRESSURE or STRESS			
lbf	poundforce	4.45	newtons	N
lbf/in^2	poundforce per square inch	6.89	kilopascals	kPa

APPROXIMATE CONVERSIONS FROM SI UNITS

Symbol	When You Know	Multiply By	To Find	Symbol
	LENGTH			
mm	millimeters	0.039	inches	in
m	meters	3.28	feet	ft
m	meters	1.09	yards	yd
km	kilometers	0.621	miles	mi
	AREA			
mm^2	square millimeters	0.0016	square inches	in^2
m^2	square meters	10.764	square feet	ft^2
m^2	square meters	1.195	square yards	yd^2
ha	hectares	2.47	acres	ac
km^2	square kilometers	0.386	square miles	mi^2
	VOLUME			
mL	milliliters	0.034	fluid ounces	fl oz
L	liters	0.264	gallons	gal
m^3	cubic meters	35.71	cubic feet	ft^3
m^3	cubic meters	1.307	cubic yards	yd^3
	MASS			
g	grams	0.035	ounces	oz
kg	kilograms	2.202	pounds	lb
Mg (or "t")	megagrams (or "metric ton")	1.103	short tons (2000 lb)	T
	TEMPERATURE (exact)			
°C	Celcius temperature	1.8C + 32	Fahrenheit temperature	°F
	ILLUMINATION			
lx	lux	0.0929	foot-candles	fc
cd/m^2	candela/m^2	0.2919	foot-Lamberts	fl
	FORCE and PRESSURE or STRESS			
N	newtons	0.225	poundforce	lbf
kPa	kilopascals	0.145	poundforce per square inch	lbf/in^2

* SI is the symbol for the International System of Units. Appropriate rounding should be made to comply with Section 4 of ASTM E380

(Revised September 1993)

REFERENCES

1. ACI Committee 318, *Building Code Requirement for Reinforced Concrete Structures (ACI 318-95)*, American Concrete Institute, Detroit Michigan, 1989.

2. American Association of State Highway and Transportation Officials (AASHTO), *LRFD Specifications for Highway Bridges*, 1997 Interim Revision, AASHTO, Washington, D.C., 1997.

3. American Association of State Highway and Transportation Officials (AASHTO), *Standard Specifications for Highway Bridges*, Sixteenth Edition, AASHTO, Washington, D.C., 1992.

4. Buckner, C. Dale, "An Analysis of Transfer and Development Lengths For Pretensioned Concrete Structures", Research Report FHWA-RD-94-049. Department of Civil and Environmental Engineering, Virginia Military Institute, Lexington, VA, 1994.

5. Lane, Susan N., "A new Development Length Equation for Pretensioned Strands in Bridge Beams and Piles", Research Report FHWA-RD-98-116. Structures Division, Federal Highway Administration, McLean, VA, 1998.

6. Nawy, Edward G., *Prestressed Concrete*. Second Edition, Prentice Hall, New Jersey, 1996.

7. Prestressed Concrete Institute (PCI), *PCI Design Handbook-Precast and Prestressed Concrete*, Third Edition, PCI, Chicago, IL, 1985.

8. Russell, B. W., and Burns, N. H., " Design Guidelines for Transfer, Development and Debonding of Large Diameter Seven Wire Strands in Pretensioned Concrete Girders.", Research Report 1210-5F. Center for Transportation Research, The University of Texas at Austin, January 1993.